

Alma Mater Studiorum – Università di Bologna

DOTTORATO DI RICERCA IN

SCIENZE AMBIENTALI: TUTELA E GESTIONE DELLE RISORSE NATURALI

Ciclo XXI

Settore/i scientifico-disciplinare di afferenza: GEO/12

TITOLO TESI

Development of operational oceanography applications: environmental indicators and decision support systems

Presentata da: Dott. Giovanni Coppini

Coordinatore Dottorato

Prof.ssa Elena Fabbri

Relatore

Prof.ssa Nadia Pinardi

Esame finale anno 2010

Correlatori:

Trine Christiansen, Attilio Rinaldi e Giuseppe Montanari.

Index

1. Introduction	7
1.1. European seas environmental threats	7
1.1.1. Marine pollution and marine eutrophication in European seas	7
1.1.2. Climate change state and impacts assessment in the European seas	11
1.2. Climate change policies, European Maritime Policy, European directives and the Barcelona convention	14
1.2.1. Climate change policy framework	14
1.2.2. European Maritime Policy	14
1.2.3. Marine Strategy Framework Directive	15
1.2.4. Directives relevant to nutrient load reduction and eutrophication	16
1.2.5. The Barcelona Convention	16
1.3. European and Italian relevant stakeholders	17
1.3.1. European Environment Agency (EEA)	18
1.3.2. European Maritime Safety Agency (EMSA)	18
1.3.3. United Nations Environmental Programme/Mediterranean Action Plan (UNEP/MAP)	19
1.3.4. Regional Marine Pollution Emergency Response Centre for the Mediterranean Sea (REMPEC)	20
1.3.5. Regional Agency for Environmental Prevention in Emilia-Romagna, Oceanographic Section (ARPA-DAPHNE)	21
1.4. Operational Oceanography Marine Core Service and Downstream Services	22
1.5. Thesis objectives	25
2. Identification, definition and implementation of environmental and climate indicators ..	26
2.1. Introduction	26
2.2. Spatial Data Theme Elements	28
2.3. Temperature SDTE and related indicators	30
2.3.1. Spatial Data Theme Element relevance	30
2.3.2. Description of the SDTE OO derived products	31
2.3.3. Indicators derived from the temperature SDTE	33
2.4. Chl-a SDTE and derived indicators	38
2.4.1. Chl-a SDTE relevance	39
2.4.2. Description of the Chl-a SDTE derived products	40
2.4.3. Chl-a trend indicators derived from the Chl-a SDTE	41
2.4.4. Coastal water extension indicator derived from the Chl-a SDTE	57
2.5. Conclusions	59
3. Oil spill accidents and illegal discharges	61
3.1. Hindcast of Oil Spill Pollution during the Lebanon Crisis, July-August 2006	61
3.1.1. Summary	61
3.1.2. Introduction	62
3.1.3. Remote sensing for oil spill monitoring	63
3.1.4. The oil spill forecasting systems	65
3.1.5. Hindcast experiments of the Lebanon oil pollution event	68
3.1.6. The reference experiments	71
3.1.7. Sensitivity Experiments	80
3.1.8. Conclusions	82
3.2. The ERO exercise	83
3.2.1. Summary of the OSCAR-MED operation	83
3.2.2. Introduction	84
3.2.3. Area of the operation, participants and monitoring and forecasting systems used	86
3.2.4. Participants in the operation	87

3.2.5.	Aerial and satellite monitoring systems used in OSCAR-MED	87
3.2.6.	ERO procedures and ERO-MOON monitoring and forecasting systems.....	90
3.2.7.	The operational activities	97
3.2.8.	Results of the operation	98
3.2.9.	Conclusions.....	98
4	Example of end-user service.....	100
4.1	Introduction	100
4.2	An environmental DSS for the Adriatic Sea	100
4.3	The ARPA-DAPHNE monitoring network and data input to ADRI-DSS.....	101
4.4	ARPA-DAPHNE user requirements.....	103
4.5	ADRI-DSS architecture.....	103
4.6	ADRI-DSS products	104
4.7	Conclusions.....	109
5	Conclusions	111
	References	114

1. Introduction

1.1. European seas environmental threats

The seas around Europe are of vital importance to the people living there. They are used for fishing, for transport, for recreation, and for many other activities of economic importance such as oil and gas exploration, sand and gravel extraction and mariculture, and are influenced by land-based activities such as agricultural and industrial production. These seas are therefore under ongoing pressure from a large number of anthropogenic factors. Due to the large population living near the coast or near rivers draining into the European seas, many contaminants and nutrients are discharged into the sea areas not only by the rivers and sewage systems but also from the atmosphere, which carries some contaminants far from their original source and deposits them in the sea according to air currents. These activities also lead to species and population loss, physical damage to marine habitats, nutrient and chemical pollution, littering of the sea, introduction of non-indigenous species, and noise exposure. Man's impact on the atmosphere also affects the sea in a more physical way: the build-up of carbon dioxide and other greenhouse gases in the atmosphere is contributing to an increase in temperature, both in the air and in the sea. Moreover, anthropogenic climate change further adds to these diverse pressures, altering water sea levels and the pH levels of marine waters. All these elements can have an additive impact on marine habitats.

In the following paragraph of this section we will introduce some of environmental threats relevant to our work. This introduction is based, *inter alia*, on the EEA report on the European environment published in 2007 (EEA, 2007), the ICES report on the environmental status of European seas published in 2003 (ICES, 2003), the paper by Markus Salomon on recent European initiatives in marine protection policy (Salomon, 2009) and the EEA report on climate change and its impact published in 2008 (EEA, 2008). Moreover, we also collect information from EEA CSI 021 (Core Set of Indicator, Nutrients in transitional, coastal and marine waters), the latest assessment of which was published in Jan 2009 (CSI021, 2009) and CSI 023 - (Chlorophyll in transitional, coastal and marine waters), the latest assessment of which was published in Jan 2009 (CSI023, 2009).

1.1.1. Marine pollution and marine eutrophication in European seas

Marine pollution is a consequence of human pressure on the marine environment. Several economic sectors such as agriculture, shipping and sewage discharge from mega-towns on the coasts contribute through emission and direct discharge to polluting European seas. Specifically,

eutrophication is linked to the excessive input of nutrients into the marine environment.

1.1.1.1. Some of the relevant economic sectors and their pressures on the marine environment

Shipping is an important activity affecting the marine environment, with some of the busiest shipping lanes in the world found in the North Sea, Baltic Sea and Mediterranean Sea. Despite mandatory global and regional regulations against discharges of oil and litter from ships, such discharges nevertheless represent a source of chronic impact from shipping. Major concerns include illegal discharges of oil and waste, atmospheric emissions of nitrogen oxide (NO_x), sulphur dioxide (SO₂), particulates and CO₂, noise, and accidental discharges of hazardous substances. There is also the risk of accidents, which can be particularly serious if oil tankers are involved.

In terms of oil inputs to marine waters, the main sources in the North Sea are the offshore oil and gas industry. In addition, there is considerable oil production in some countries bordering the Mediterranean Sea. Refineries are distributed all around the Mediterranean coasts, often in association with petrochemical plants, and these may have discharges to sea. Shipping traffic, carrying both crude oil and its refined products, travels through all the seas of the North Atlantic and adjacent seas, except for the high Arctic.

The European seas are crisscrossed by some of the busiest shipping routes in the world. Shipping activities have a range of impact on the marine environment ranging from impact on the coastal zone – resulting from the development and daily activities of large-scale port facilities – to the stirring up of contaminated sediments by dredgers working to keep the shipping channels open (ICES, 2003). Ships can also have an effect on the marine environment if they suffer an accident and lose their cargo.

Many cities and towns are located near the coast, and urbanization claims large expanses of coastline in northwestern Europe and on the northern coast of the Mediterranean Sea. This large urbanization leads to an input of contaminants into the marine environment. Tourism too is a growing source of disturbance in coastal areas, and brings an increase of the population in these areas during the tourist season.

Agriculture is among the land-based economic activities that have considerable influence on the seas. The sector is responsible for a major part of nutrient inputs into the North Sea and Baltic (HELCOM, 2003; ICES, 2003, 2007).

1.1.1.2. Contaminants and oil pollution

Contaminants are chemical substances that are detected in locations where they should not normally be found and can be either natural or manmade. Contaminants in the marine environment fall into four main groups:

- 1 Trace metals: metals such as cadmium and mercury, which are generated in metallurgic industries such as the manufacture of batteries, and copper, which is widely used in antifouling;
- 2 Organic compounds: includes pesticides and herbicides that occur in agricultural runoff;
- 3 Oil: from energy extraction and marine transport;
- 4 Radioactive elements: radioactive caesium is released from nuclear reprocessing operations.

In this paragraph we will focus only on category 3 of the above list, and specifically oil from marine transport and accidents at sea. Chapter 3 of this thesis is in fact dedicated to presenting cases in the Mediterranean Sea of oil pollution at sea and proposing possible strategies for marine pollution emergency management.

The impact of offshore oil and gas exploration and production and of major accidental oil spills at sea have been studied within the North Sea and consequently in large accidents such the *Haven* in the Ligurian Sea and the *Prestige* in the northern Spanish coast. Oil discharges from ships represent a significant threat to marine ecosystems. These discharges may occur during normal activities (operational) or may be accidental or illegal. Illegal discharges of oil from ships are often limited in size and scattered, but, surprisingly, their sum is higher than that from oil spills, and they may create a chronic impact of oil in certain areas. There have been a number of large oil spills from tankers in the European Seas area over the last few decades, with examples including:

- The *Torrey Canyon* off England in 1967 (93,000 t);
- The *Amoco Cadiz* off Brittany in 1978 (260,000 t);
- The *Haven* off Genoa, Italy, in 1991 (114,000 t of crude oil, most of which burned);
- The *Aegean Sea* off northwest Spain in 1992 (80,000 t);
- The *Braer* off Shetland in 1993 (85,000 t of crude oil);
- The *Sea Empress* off Wales in 1996 (72,000 t of crude oil);
- The *Erika* off Brittany in 1999 (of the 30,000 t of heavy fuel oil on board, more than 10,000 t got into the marine environment);
- The *Prestige* off northwest Spain in late 2002 (more than 25,000 t of heavy fuel oil, with 50,000 t remaining in the wreck).

The environmental impact of all these spills has been thoroughly studied, with monitoring studies ongoing for two or more years following most of the spills mentioned above. In all cases, the spills had both immediate and longer-term effects, including contamination of farmed fish and shellfish for human consumption. Taking the *Erika* as an example, heavy fuel oil came ashore along over 400 km of the coast of western France, from south Finisterre to the Vendée. Initial mortality of shellfish in coastal waters was accompanied by contamination of seawater, which persisted for several months. Oil, and heavy fuel oil in particular, stranded on rocky coasts and trapped in inshore sediments causes direct kills and habitat losses, but is also likely to remain there for long periods. This provides a long-term source of contamination, which impacts on coastal habitats and resources, e.g., preventing the re-opening of some coastal fisheries (ICES, 2003).

1.1.1.3. Nutrients and eutrophication

Nutrients and light are essential for the growth of marine plants, including phytoplankton, which form the base of the food chain which leads up through fish to man. In addition to upwelling, human activities contribute important additional sources of nutrients from:

- River runoff – including inputs from industry, municipal discharge, and agriculture;
- Direct inputs of municipal discharge and industrial waste;
- The atmosphere – emissions from agriculture, fuel combustion, including traffic;
- Marine activities such as fish farming.

These sources lead to increased concentrations of nutrients in coastal waters and, in particular, partially enclosed sea areas. Excessive nutrient enrichment from human activities is termed eutrophication and can cause reduced water transparency, algal blooms (red tides, foam or green tides on beaches), fish and benthos kills owing to decreased amounts of oxygen in the bottom waters, bad smells (hydrogen sulphide), and changes in the communities and biodiversity of planktonic and bottom living organisms (ICES, 2003). The two most important nutrients that are needed for plant growth are nitrogen and phosphorus. Marine phytoplankton takes up nitrogen and phosphorus in a ratio of about 16:1. Under normal conditions in the marine environment, nitrogen is the limiting nutrient, but recent major reductions in phosphorus inputs, due amongst other reasons to the introduction of phosphate-free detergents and municipal wastewater treatment, has led to a condition where phosphorus limitation of phytoplankton production now occurs in certain coastal areas. Nitrogen inputs, on the other hand, are much more difficult to control, as there are many diffuse sources, including agriculture and fuel combustion. This has led to an excess of nitrogen over phosphorus in the coastal waters of some European seas, which can result in an altered phytoplankton species composition and an enhanced growth of nuisance algae.

There are long-standing eutrophication hot spots in the Mediterranean, for instance in the Venice area, and the Gulf of Lion. Others occur in the Baltic Sea, Black Sea, Great and Little Belts, Kattegat, in the Norwegian fjords and the North Sea's Wadden Sea (EEA, 2007). More widely, eutrophication of coastal waters also reduces the transparency of the water and causes a decline or shift in life on the seabed. Thus, red algae beds have disappeared from wide areas of the Black Sea, and sea grass beds from the Baltic (EEA, 2007). Problems appear in most cases to be directly related to the volume of fertilizer use on land. Thus, eutrophication in the Black Sea reduced during the 1990s when the economic downturn led to less fertilizer being applied. Reductions were also observed in the Baltic and North Seas following constraints on direct discharges into the Rhine (EEA, 2007).

The latest results of the EEA indicator on nutrients in coastal waters (CSI021,2009) assessed that:

- The highest winter oxidized nitrogen and orthophosphate concentrations were observed in coastal areas and estuaries and are at many locations associated with nutrient inputs from major rivers.
- Decreasing trends in oxidized nitrogen concentrations were found at 12% of stations reported to the EEA in 2005, increasing trends were found at 3% of stations, and the majority of stations (85%) indicate no statistically significant change in concentration.
- Decreasing trends in orthophosphate concentrations were found at 11% of stations reported to the EEA in 2005, increasing concentrations were found at 7% of stations, and, as for oxidized nitrogen, the majority of stations (82%) indicate no statistically significant change in orthophosphate concentration.

The latest results of the EEA CSI023 on chl-a trends in the coastal zones assesses that the highest summer chlorophyll-a concentrations were observed in coastal areas and estuaries and are at many locations associated with nutrient inputs from major rivers. Of the 413 stations reported to the EEA in 2005 with more than 5 years of observations, decreasing trends in summer chlorophyll-a concentrations were found at 7% of stations, increasing trends were found at 8% of stations, and the majority of stations (85%) indicate no statistically significant change in concentration. The stations with decreasing trends are located either in the Baltic Sea or along the coast of Italy.

1.1.2. Climate change state and impacts assessment in the European seas

Climate change can be defined as a change in the state of the climate that can be identified (e.g. using statistical tests) by changes in the mean and/or the variability of its properties and that persists

for an extended period, typically decades or longer (IPCC). In this case it refers to any change in climate over time, whether due to natural variability or as a result of human activity. A second possible definition of climate change is the one provided by the United Nations Framework Convention on Climate Change (UNFCCC), which define climate change as a change of climate that is attributed directly or indirectly to human activity that alters the composition of the global atmosphere and that is additional to natural climate variability observed over comparable time periods. In this introductory part of the thesis the candidate aims to present a general description of climate change state and impacts in the European Seas as reported by the recent scientific literature and European reports (i.e. ICES, 2003 and EEA, 2008).

The effects of Climate Change are evident: natural systems appear to be affected by regional climate changes, particularly temperature increases. Effects include: shifts in ranges and changes in algal, plankton and fish abundance in high-latitude oceans; increases in algal and zooplankton abundance in high latitudes; and range changes and earlier fish migrations in rivers. Sea level rise and human development are together contributing to losses of coastal wetlands and mangroves and increasing damage from coastal flooding in many areas.

Warming of the climate system is unequivocal, as is now evident from observations of increases in global average air and ocean temperatures, widespread melting of snow and ice and rising global average sea level (IPCC, 2007 and Trenberth et al., 2007). Climate change impact is observed in all European seas (Halpern et al., 2008), although the extent to which these have been documented in time and space varies.

One of the most visible consequence of increased temperature of the ocean is the reduced area of sea ice coverage in the Arctic polar region, and there is an accumulating body of evidence suggesting that many marine ecosystems are responding both physically and biologically to changes in regional climate caused predominantly by the warming of air and SST. Recruitment in cold temperate species is often synchronized with seasonal production cycles of phytoplankton. If warming results in advancement of the timing of reproduction of these species, this may result in a mismatch with the presence of their main food source (phytoplankton). Any subsequent decrease in recruitment success will inevitably lead to shifts in species composition.

In general, a rapidly warming environment would be expected to result in a poleward movement of species. Since warming accelerated in the late 1980s, poleward advances of southern species and retreats of northern species have been recorded in zooplankton, fish and benthic species, including those found on rocky shores (Brander et al., 2003; Southward et al., 2005).

Rapid warming can accelerate establishment of non-indigenous species, many of which have been shown to do better under the warmer conditions experienced in recent years (Stachowicz et al.,

2002).

Sea level observations show that increases in sea level are evident and consistent with warming. Global average sea level rose by around 0.17 m (1.7 mm/year) during the 20th century. In Europe rates of sea level rise (SLR) ranged from – 0.3 mm/year to 2.8 mm/year. The sea level is not raising uniformly (EEA, 2008). Table 1.1 presents the SLR rates for the different European seas as calculated in the period October 1992-June 2008 from satellite altimetry. Since the beginning of the 1990s, the sea level has been precisely measured by satellite altimetry with a global coverage. The rate of rising seems to show acceleration with a value of 3.1 mm/year. However, satellite altimetry has revealed that sea level is not rising uniformly (Table 1.1). The satellite observations indicate a large spatial variability of SLR trends in the European seas (Guinehut and Larnicol in EEA, 2008): North Atlantic (50°N to 70°N) 3.4 mm/yr, Central North Atlantic (30°N to 50°N) 1.1 mm/yr, Mediterranean Sea 1.7 mm/yr and Black Sea 3.3 mm/yr. These local variations could be explained by variability of the North Atlantic Oscillation (NAO), inter-annual wind variability, changes in global ocean circulation patterns, or specific local structures of the circulation (e.g. gyres) (Demirov and Pinardi, 2002 and Lombart et al., 2006). Recent studies have attempted to close the sea level budget for the recent period by assessing the different contributions (thermal expansion from Argo, mass variation from GRACE). The main conclusion from Cazenave et al. (2009) could be summarized as followed: since 2003, the sea level has continued to rise but at a rate of 2.5 mm/y. For this period, ocean mass has increased at an averaged rate of 1.9 mm/y, whereas the thermal expansion has a smaller contribution of about 0,3 mm/y. These results are slightly different than those obtained for the last decade, where thermal expansion explains half of the sea level rise.

European seas	Sea-level rise (mm/year)
North Atlantic (50°N to 70°N)	3.4 mm/yr
Central North Atlantic (30°N to 50°N)	1.1 mm/yr
Mediterranean Sea	1.7 mm/yr
Black Sea	3.3 mm/yr

Table 1.1 Average sea-level rise in some European seas (satellite observations) (October 1992–June 2008). Courtesy of Durando and Larnicol, CLS, France.

Rising sea levels have a certain impact on coastal areas by increasing numbers and intensity of storm surges and coastal flooding. They endanger industrial and living areas and may cause migration after depleting small, flat islands as well as flat coastal areas (EEA, 2008).

An improved understanding of sea level rises and their variability will contribute to monitoring of the global change and better management of the coastal zones by improving the planning of development of infrastructures for coping with flooding or erosion of sandy beaches, for instance (EEA, 2008).

1.2. Climate change policies, European Maritime Policy, European directives and the Barcelona convention

In these paragraphs we will briefly overview the most relevant European Directives and international conventions that compose the policy framework for climate change, marine eutrophication and oil spill pollution.

1.2.1. Climate change policy framework

Since the early 1990s, most industrialized nations and many developing countries have implemented climate change-related policies. During 2008 the European Commission proposed a package of actions that will deliver on the European Union's ambitious commitments to fighting climate change and promoting renewable energy up to 2020 and beyond. The EU is committed to reducing its overall emissions to at least 20% below 1990 levels by 2020, and is ready to scale up this reduction to as much as 30% under a new global climate change agreement when other developed countries make comparable efforts. It has also set itself the target of increasing the share of renewables in energy use to 20% by 2020 (http://ec.europa.eu/climateaction/index_en.htm).

The maritime dimension of climate change is evident and the European Commission has shown with recent actions that oceans, seas and coasts deserve special attention in the climate change context. The European Commission has recently started to set up an EU Framework on Adaptation to Climate Change with the publication of the White Paper that sets out a framework to reduce the EU's vulnerability to the impact of climate change. The White Paper gives special attention to coastal and marine environments. The strategy proposed in the White Paper commits the Commission to ensuring that adaptation in coastal and marine areas is taken into account in the framework of the Integrated Maritime Policy (see paragraph 1.2.2), in the implementation of the Marine Strategy Framework Directive (see paragraph 1.2.3) and in the reform of the Common Fisheries Policy.

1.2.2. European Maritime Policy

On 10 October 2007 the Commission presented its vision for an Integrated Maritime Policy for the European Union. The vision document (also called the Blue Book¹) proposes an Integrated Maritime Policy for the European Union, based on the clear recognition that all matters relating to Europe's oceans and seas are interlinked, and that sea-related policies must develop in a joined-up way.

Along with its other objectives, EU maritime policy is developing and delivering programmes of

1 <http://eur-lex.europa.eu/LexUriServ/LexUriServ.do?uri=COM:2007:0575:FIN:EN:PDF>

work in the following sectors:

- A European Strategy for Marine Research
- National integrated maritime policies to be developed by member states
- A roadmap towards maritime spatial planning by member states
- A strategy to mitigate the effects of climate change on coastal regions
- A European network of maritime clusters

1.2.3. Marine Strategy Framework Directive

In the framework of the marine and maritime EU policy the European Marine Strategy Framework Directive (2008/56/EC) (MSFD) was launched on 17 June 2008 and represents the most important recent initiative for the protection of marine ecosystems in Europe. EU member states are required by law to formulate strategies to aim at the conservation of marine ecosystems. This approach should include protected areas and should address all human activities that have an impact on the marine environment. The main target of the Marine Strategy Framework Directive is to reach good environmental status (GES) in European waters by 2020. Definition of GES is under definition by expert working groups in consultation with member states on the basis of the MSFD descriptor definitions.

The marine strategies to be developed by each Member State must contain a detailed assessment of the state of the environment, a definition of GES at regional level and the establishment of clear environmental targets and monitoring programmes.

A strategic aspect is that the MSFD calls for cooperation between neighbouring states and regions and for coordination in developing programmes of measures, risk assessments and monitoring programmes.

To be mentioned in this context is the fact that the MSFD identifies an indicative lists of characteristics, pressures and impacts in Annex II of the Directive which include physical and chemical features such as: annual and seasonal temperature regime and ice cover, current velocity, upwelling, wave exposure, mixing characteristics, turbidity, residence time and the spatial and temporal distribution of salinity.

Preparations for the implementation of the MSFD are now underway in the Commission and the Member States. Recently during their meeting in Brno (CZ), Marine Directors agreed on 29 May 2009 on a work structure for an informal Common Implementation Strategy (CIS) at EU level, which consists of:

- Marine Directors;
- Marine Strategy Coordination Group + a small number of working groups, initially a working group on good environmental status and one on data, information and knowledge

exchange.

Where the Directive attributes responsibilities the European Commission assisted by an official Committee, the CIS will prepare materials that will also be considered by that official Committee.

1.2.4. Directives relevant to nutrient load reduction and eutrophication

There are a number of EU Directives aimed at reducing the loads and impacts of nutrients. These include: the Nitrates Directive (91/676/EEC), aimed at reducing nitrate pollution from agricultural land; the Urban Waste Water Treatment Directive (91/271/EEC), aimed at reducing pollution from sewage treatment works and certain industries; the Integrated Pollution Prevention and Control Directive (96/61/EEC), aimed at controlling and preventing pollution of water from industry; and the Water Framework Directive (2000/60/EC), which requires the achievement of good ecological status or good ecological potential of transitional and coastal waters across the EU by 2015.

Measures also arise from a number of other international initiatives and policies including: the UN Global Programme of Action for the Protection of the Marine Environment against Land-based Activities; the Mediterranean Action Plan (MAP) 1975; the Helsinki Convention 1992 (HELCOM) on the Protection of the Marine Environment of the Baltic Sea Area; the OSPAR Convention 1998 for the Protection of the Marine Environment of the North East Atlantic; and the Black Sea Environmental Programme (BSEP).

1.2.5. The Barcelona Convention

The Barcelona Convention aims for the protection of the marine environment and the coastal region of the Mediterranean. The European Community and the countries surrounding the Mediterranean are parties to this convention implemented through the Mediterranean Action Plan (MAP). This assists the Mediterranean countries to assess and control marine pollution, to formulate their national environment policies for protecting biodiversity and the marine and coastal environment, and to improve the ability of governments to identify better options for alternative patterns of development.

Seven Protocols addressing specific aspects of Mediterranean environmental conservation complete the MAP legal framework:

- Dumping Protocol (from ships and aircraft)
- Prevention and Emergency Protocol (pollution from ships and emergency situations)
- Land-based Sources and Activities Protocol
- Specially Protected Areas and Biological Diversity Protocol
- Offshore Protocol (pollution from exploration and exploitation)

- Hazardous Wastes Protocol
- Protocol on Integrated Coastal Zone Management (ICZM)

In 2008, the parties to the Barcelona Convention signed a Protocol on Integrated Coastal Zone Management in the Mediterranean, identifying adaptation to climate change as a priority. The Marrakesh Declaration, adopted by the Barcelona Convention in November 2009, highlights the need for urgent action to counter the serious impacts of climate change on ecosystems and resources.

Of the seven protocols, we would like to focus on the one related to prevention and emergency (pollution from ships and emergency situations), since is very relevant to the activities presented in Chapter 3 of this thesis. The Protocol Concerning Cooperation in Preventing Pollution from Ships and, in Cases of Emergency, Combating Pollution of the Mediterranean Sea is the legal framework within which regional cooperation in the Mediterranean region in the fields of prevention of and response to marine pollution is developing. The Protocol was adopted on 25 January 2002 in Malta and entered into force on 17 March 2004. The states that adopted the protocols cooperate to implement international regulations to prevent, reduce and control pollution of the marine environment from ships; and take all necessary measures in cases of pollution incidents.

The Protocol also promotes bilateral or multilateral cooperation and the preparation of contingency plans for preventing and combating pollution incidents. These means shall include, in particular, equipment, ships, aircraft and personnel prepared for operations in cases of emergency, the enactment, as appropriate, of relevant legislation, the development or strengthening of the capability to respond to a pollution incident and the designation of a national authority or authorities responsible for the implementation of the Protocol. The parties that signed the Protocols shall also take measures in conformity with international law to prevent the pollution of the Mediterranean Sea area from ships. The parties shall develop and apply, either individually or through bilateral or multilateral cooperation, monitoring activities covering the Mediterranean Sea area in order to prevent, detect and combat pollution, and to ensure compliance with the applicable international regulations (see OSCAR-MED operations described in 3.2). In case of release or loss overboard of hazardous and noxious substances, the parties to the Protocols shall cooperate as far as practicable in the recovery of such substances so as to prevent or reduce the danger to the marine and coastal environment.

1.3. European and Italian relevant stakeholders

Different European Agencies and several national authorities are involved in monitoring and combating the European sea problems described in section 1.1, and work to facilitate the

implementation of the Directives and Conventions described in section 1.2. In this introduction the candidate presents some of the most relevant at the European and Italian levels. EEA is relevant to the work carried out to establish the indicators presented in chapter 2.

The Regional Marine Pollution Emergency Response Centre for the Mediterranean Sea (REMPEC) operates to combat marine pollution and is the main user of the oil spill monitoring and forecasting system described in chapter 3. The work presented in Chapter 3 is also connected to activities carried out by the European Maritime Safety Agency (EMSA).

On the basis of the Regional Agency for Environmental Prevention in Emilia-Romagna, Oceanographic Section (ARPA-DAPHNE) requirements the candidate has designed the Adriatic Sea Decision Support System (ADRI-DSS) presented in chapter 4.

1.3.1. European Environment Agency (EEA)

The EEA is an agency of the European Union. The EEA aims to support sustainable development and to help achieve significant and measurable improvement in Europe's environment through the provision of timely, targeted, relevant and reliable information to policy-making agents and the public. Currently, the EEA has 32 member countries. The EEA provides a wide range of assessments, analysing the state of, and trends in, the environment, together with the pressures caused by economic and social driving forces. The EEA also works on scenario development, policy evaluation and data quality assurance. In addition, the EEA coordinates the European environment information and observation network (Eionet), which provides advice and input on indicators, data flows and streamlining of information. The EEA collects and analyses environmental data from its member countries, its EU partners, and international organizations. The development of a shared environmental information system (SEIS) will be at the core of the EEA's upcoming 2009-2013 strategy. The EEA will do this by building on existing reporting systems and tools (Reportnet), initiatives related to e-Government, the Infrastructure for Spatial Information in Europe (INSPIRE), Global Monitoring for Environment and Security (GMES) and the Global Earth Observation System of Systems (GEOSS).

To support data collection, management and analysis, the EEA has established and manages European topic centres (ETCs) covering the major environmental and operational areas of the EEA's work programme.

1.3.2. European Maritime Safety Agency (EMSA)

The European Maritime Safety Agency, created in the aftermath of the *Erika* disaster, contributes to the enhancement of the overall maritime safety system within the Community. Its goals are, through its tasks, to reduce the risk of maritime accidents, marine pollution from ships and the loss of

human lives at sea.

In general terms, the Agency provides technical and scientific advice to the Commission in the field of maritime safety and prevention of pollution by ships in a continuous process of updating and developing new legislation, monitoring its implementation and evaluating the effectiveness of the measures in place. Agency officials closely cooperate with member state maritime services.

To support member states and the Commission in the field of oil pollution, EMSA, among other activities, manages a satellite-based monitoring system for marine oil spill detection and surveillance in European waters (CleanSeaNet). This service provides a range of detailed information including oil spill alerts to member states and rapid delivery of available satellite images and oil slick position.

1.3.3. United Nations Environmental Programme/Mediterranean Action Plan (UNEP/MAP)

In 1975, 16 Mediterranean countries and the European Community adopted the Mediterranean Action Plan (MAP) as a Regional Seas Programme under UNEP's umbrella. The main objectives of the MAP were to assist the Mediterranean countries to assess and control marine pollution, to formulate their national environment policies, to improve the ability of governments to identify better options for alternative patterns of development, and to optimize the choices for allocation of resources. Later, in 1995, the Action Plan for the Protection of the Marine Environment and the Sustainable Development of the Coastal Areas of the Mediterranean (MAP Phase II) was designed, taking into account the achievements and shortcomings of the MAP in the context of recent developments. Today MAP involves 21 countries bordering the Mediterranean as well as the European Community.

Key MAP priorities are:

- To bring about a massive reduction in pollution from land-based sources;
- To protect marine and coastal habitats and threatened species;
- To make maritime activities safer and more conscious of the Mediterranean marine environment;
- To intensify integrated planning of coastal areas;
- To monitor the spreading of invasive species;
- To limit and intervene promptly on oil pollution.
- To further promote sustainable development in the Mediterranean region

The Secretariat of the Mediterranean Action Plan (MAP), based in Athens, is responsible for the implementation of the MAP legal instruments and activities, notably:

- The MEDPOL Programme for the Assessment and Control of Pollution in the Mediterranean Region;
- The REMPEC to prevent maritime accidents and illegal discharges from ships;
- The Priority Actions Programme Regional Activity Centre (PAP/RAC) dealing with the protection of the Mediterranean coasts from the impact of unrestrained development and its effects on the marine environment;
- The Specially Protected Areas Regional Activity Centre (SPA/RAC) safeguarding the natural and cultural resources;
- The Information and Communication Regional Activity Centre (INFO/RAC) designing and implementing the Information and Communication Strategy for the Mediterranean Strategy for Sustainable Development (MSSD).

1.3.4. Regional Marine Pollution Emergency Response Centre for the Mediterranean Sea (REMPEC)

REMPEC assists the Mediterranean coastal states in ratifying, transposing, implementing and enforcing international maritime conventions related to the prevention of, preparedness for and response to marine pollution from ships.

In cases of marine pollution emergency, contracting parties to the Barcelona Convention can request assistance from other through the existing bilateral or multilateral agreements or through REMPEC. Within this framework the MOON-REMPEC agreement presented in Section 3.2.2.2 enforces REMPEC capabilities to respond to contracting parties' requests of assistance.

REMPEC's main fields of action for the prevention of pollution of the marine environment from ships and the development of preparedness for, and response to, accidental marine pollution and cooperation in case of emergency consist of:

- Strengthening the capacities of the coastal states in the region with a view to preventing pollution of the marine environment from ships and ensuring the effective implementation in the region of the rules that are generally recognized at the international level relating to the prevention of pollution from ships, and with a view to abating, combating and, to the fullest possible extent, eliminating pollution of the marine environment from shipping activities, including pleasure craft;
- Developing regional cooperation in the field of the prevention of pollution of the marine environment from ships, and facilitating cooperation among Mediterranean coastal states in order to respond to pollution incidents which result or may result in a discharge of oil or other hazardous and noxious substances and which require emergency actions or other

immediate response;

- Assisting coastal states of the Mediterranean region which so request in the development of their own national capabilities for response to pollution incidents which result or may result in a discharge of oil or other hazardous and noxious substances and facilitating the exchange of information, technological cooperation and training; and
- Providing a framework for the exchange of information on operational, technical, scientific, legal and financial matters, and promoting dialogue aimed at conducting coordinated action at the national, regional and global levels for the implementation of the Prevention and Emergency Protocol;
- Assisting coastal states of the region, which in cases of emergency so request, either directly or by obtaining assistance from the other parties, or when possibilities for assistance do not exist within the region, in obtaining international assistance from outside the region.

1.3.5. Regional Agency for Environmental Prevention in Emilia-Romagna, Oceanographic Section (ARPA-DAPHNE)

ARPA stands for Agenzia Regionale per la Prevenzione e l'Ambiente dell'Emilia-Romagna (Regional Agency for Environmental Prevention in Emilia-Romagna). ARPA is an environmental control technical support body to the regional, district and local authorities and is administratively and technically independent. ARPA's functions, activities and tasks cover all aspects of environmental control, including:

- Monitoring of the various environmental components
- Management and surveillance of human activities and their territorial impact
- Activities in support of the environmental impact assessment of plans and projects
- Creation and management of a regional environmental information system

The Agency's activities are aimed at local, regional and national institutional customers, the business world and private citizens.

The DAPHNE Oceanographic Structure (ARPA-DAPHNE) is responsible for monitoring marine-coastal ecosystems, operating with an oceanographic motor vessel equipped for monitoring and studying the evolution of the North Adriatic ecosystem. It provides specialist biochemical analytical services in support of safeguarding the ecosystem and drawing up plans and projects for planning, improvement and protection.

1.4. Operational Oceanography Marine Core Service and Downstream Services

Operational Oceanography (OO) represents a knowledge-base service for the protection and management of marine areas and OO systems are currently in transition from research to sustainable operations.

Operational oceanography started to be coordinated in Europe with the signing in Rome of the EuroGOOS Memorandum of Understanding in 1995 (<http://www.eurogoos.org/>). The service was developed with a European regional seas strategy and service were initially developed at the level of three regional seas, in task team: MOON, BOOS, IBI-ROOS and NOOS (see Fig. 1.1).

At the same time, a comprehensive effort to connect European regional seas to the global ocean started with the advent of the MERSEA Integrated Project, funded by the FP6 GMES program from April 2004 to March 2008. The GMES service, integrated and interoperable between regional seas and the global ocean, also started to be developed in a precursor GMES FP5 EU project, MERSEA Strand-1, where four European regional seas (Arctic, Baltic, North Eastern Atlantic and Mediterranean) started to develop and implement common quality control protocols for ocean products (<http://strand1.mersea.eu.org/>).

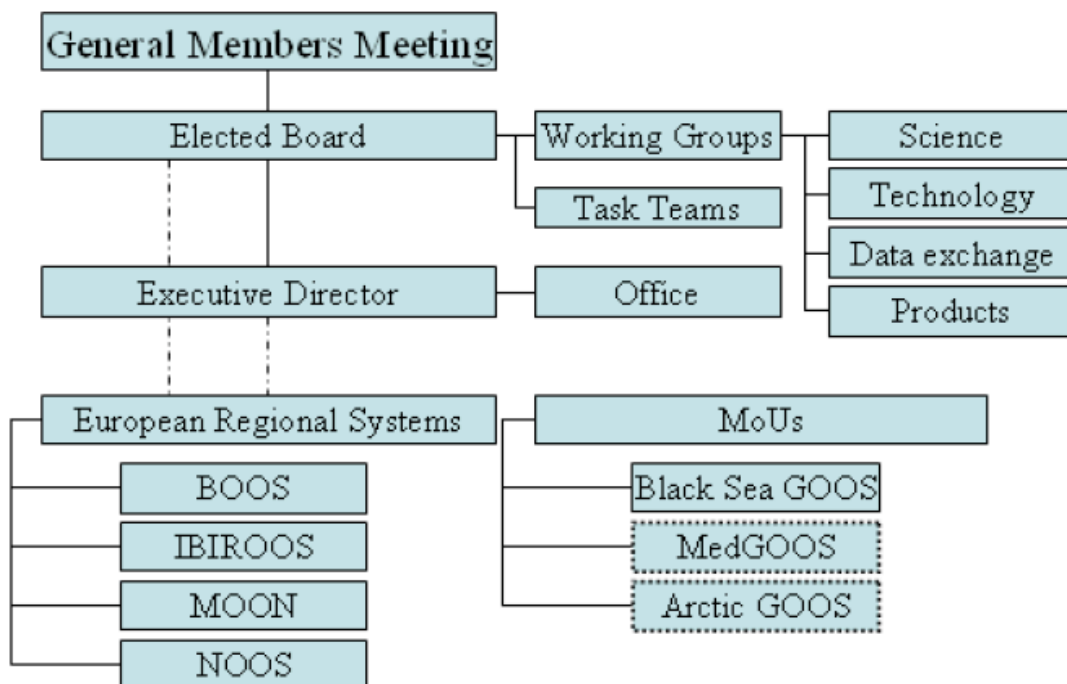


Figure 1.1. The structure of the EuroGOOS association and related European Regional Systems services.

The OO systems have been further developed and integrated within the MERSEA Integrated project and then in the GMES follow-up project BOSS4GMES (2006-2009). Finally, the final step towards operations of the Marine Core Service (MCS) will be achieved in the MyOcean project (2009-2012).

With the GMES program and its Marine Core Service (MCS) fast-track, the European community is consolidating past efforts in pre-operational ocean monitoring and forecasting capacity in Europe through precursors run in FP6 MERSEA and BOSS4GMES or GSE MARCOAST and POLARVIEW.

The MyOcean consortium has started to deliver a pan-European MCS product and service portfolio through a robust and optimized ocean monitoring and forecasting core infrastructure. The validation process planned through a 3-year experience will enable to organize the user-driven service up to pre-operational phase with propositions addressing the MCS long-term roadmap.

Thanks to the existing community and efficient networks like EuroGOOS, MyOcean is providing core information on the ocean in all areas of benefit – identified by the MCS Implementation Group – to key categories of users: EU agencies (EEA and EMSA), member state service providers (met offices, coast guards), intergovernmental bodies or their members (OSPAR, HELCOM).

The global ocean and the European seas will be monitored with an eddy-resolving capacity based on assimilation of space and in-situ data into 3D models representing the physical state, ice and the ecosystems of the ocean; in the past (25 years), in real time and in the future (1-2 weeks). The high-quality products will rely on the aggregation of European modelling tools and the scientific methods will be produced through a strong cross-fertilization between operational and research communities. Observations, model-based data, and added-value products will be generated – and enhanced by dedicated expertise – by the following production units (Figure 1.2):

- Six Thematic Assembly Centres, each of them dealing with a specific set of observation data: sea level, ocean colour, sea surface temperature, sea ice, in-situ data and wind data,
- Seven Monitoring and Forecasting Centres to serve the global ocean, the Arctic area, the Baltic Sea, the Atlantic North-West shelves area, the Atlantic Iberian-Biscay-Ireland area, the Mediterranean Sea and the Black Sea.

Intermediate and final users will discover, view and get the products by means of a central web desk, a central re-active manned service desk and experts within regional services. Routine/bulk delivery, expert forecaster interpretation, human support for emergencies, response to specific queries (non-emergency) and user training will be the proposed types of service.

In addition, the MyOcean consortium commits to provide users with operational and qualified products and services. Therefore, certifications throughout the whole operational chains will be undertaken by a Quality Management System with dedicated key performance indicators and metrics. The operational commitments – in compliance with users' requirements – are defined in contractual agreements between data suppliers, production units and users at the levels of

procurement, production and service, respectively. The work described in chapter 2 will be part of a Service Level Agreement between MyOcean and EEA and will represent an example of operational commitment.

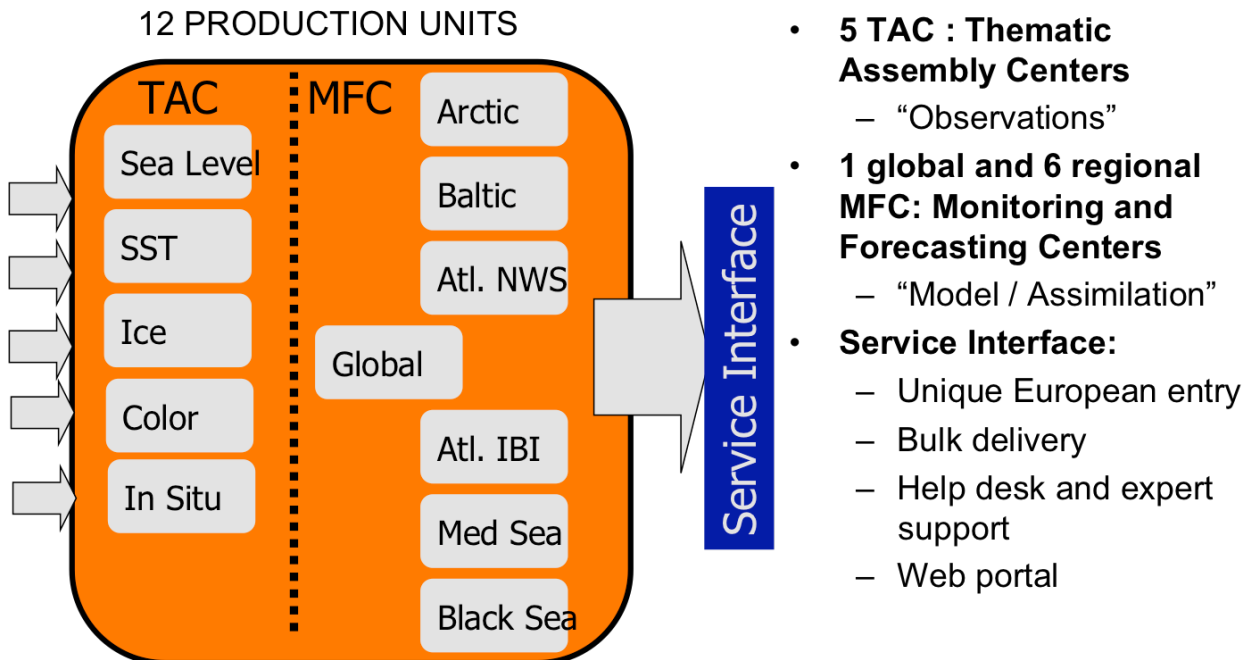


Figure 1.2. The MyOcean Production Units.

Several operational downstream services can be implemented with an operational capability in oil spill pollution monitoring and forecasting, climate change state monitoring and ecosystem health assessment.

As mentioned above in the Mediterranean Sea OO is organized in the Mediterranean Operational Oceanography Network (MOON, <http://www.moon-oceanforecasting.eu>) that is an evolution of the EuroGOOS Mediterranean Task Team. It brings together marine research centers from the region to contribute to the planning and implementation of the operational ocean observing and forecasting system in the Mediterranean, promoting the development and optimization of the scientific base, the technology and the information system for operational oceanography, and targeting the GOOS goals to consolidate and expand the concerted monitoring and forecasting systems for Sustainable Development, Marine State Assessment and Risks Management. MOON is led by the Istituto Nazionale di Geofisica e Vulcanologia (Italy) and Mercator-Ocean (France).

At the national Italian level, Operational Oceanography is coordinated by the National Operational Oceanography Group (GNOO) (<http://gnoo.bo.ingv.it>) of Istituto Nazionale di Geofisica e

Vulcanologia. GNOO coordinates the Italian institutes that operate in OO fields and works to enforce the monitoring and forecasting systems of the Italian seas and develop their sustainability at the operational level.

1.5. Thesis objectives

The main objective of this thesis is to develop methodologies to utilize operational oceanography products for: 1) developing environmental and climate change indicators; 2) forecasting oil spill at sea and managing emergencies; 3) developing decision support systems for state of environment assessment.

The identified methodologies aim to facilitate the achievement of the standards planned by European Directives, the Barcelona Convention and the EU Maritime Policy. This thesis will develop application examples for each objective mentioned above.

The thesis is organized as described in the following part of this paragraph. The second chapter defines the methodology for identifying and implementing indicators for climate change state assessment (see paragraph 2.3) and for pan-European eutrophication monitoring (see paragraph 2.4). The third chapter contains the examples related to the usage of operational oceanography products for oil spill monitoring and forecasting: the first example is dedicated to the hindcast of oil spill pollution during the Lebanon Crisis occurred in July-August 2006 (see paragraph 3.1) while the second example (see paragraph 3.2) consists of the description of the MOON-REMPEC agreement and the Emergency Response Office (ERO) activities. ERO has been created to support REMPEC to manage emergencies and the second example of chapter 3 consists in the description of ERO contribution to the OSCAR-MED operation (Coordinated Surveillance Operation in the Western Mediterranean). The work related to the ERO and the operational activities described in the context of OSCAR-MED have been carried in close collaboration with REMPEC to serve the implementation of the Barcelona Convention. The fourth chapter describes how, through the strong involvement of key user such as ARPA-DAPHNE, we have designed and implemented a Decision Support System, namely ADRI-DSS, for state of environment assessment in the northern Adriatic Sea.

2. Identification, definition and implementation of environmental and climate indicators

2.1. Introduction

Operational Oceanography (OO) represents a knowledge base service for the protection and management of marine areas, and OO systems are currently in transition from research to sustainable operations. In this chapter the candidate reviews and discusses how such systems can be used to support and strengthen EEA indicator reporting and assessment of European regional seas. Indicators play a vital part in focusing and illuminating the significance of environmental change and the progress towards sustainable development. In consideration of the step-by-step approach in selection and development of indicators, the following five criteria are commonly used: clearly defined, linked to policies, easy to understand and interpret (scientifically reliable and significant), limited in number and based on acknowledged (official) and accessible data.

OO systems can profoundly broaden the way our marine environment is observed and known. We now have at our disposal observations, data, analyses, forecasts and hindcasts in four dimensions (space and time) at unprecedented resolution and coherence. Work is needed to distil this wealth of information into summary indicators fit for EEA purposes, but the generic databases are in place at a pan-European level. Prior to the adoption of the Marine Strategy Framework Directive (MSFD), the European Marine Monitoring and Assessment (EMMA) Working Group agreed to develop a common pan-European set of marine indicators to assess issues of pan-European relevance, which should also be able to reflect regional specificities (see Emblow and Gelabert, 2008). Part of this set would be based on existing regional sea and EEA indicators for the determinants in MSFD Annex III (characteristics, pressures and impacts), which has been taken as a guideline for wider marine assessments. The EEA has been contributing to the fulfilment of several objectives of the EMMA roadmap. It supports the implementation of the European Marine Strategy (EMS) and the MSFD, and will further develop its own pan-European marine assessments.

EMMA noted that the EEA would lead such an analysis in two phases. The first phase would be during the second halves of 2007 and 2008 (Priority 1) and the second one afterwards (Priority 2). Analysis will be performed as follows:

- Priority 1.1: ‘temperature’; ‘Chlorophyll-a’; ‘fish abundance’; ‘nutrient concentrations’; ‘hazardous substances in biota’; ‘oil slicks’; ‘input of nutrients’ (riverine and direct discharges); and ‘atmospheric deposition’ of non-toxic contaminants).
- Priority 1.2: for other ‘physical and chemical’ determinants’ (e.g. ‘currents’, ‘water exchange’, ‘salinity’, and ‘bathymetry’ as well as ‘water transparency’).

This chapter proposes a role for the operational systems developed within Marine Core Services (MCS) towards the development of indicators to fulfil EEA objectives.

MCS can contribute to the DPSIR (Driving Forces-Pressures-State-Impacts-Responses) assessment framework mainly by assembling information about the State, Pressure and Impact parts of the cycle.

Insofar as the State element is concerned, MCS will advance the European capacity to release high quality real-time and delayed mode information on:

- a) Temporal and spatial variability of the physical state variables describing the ocean, i.e., temperature, salinity, sea level, wind and waves, currents in the whole water column;
- b) Temporal and spatial variability of sea ice;
- c) Temporal and spatial variability of suspended materials in the water, from biologically active tracers (Chlorophyll), to sediments and other non photosynthetic materials (CDOM) and pollution (oil spills)

For Pressure and Impact, the MCS will help to:

- a) Develop new indicators of higher quality, uniformly computed for all the European seas based upon the State variables described above
- b) Manage crises and increase awareness of episodic events that affect the state of the marine environment
- c) Provide context for in-situ sampling (adaptive or optimal sampling).

Regarding the specific needs of the proposed Marine Strategy Directive, the GMES MCS can contribute to three marine thematic assessments:

- a) Climate Change
- b) Eutrophication
- c) Pollution (with emphasis on oil spills).

The present chapter describes the Spatial Data Theme Elements (SDTEs) produced by OO services that contribute to the development of indicators prioritized within EMMA and dedicated to the evaluation of the state of climate change and eutrophication. SDTEs are defined following the

INSPIRE Directive² and are ocean state variables with specified spatial and temporal resolution. The SDTEs listed in this chapter are aimed at contributing to the development of (as far as is possible) pan-European uniform coverage indicators. Regional differences are considered in order to achieve maximum accuracy in the SDTEs and regional ecosystem characteristics.

This chapter presents the work done in developing indicators for two advanced SDTEs, namely Temperature and Chl-a. Temperature-derived indicators, i.e., the Sea Surface Temperature indicator, have been included in the most recent EEA climate change and State of the Environment reports:

- Impacts of Europe's changing climate: 2008 indicator-based assessment (http://www.eea.europa.eu/publications/eea_report_2008_4)
- 2010 EEA State of the Environment Report (<http://soer2010.ew.eea.europa.eu/>)

The Chl-a trend indicator has been included in the 2010 EEA State of the Environment Report (<http://soer2010.ew.eea.europa.eu/>)

Developed indicators are used by EEA, and to facilitate this utilization a dedicated service will be established between EEA and MyOcean³ Project (principal data and indicator provider).

Paragraph 2.2 briefly describes the SDTEs that will contribute to the indicators listed in Priority 1.1 (Temperature, Chlorophyll-a) and Priority 1.2 (Current, Water Exchange, Salinity and Water Transparency). Paragraph 2.3 describes the Temperature SDTE and the indicators that have been derived for EEA. Paragraph 2.4 describes the Chl-a SDTE and the indicators that have been derived for EEA.

2.2. Spatial Data Theme Elements

Referring to SDTEs to describe marine state variables at specified space and time resolutions we should help to distinguish between SDTEs such as 'Temperature' and the derived set of indicators such as temperature anomaly time series, heat content anomaly trends, etc.

For each SDTE the data availability and products from the GMES MCS are presented (Table 2.1= and the candidate then discusses the possibility to develop indicators from the SDTE for two of the SDTEs that may contribute to the development of the Indicators Proposed by EMMA in Priority 1.1 (Temperature, Chlorophyll-a).

² <http://inspire.jrc.ec.europa.eu/> and <http://eur-lex.europa.eu/JOHtml.do?uri=OJ:L:2007:108:SOM:EN:HTML>

³ <http://www.myocean.eu.org/>

The Temperature and Chlorophyll-a (Chl-a) SDTEs appear the most mature and only for these SDTEs is an indicator development test phase shown in this chapter. In particular, the OO Chl-a SDTE, deduced from satellite data, will be able to contribute to the further development of the CSI023 Chl-a indicator.

Sea Level and Ice SDTEs are also well developed and climate indicators have been developed but they are not shown in this work. Marine Current and Salinity SDTEs appear less ready for the development of new indicators at a pan-European level because their correlation with environmental aspects is not yet well recognized in all European marine areas. The Transparency SDTE appears mature, but more effort should be put into relating the indicator to in-situ measurements.

Table 2.1 summarizes the state of development of the SDTEs (Chl-a and SST only) partially analysed in this chapter.

Spatial Data Theme Element (SDTE)	Suitability as future indicator ¹	Spatial coverage ²	Availability ⁵	Source ⁶	Accuracy ⁴	Temporal coverage ³	Priority ranking ⁷
Temperature	High	All	Yes	IO	High	1871 - present	2
				M	High	2000-present	
				EO	High	1985-present	
Chlorophyll-a	High	All	Yes	EO	High	1980-1986 1997-present	1
Marine Currents	Moderate	NE Atlantic, North Sea, Baltic Sea, Mediterranean	2009	M	Moderate	2000-present	6
Salinity	Moderate	NE Atlantic, North Sea, Baltic Sea, Mediterranean	Yes	M	High	2000-present	7
				IO	High	1900-present	
Transparency	High	All	2009	SO	Moderate	1997-present	3
Sea level	High	All	Yes	IO	High	1900-present	4
				M		2000-present	
				EO		1992-present	
Ice	High	Arctic Ocean Baltic Sea	Yes	M, EO	High	1979-present	5

Table 2.1 Spatial Data Theme Element summary table.

- 1) A subjective scale of low, moderate or high has been used
- 2) Seas: Global, NE Atlantic, North Sea, Baltic Sea, Mediterranean, Black Sea, and Arctic Ocean.
- 3) The longest period covered is mentioned

- 4) A subjective scale of low, moderate or high has been used
- 5) 'Yes' has been used, or alternatively the year when product will start has been indicated
- 6) M means Model, IO means In-situ Observations, EO means Earth Observation from Satellite
- 7) SDTEs have been prioritized in the order 1-7.

2.3. Temperature SDTE and related indicators

The SDTE presented in this paragraph is the temperature of the ocean estimated from satellite, in-situ and model datasets by the OO services. The description of the Temperature SDTE for the sea surface temperature (SST) is separated from the water column temperature. This subdivision reflects the different sources (Satellite for SST and in-situ and models for deeper temperatures) and also the fact that the EEA is already using an SST indicator in the climate change reports, whereas it is not using any indicator on deeper temperatures.

The EEA has since 2008 started to include the SST indicator in its Climate and State of the Environment reports:

- Impacts of Europe's changing climate: 2008 indicator-based assessment (http://www.eea.europa.eu/publications/eea_report_2008_4) (EEA, 2008)
- 2010 EEA State of the Environment Report (<http://soer2010.ew.eea.europa.eu/>)

In the 2008 and in the 2010 reports, the SST indicator has been improved using OO high-resolution remote-sensing regional products in the Mediterranean, Baltic and North Seas.

Even if there are no specific policies in place that specifically target SST, the EEA is using these indicators because SST is relevant for monitoring climate change because it partly reflects the heat content of the ocean and because long time series are available. It thus reflects the speed of global warming and the extent to which global warming has impacted the ocean. In the EEA context and EEA reports SST indicators have been used to answer the relevant policy questions:

- 1) *Is the sea surface temperature of the global and European seas increasing compared to the long-term average?*
- 2) *What is the spatial distribution of the rate of change in European seas?*

2.3.1. Spatial Data Theme Element relevance

SST is supposed to indicate the temperature of the first metres of the water column. SST is a relevant SDTE because it influences air-sea interactions, heat fluxes and gas exchange. Moreover, SST influences metabolic rates of phytoplankton and bacteria in the marine environment. SST can produce, and is related to, changes in atmospheric circulation and precipitation regimes, air temperature on land, etc. These changes are at the start of a chain of events that impacts human

health and activities such as energy demand, agricultural yields, and ecosystem services. The SST anomalies track global change due to greenhouse-gas warming.

SST meaning is variable with seasons: during winter, over most of the European seas, SST is a good approximation of the whole water column temperature, while during summer SST mainly describes the temperature of the first few metres or less of the water column. Two main problems are connected with the SST indicator:

- 1) During summer the SST is only the temperature of the first few metres or less of the water column;
- 2) SST measured from satellite could be affected by large errors due to clouds and surface skin effects. The usage of satellite multisensor SST, a combination of infrared and microwave radiometers, is now recommended to partially solve cloud contamination.

High-accuracy water column temperature SDTE is produced by in-situ observing systems and hydrodynamic models. The analysis of the deep ocean temperature changes will allow estimating the net ocean heat content changes that are very closely tied to the net radiative imbalance of the planet since the ocean component of the climate system has by far the biggest heat capacity. Deep ocean temperatures are thus a key indicator of the system response to changes in CO₂ and the other radiative forcings. Evaluating the impact of global warming in the oceans and European seas is then connected to the vertical integral of temperature in the water column, the so-called heat content. Surplus heat arriving at the air-sea interface produces warming in the entire water column with significant time delays, of the order of weeks, months and years.

Subsurface temperature increase will have a direct impact on the thermal expansion of the ocean and hence lead to sea-level rise unless it is compensated by a salinity increase that keeps the density unchanged. The temperature has a direct effect on the biochemical state of the ocean, in particular on primary and higher trophic level productivity. Temperature stratification is directly related to anoxic events that might be produced in stratified eutrophic shelf and coastal areas.

2.3.2. Description of the SDTE OO derived products

2.3.2.1. Present SST products, databases

SST OO products have been used in the 2008 EEA climate change report and in the EEA State of the Environment report 2010 and are:

1) The Medspiration products, developed by a European initiative to combine data measured independently by different satellite systems into a set of data products that represent the best measure of SST;

2) The MyOcean and EuroGOOS regional seas Task Team products from the global to the regional scale. These SST products have different resolution in different European seas and integrate the satellite SST with the whole water column temperature.

OO is the framework for the future development of high-accuracy and high-resolution SST data products (the so-called L4 products) needed to be included in the SST indicator related to changes in the past 120 years. Regional high-resolution datasets are now available for the North Sea, Baltic Sea, North Atlantic and Mediterranean Sea.

Examples of available SST L4 OO products are:

a Global products:

- CERSAT-GLOB-ODYSSEA-SST-NRT-OBS (Geographic coverage: -90°S-90°N, 180°W-180°E; Temporal coverage: 1990-03-01 ongoing; Spatial resolution 0.1°-0.5°; Producer: IFREMER/CERSAT, FR);
- OSTIA: (Geographic coverage: -90°S-90°N, 180°W-180°E; Temporal coverage: 2006-04-01 ongoing; Spatial resolution 1/20°; Producer: UK METOFFICE, UK)

b Atlantic products (Geographic coverage: 70°S-90°N, 100°W-45°E; Temporal coverage: 2005-02-01 ongoing; Spatial resolution: 1-25 km; Producer: CMS, MÉTÉOFRANCE, FR)

c North Sea product: (Temporal coverage: 1969 ongoing; Spatial resolution 20 km; Producer: BHS, DE)

d Mediterranean products:

d.1 GOS-MED-L4-SST-DT_{v1}-OBS is a multisensor product (AVHRR, ATS, Severi, Aqua and Terra) (Temporal coverage: 2006 ongoing; Spatial resolution: 6 km; Producer: CNR-ISAC, IT),

d.2 Med-Re-Analysis (RA_{v0}): is a reanalysis of AVHRR Pathfinder SST time series from 1985 to 2007 for the whole Mediterranean Sea This analysis has been conducted by CNR-ISAC in collaboration with the ENEA.

d.3 MEDSPIRATION-MED-SST-OBS (Temporal coverage: 2005 ongoing; Spatial resolution: 2 km; Producer: MEDSPIRATION, ESA),

e Baltic Sea product (Temporal coverage 1990 ongoing; Spatial resolution 20 km; Producer: BHS, DE).

Most of the products mentioned above are also part of the Global High-Resolution Sea Surface Temperature (SST) Pilot Project (GHRSSST-PP). Most of these products are now available through MyOcean.

2.3.2.2. Present Subsurface ocean temperature products (in-situ and model data)

OO produces an estimate of the whole water column temperature from in-situ and hydrodynamic models, merged with satellite and in-situ data (analyses). The OO products are:

- Temperature analyses and re-analyses;
- Observational maps from in-situ temperature.

The temperature analyses/re-analyses and observational maps have different space-time resolutions from the global to the European regional seas. The observational maps are now possible because of the large coordinated observational programmes such as ARGO, VOS (Voluntary Observing Ships) and SOOP (Ship Of Opportunity Programme) that collect profiles of temperature and salinity data everywhere. 3000 ARGO floats, giving temperature and salinity profiles from the surface to 1000-2000 metres, have been launched in the Global Ocean and the Arctic, Mediterranean and Black Seas, giving quality-controlled temperature profiles from the surface to about 2000 m. They are available in near-real time from the Coriolis Data Centre or the regional EuroGOOS data centres. SOOP and VOS provide near-real-time XBT temperature profiles. Other temperature observations from moored or drifting buoys and research vessels are also available in near-real time.

Long timeseries of model re-analyses are and will be available through the MyOcean project. Model products are available through the MyOcean project for the Global Ocean, Arctic Ocean, Mediterranean Sea, North East Atlantic and Black Sea.

Model validation and verification is one of the fundamental steps in delivering reliable products. As far as the Temperature SDTE from model analyses is concerned, the accuracy varies from few tens °C in the deep part of the water column up to 1°C in the thermocline and the surface. Moreover, the error presents a seasonal variability with maximum values during summer time. The differences along the water column are due to the higher variability of the upper part of the ocean compared to the deeper one. The highest values of the error during the summer are mainly due to the model's inaccuracy in representing the depth of the seasonal thermocline.

2.3.3. Indicators derived from the temperature SDTE

Different indicators can be derived from the temperature SDTE. A first set is related to climate change and monitors the SST with the longest available datasets. It will be possible to develop

additional indicators that consider the whole water column temperature and could be indicative of long-term effects and extreme events. The latter are very relevant for ecosystems dynamics and possible stresses.

Using the temperature SDTE from OO products, several indicators can be defined for the Global Ocean and each European sea:

a) SST indicators:

- Annual basin average SST anomalies (1871-present);
- SST anomaly linear trends of the period (1871-present) and maps showing the spatial distribution of SST linear trends;
- Real-time SST anomaly maps (timescale from daily to monthly);

b) Deep ocean temperature indicators

- Annual basin average Heat Content (HC) anomalies (1985-present);
- HC linear trends and maps of the spatial distribution of HC linear trends (1985-present);
- Real-time temperature anomaly profiles in the water column;
- Mixed-layer depth anomaly time series.

Only the SST indicators for climate change state monitoring (SST anomaly timeseries and SST trends) will be presented in this chapter since they are the ones now accepted by the EEA. SST indicators for climate change monitoring are presented, as they have been prepared with the collaboration of the EEA in the indicator fact sheet. The SST indicator fact sheet represents an effort to present the scientific results and products underlining the following aspects:

- ‘Key messages’ synthesize the main relevant messages useful for sending a clear message to the public
- ‘Rationale’ explains the relevance of the indicator in the context of climate change
- ‘Policy Context’ identifies the policy implementations, if any, to which the indicator is contributing
- ‘Policy questions’ reflect the important questions that are clarified by using the indicator. By answering these questions, the main results are presented.
- ‘Methodology’ describes the calculations done to get to the results presented by the indicator. This paragraph of the fact sheet is also designed to describe the technical aspects

of the indicator preparation and together with the paragraph on ‘data sources’ would help for any reproduction of calculations by interested parties.

- ‘Data specification sources’ describe where the data have been collected and who are the data providers.
- ‘Time series length’: for each of the different data typology the time extensions of the time series is described
- ‘Evaluate the data situation’: this is the paragraph that presents different aspects of the data used for the indicator calculation, such as:
 - Geographical coverage: describe the area covered by the data used such as which European seas, and whether the data are available at the Global Ocean level.
 - Expected source and references: this is the paragraph in which the list of experts is mentioned, these scientists are those considered experts in the data and potential support for report preparation by the EEA.
 - Uncertainties: this important paragraph highlights the existing uncertainties of the datasets and of the indicator itself.

The SST indicator fact sheet is updated every year: the timeseries are updated and the contents are revised on the basis of the latest scientific results.

The following SST indicator products are presented in the indicator fact sheet and have been included in EEA reports (i.e. EEA, 2008):

- 1) Annual and basin average SST anomalies (1871-2008) (see Figure 2.1),
- 2) Linear trends of the last 136 years and of the last 24 years,
- 3) A map showing the spatial distribution of linear trends of the last 24 years (1985-2008) for the European seas (see Figure 2.2).

The SST indicators presented in this paragraph show that SST in European seas is increasing more rapidly than in the global oceans (Figure 2.1). The rate of increase is higher in the northern European seas and lower in the Mediterranean Sea (EEA, 2008). The rate of increase in sea surface temperature in all European seas during the past 25 years (1984-2008) has been about 10 times faster than the average rate of increase during the past century (see also EEA, 2008). The rate of increase observed in the past 25 years is larger than in any previous 25-year period (EEA, 2008). The SST changes in the European regional seas are stronger than in the global oceans (Table 2.2). The strongest trend in the last 25 years is in the Baltic Sea and the North Sea, while the rates are lower in the Black Sea and Mediterranean Sea. The regional seas experienced warming rates that

are up to six times larger than those in the global oceans in the past 25 years.

Sea	1871–2008 annual rate °C/year (past 138 years)	1984–2008 annual rate °C/year (past 25 years)
Global ocean	0.004	0.008
North Atlantic Ocean	0.003	0.030
Baltic Sea	0.006	0.064
North Sea	0.006	0.049
Mediterranean Sea	0.004	0.039
Black Sea	0.003	0.044

Table 2.2 Summary of sea surface temperature changes in the global ocean and the four European regional seas during the last 138 years (central column) and during the last 25 years (right column).

These changes have not been observed in any other 25-year period since systematic observations started more than a century ago (EEA, 2008). The spatial distribution of trend over the European seas shows that the positive temperature trend is more pronounced in the North Sea, Baltic Sea, the area south of the Denmark Strait, the eastern part of the Mediterranean, and the Black Sea (figure 2.2). Absolute maxima are located in the North Atlantic around 50°N, in the North Sea and Baltic Sea, with values over 0.06–0.07 °C/year. Negative trends are detected in the Greenland Sea. Here, the estimates also depend on the extent of the ice (EEA, 2008).

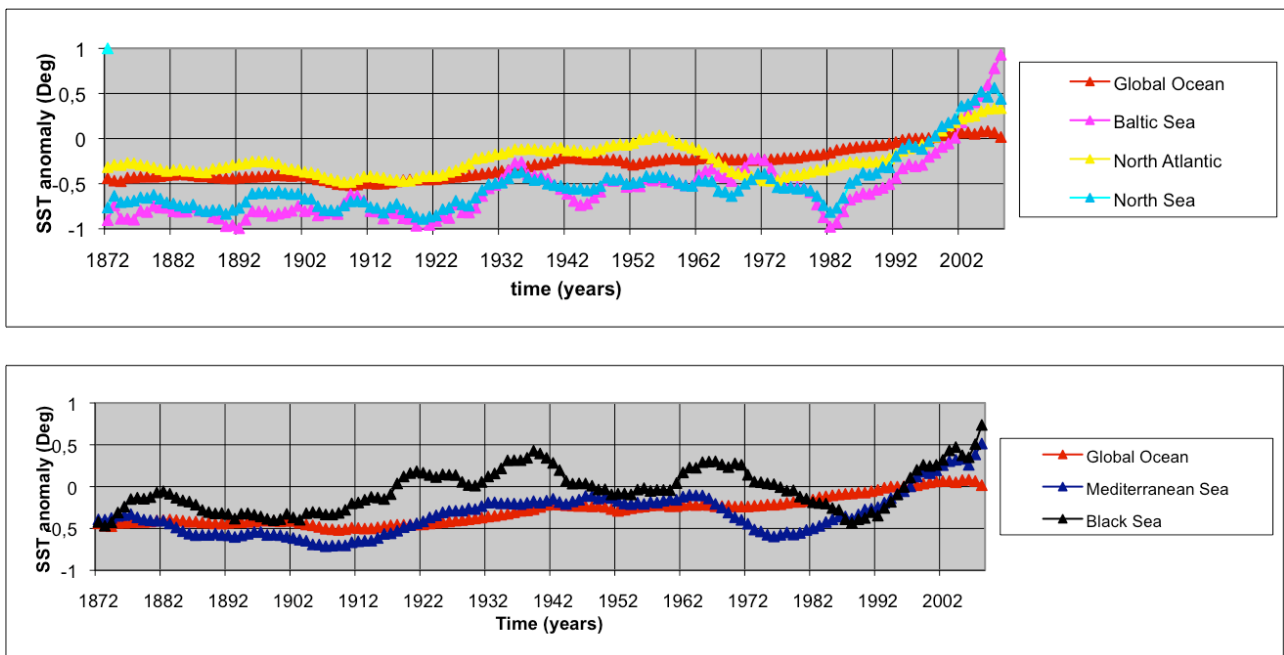


Figure 2.1. Annual and basin-average SST anomalies:

- For the Global Ocean (red, upper and lower panels) for the period 1872–2008 relative to the 1985–2008 mean from the Hadley Centre SST dataset;
- For the Mediterranean Sea (blue, lower panel) for the period 1985–2008 relative to the 1985–2008 mean from the MOON dataset and for the period 1872–1984 relative to the 1985–2008 mean from the Hadley Centre SST dataset,
- For the Black Sea (black, lower panel) for the period 1872–2008 relative to the 1985–2008 mean from the Hadley Centre SST dataset;

- For the North Sea (cyan, upper panel) for the period 1969-2008 relative to the 1985-2008 mean from the BSH dataset and for the period 1872-1968 relative to 1985-2008 mean from the HADSST1 dataset;
- For the North Atlantic (Lat: 30N-70N; Lon: 40W-0E) (yellow, upper panel) for the period 1872-2008 relative to the 1985-2008 mean from the HADSST1 dataset;
- For the Baltic Sea (magenta upper panel) for the period 1990-2008 relative to the 1990-2008 mean from the BSH dataset and for the period 1872-1989 relative to the 1985-2008 mean from the HADISST1 dataset.

The SST time series presented in Figure 2.1 present the annual average SST anomalies with respect to the 1985-2008 mean. SST anomalies have been calculated from the four different datasets as presented in Table 2.2 for the different ocean domains presented in Table 2.3. The time series of the anomalies have been smoothed with a running mean filter with a window of 11 years.

Dataset	Spatial resolution	Temporal resolution	Time frame used	Access to data
HADSST	1°x1° global	monthly	1871-2008	http://hadobs.metoffice.com/hadisst/data/download.html
BSH	20km	weekly	Baltic 1990-2008 North Sea 1969-2008	http://www.bsh.de/en/Marine_data/Observations/Sea_surface_temperatures/index.jsp dataset have been provided by BOOS Partner BSh, (contact Peter Loewe peter.loewe@bsh.de)
MOON	1/16°x1/16°	daily	1985-2008	http://gos.ifa.rm.cnr.it/index.php?id=407 The dataset is produced by MOON partner CNR-ISAC. Dataset have been provided by MOON Partner ENEA, (contact Salvatore Marullo salvatore.marullo@enea.it)

Table 2.3. Datasets used in the calculation of the SST anomaly indicators (Figure 2.1).

Region	Lon	lat
Global Ocean	0E-360E	50S-90N
North Atlantic	50W-0E	30N-80N
Black Sea	28E-43E	40N-49N
Mediterranean	6W-39E	30N-47N
North Sea	5W-10E	51N-61N
Baltic Sea	9E-31E	53N-68N

Table 2.4. Definition of the domains of the regions used in the calculation SST anomaly indicators (Figure 2.1)

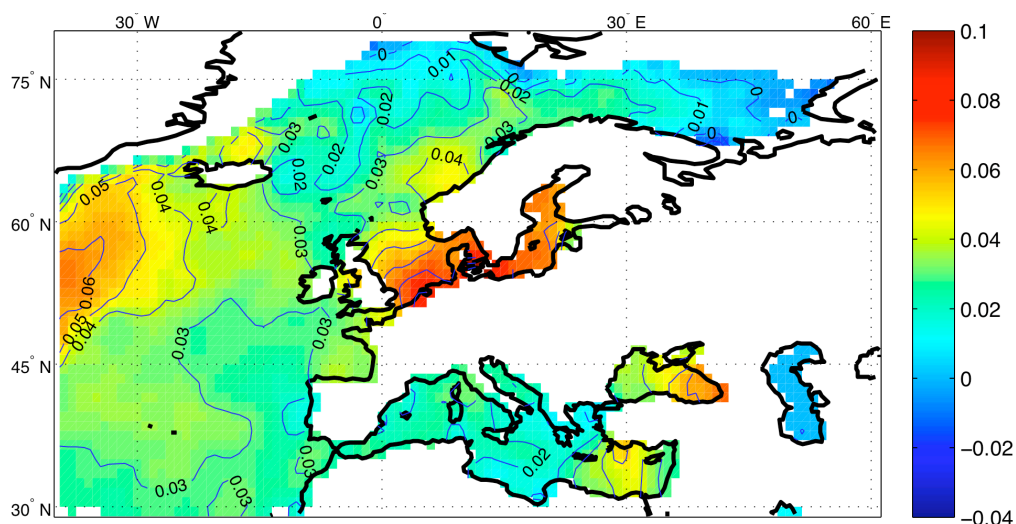


Figure 2.2. Spatial distribution of linear trends of the past 24 years (1985-2008) for the European seas as calculated from HADISST1 dataset. The units are °C/yr.

The SST trend map presented in Figure 2.2 describes the SST trends for the European Seas over the period from January 1985 to December 2008. Trends have been calculated from HADSST1 dataset. The dataset is available at the following address: <http://hadobs.metoffice.com/hadisst/data/download.html>.

SST trend maps have been masked for the region where ice coverage was higher than 20% of the seawater. To mask this region the sea ice dataset from the Hadley Centre has been used: <http://hadobs.metoffice.com/hadisst/data/download.html>.

2.4. Chl-a SDTE and derived indicators

The SDTE from OO presented in this paragraph is Chlorophyll-a (Chl-a) estimated from satellite data. The present EEA indicator related to Chl-a is CSI 023 (Chlorophyll in transitional, coastal and marine waters) estimated from in-situ data. A description of the CSI 023 indicator is given on the following website:

http://themes.eea.europa.eu/IMS/ISpecs/ISpecification20041007132031/IAssessment1116504836843/view_content

Section 2.4.1 describes Chl-a's relevance for environmental monitoring and Section 2.4.2 overviews the different products that can be derived from this SDTE. Section 2.4.3 focuses on the calculation of a new indicator from OO Chl-a SDTE to complement the existing CSI 023.

The second indicator is called coastal water extension and is presented in Section 2.4.4.

2.4.1. Chl-a SDTE relevance

Measurements of the water-leaving radiance through satellite radiometers in the visible range (ocean colour remote sensing) can be used nowadays to determine the Chl-a concentration, which is an indicator of phytoplankton biomass and can be related to primary production. Chl-a is an indicator of algal photosynthetic activity and is thus related to carbon synthesis by living marine organisms. Chl-a can now be estimated from satellite radiometers in the visible range at high spatial and temporal resolutions (daily and 250 metres horizontal resolution). Ocean colour satellites available now are SeaWiFS, MERIS-Envisat and MODIS-AQUA: the future Sentinel-3 GMES satellite will also have an ocean colour sensor ensuring continuous monitoring for the period 1997-2030. The first ocean colour sensor was CZCS, working approximately from 1980 to 1986; nothing was then in operation until 1997, when SeaWiFS started ocean colour monitoring again.

The in-situ phytoplankton monitoring systems, working on in-situ water samples, are only local and mainly coastal, thus providing a very accurate measure of Chl-a but at low temporal and spatial resolutions. On the contrary, Chl-a estimated by satellites covers vast areas at a daily temporal resolution, but the accuracy is lower.

The estimate of Chl-a from ocean colour is an integral over the water depth corresponding to the e-folding scale of light in the water. The ocean colour transformation algorithms have been calibrated with in-situ data at a global scale and are thought to be regionally dependent: the algorithm developed for the Mediterranean Sea has been specifically calibrated on datasets acquired in the Mediterranean Sea. Oceanic waters can be classified into Case 1 or Case 2 waters, (Morel and Prieur, 1977; Gordon and Morel, 1983; Prieur and Sathyendranath, 1981). By definition, Case 1 waters are those waters in which phytoplankton (with their accompanying and covarying retinue of other biological origin material) are the principal agents responsible for variations in optical properties of the water. On the other hand, Case 2 waters are influenced not just by phytoplankton and related biological particles, but also by other substances that vary independently of phytoplankton, notably inorganic particles in suspension and yellow substances. This classification implies that all the optical properties of Case 1 waters can be modelled as a function of Chlorophyll-a concentration. The simplicity of single-variable models has to be abandoned when dealing with Case 2 waters, since at least three relevant quantities (phytoplankton, suspended material and yellow substances, and perhaps even bottom reflectance) can vary independently of each other and specific algorithms should be used.

In shelf and coastal waters, Case 2 waters, suspended inorganic matter and yellow substances (coloured organic dissolved matter, CDOM) significantly influence the water-leaving radiance

making the retrieval of Chl-a from satellites less accurate. However, the CDOM information is important and should be used in the future as a new indicator of river influence in coastal areas.

Time series of satellite Chl-a averaged on a certain area can indicate the timing of the blooms that show the annually recurring life cycle of major phytoplankton species, and provide a sensitive indicator of climate change (Edwards and Richardson, 2004).

2.4.2. Description of the Chl-a SDTE derived products

OO provides real time products of Chl-a from satellites at high accuracy since ocean colour regional algorithms have been developed. Part of the OO products consists of re-analyses done with regionally calibrated algorithms that provide a consistent monitoring of phytoplankton biomass in European regional seas from 1997 onwards.

Ocean colour products are available at a global scale and specific regional products have been produced in the framework of OO. Example of OO ocean colour products are listed below:

Global products (from JRC): Geographic coverage -90°N-90°N, 180°W-180°E

- Product JRC-GLOBAL-SEAWIFSCHL-OBS: Temporal resolution (availability): Monthly- with 3 months' delay - Temporal coverage: 1997-09-ongoing - Spatial resolution: 9 km. Sensor: SeaWiFS.
- Product JRC-GLOBAL-MODISCHL-OBS: Temporal resolution (availability): Monthly- with 2 months' delay - Temporal coverage: 2002/07-ongoing - Spatial resolution: 9 km. Sensor: MODIS-AQUA.

Mediterranean products (from CNR-ISAC): Geographic coverage 30°N-46°N, 6.0°W-36.5°E –

- Product Mediterranean reanalysis: Temporal resolution (availability): daily - Temporal coverage: 1997-09 2006 - Spatial resolution: 1 km. Produced with specified Mediterranean algorithm. Sensor: SeaWiFS
- Product reanalysis: Temporal resolution (availability): daily and monthly- Temporal coverage: 2002-07-ongoing - Spatial resolution: 1 km. Produced with specified Mediterranean algorithm. Sensor: MODIS-AQUA

North Sea products (from PML):

- Product 1: Temporal resolution: daily – Spatial resolution; 1.1 km - Temporal coverage: 1997 - December 2004; - Sensor: SeaWiFS
- Product 2: Temporal resolution: daily and weekly. spatial resolution: 4.4 km – Temporal coverage: November 2005 - present day - Sensor: SeaWiFS
- Product 3: temporal resolution: daily and weekly – temporal coverage: 2002 - present day (produced with specifically calibrated algorithm) Sensor: MODIS-AQUA

European products (from JRC): Geographic coverage 80.0°N-10.0°N, 40°E-40°W - Temporal resolution (availability): Monthly - Temporal coverage: 1997-09 2006-09 - Spatial resolution 2 km produced with standard algorithm. Sensor: both MODIS-AQUA and SeaWiFS

2.4.3. Chl-a trend indicators derived from the Chl-a SDTE

The EEA would like to develop a method for using satellite-derived ocean colour products to complement the EEA CSI023 indicator of eutrophication, which is based on in-situ observations of Chlorophyll-a. To accomplish this, work was done to compare observations based on in-situ data to ones based on ocean colour, and to develop a method for calculating trends.

Ocean colour has a much higher spatial and temporal resolution than the in-situ observations. The ocean colour observations are, however, based on indirect measurements of the optical properties of the ocean, which are transformed to Chl-a using an appropriate algorithm. This algorithm can be either a global algorithm that reproduces the average global Chl-a concentrations well, or one that is adjusted to specific regional conditions.

The work done for the EEA has been based on a dataset readily available, through the product portfolio of JRC-MERSEA, Global Ocean JRC-SeaWiFS (Table 2.4), based on a global ocean algorithm calibrated on open ocean waters and a second dataset, Mediterranean CNR-SeaWiFS (Table 2.4), produced with a regional algorithm calibrated for the open ocean water of the Mediterranean Sea. The work will be continued using global and regional MyOcean products.

The work has been comprised of comparison between in-situ observations and ocean colour, and proposes a preliminary methodology for analysing trends comparable to the method EEA uses for their CSI23 indicator. The analysis has revealed the need for regional ocean colour products to be available to develop support of the EEA indicator and also that there is potential in a long-term trend analysis based on ocean colour because large-scale and in some cases even regional-scale changes appear to be captured by the satellite images. In order to build confidence in this analysis, it is however clear that it needs to be based on the best possible regional products, which at present are not available to the EEA.

2.4.3.1. Objectives

EEA is using an indicator based on in-situ Chlorophyll-a (Chl-a) trends to monitor eutrophication in the European seas, referred to as CSI023 in the EEA system. (For a complete overview on the indicator please refer to the following web site:

http://themes.eea.europa.eu/IMS/IMS/ISpecs/ISpecification20041007132031/full_spec).

CSI023 evaluates the trends of Chl-a for seasonal⁴ mean of Chl-a from in-situ collected samples, integrated in the first 10 metres of the water column. The objective of the CSI023 indicator is to demonstrate the effects of measures taken to reduce discharges of nitrogen and phosphate on coastal concentrations of Chl-a and it is thus an indicator of eutrophication.

The last assessment was done in 2009 and results are presented in terms of concentration of Chl-a in the European seas and trends from 1985 to 2004 and 2005.

A methodology to supplement the indicator with observations based on ocean colour from space has been developed, and this new indicator is called CSI023. Ocean colour products are widely available at daily time scales in all European coastal/shelf and open ocean waters and if compared to the in-situ observations they show a higher spatial coverage (i.e., 1km resolution) and higher temporal resolution (i.e., daily). Higher temporal resolution can be achieved in southern European regional seas due to lower cloud coverage if compared to the northern European seas.

The Sentinel-3 GMES satellite will also have an ocean colour sensor ensuring continuous monitoring for the period 1997-2030.

Finally, the trend estimates from an improved CSI023 have the potential to be more representative of the eutrophication state of European seas with uniform standards.

2.4.3.2. Methods

a) Data

Dataset name	Domain	Spatial resolution	Time frame and resolution	Algorithm	Reference to validation	Provider
Global Ocean JRC-SeaWiFS	Global Ocean	9x9 km	1998-2007 monthly	Global – OC4v4	O’Reilly, 2000	JRC
Mediterranean CNR-SeaWiFS	Mediterranean Sea and Black Sea	1x1 km	1998-2004 daily 2004-2008 monthly	Mediterranean – MEDOC4	Volpe, 2007	CNR-ISAC

Table 2.5. Overview of ocean colour data used in the calculation of Chl-a trends.

In this work we use two different SeaWiFS datasets (Table 2.4). The first is the global product obtained with standard SeaWiFS chlorophyll algorithm (OC4v4); the second is the Mediterranean product produced with the regional algorithm MedOC4 (Volpe *et al.*, 2007). The SeaWiFS products have been in general extensively validated (O’Reilly, 2000) with in-situ measurements showing that the standard SeaWiFS chlorophyll algorithm (OC4v4) generally performed well, but significantly over-estimated Chl-a where inorganic suspended sediment was present (Lavander *et al.*, 2004),

⁴ June to September for stations north of 59 degrees in the Baltic Sea (Gulf of Bothnia and Gulf of Finland) and from May to September for all other stations

Moreover, the Mediterranean algorithm and dataset too have been validated and MedOC4 results as the best algorithm matching the requirement of unbiased satellite chlorophyll estimates and improving the percentage of the satellite uncertainty (Volpe *et al.*, 2007). It is important to underline that both the global algorithm and the Mediterranean is calibrated for open ocean waters and not specifically for coastal waters, and therefore an overestimation of Chl-a concentration by the ocean colour products in the coastal zone is expected. The datasets and comparisons are summarized in Table 2.5.

Regional Sea	In-situ data	Ocean colour data/products	
		Name of the ocean colour dataset	Usability in specific regional sea
Baltic	In-situ station observations reported to EEA 1997-2007	Global Ocean JRC-SeaWiFS	Problems expected due to high levels of dissolved organic matter in the Baltic,
Mediterranean Sea	In-situ station observations reported to EEA 1997-2007	Global Ocean JRC-SeaWiFS	Problems expected due to the global algorithm used
North Sea	In-situ station observations reported to the EEA 1997-2007	Global Ocean JRC-SeaWiFS	Problems expected due to the global algorithm used
Mediterranean Sea	In-situ station observations reported to EEA 1997-2007	Mediterranean CNR-SeaWiFS	Better correlation expected due to the regional algorithm used

Table 2.6. Overview of data compared.

b) Validation of products

Our specific validation presented here is performed by comparing the ocean colour products with in situ ones with the objective of evaluating the capability of ocean colour products to estimate trends of Chl-a on with respect to the estimation performed using in situ products. This validation compare the Pan-European SeaWiFS dataset of Chl-a concentration with the in situ data made available by ICES that include also EIONET Chl-a data. Since we are mainly interested in investigating trends we need to use the longest available timeseries and therefore we decided to compare in situ and ocean colour data only at locations where at least 9 years of data are available. For both datasets data above 64 mg/m³ have been removed.

When using the Global Ocean JRC-SeaWiFS, since the data spatial resolution in 9km, to allow comparison between point observations (stations) and these ocean colour data, the in situ observations are averaged to a 9km grid.

The comparison between in-situ data and ocean colour is generally not so favourable for individual regional seas. Both the comparison of monthly and seasonally aggregated Chl-a values shows a poor correlation between in-situ and satellite observations. This result is attributed to the difficulty

of deriving two comparable datasets when the in-situ observations are based on point measurements and the ocean colour observations are average values in a 1 x 1 km grid in the Mediterranean Sea or a 9x9 km grid in all other areas. Furthermore, except for the Mediterranean, the ocean colour data set is based on a global algorithm, which is not suitable for water heavily influenced by river run-off such as the Baltic or the North Sea. Comparison of yearly summer means of Chl-a concentration shows that ocean colour concentrations tend to be higher than in-situ observations.

In the southern European seas, where high spatial resolution ocean colour data were available, trends of Chl-a are analysed in the coastal areas (Chl-a areas). Chl-a trends estimated with ocean colour show a large area with decreasing Chl-a concentrations in the Black Sea, in the Northern Adriatic Sea, and in the Skagerrak, whereas a large area with increasing trends is observed in the Bay of Biscay and in the Baltic Sea.

Different qualitative validations have been performed and are presented in Table 2.6.

Test # and variables compared	Aggregation level	Result of comparison
Test 1 Chl-a concentration	Summer mean and European seas (Figure 2.4, 2.5 and 2.6)	Good correlation ($R^2=0.6$) if the analysis is performed for all the available stations in the European seas (Fig 2.4), expected also because of the wide range of values observed on an EU scale. Low correlation ($R^2=0.3$) if the analysis is performed for Mediterranean Sea stations (Fig 2.5). Low correlation ($R^2=0.2$) if the analysis is performed for Baltic Sea stations (Fig 2.6)
Test 2 Chl-a concentration	Summer Mean for 2005 (Figure 2.7)	Relevant similarities but areas such as the Gulf of Finland and Botnian Bay are also highlighted, in which ocean colour seems to over estimate in situ Chl-a concentration
Test 3 Chl-a concentration	Basin and summer mean (Figures 2.8, 2.9, 2.10 and 2.11)	Monthly mean of Chl-a concentration in summer time estimated by ocean colour overestimates the in-situ measurements: Figures 2.8, 2.9, 2.10 and 2.11 show that trends are similar in the Mediterranean and Baltic Seas but not in the North Sea
Test 4 Chl-a concentration	5 days average concentration for Chl-a areas (Figure 2.12)	Daily Chl-a concentration values estimated by MedOC4 ocean colour products are well correlated with in-situ ones.
Test 5 Chl-a concentration	Daily values average concentration for Chl-a areas (Figure 2.13)	Daily Chl-a concentration values estimated by MedOC4 ocean colour products are well correlated with in-situ ones, but in some regions ocean colour products seems to underestimate in-situ concentrations during summer period
Test 6 CSI023	Yearly summer mean (Figures 2.14 and 2.15)	Trend slope of ocean colour is similar to in-situ estimated trends in several region such as the Italian seas, Kattegat and Southern Baltic Sea while ocean colour products seem to overestimate positive trends in the northern Baltic Sea.
Test 7 CSI023	Yearly summer mean (Figures 2.16)	Trend signs of ocean colour is similar to in-situ estimated trends but ocean colour products are not able to detect negative trends in the Tyrrhenian Sea, and seem to overestimate positive trends in the southern Baltic Sea while overestimating negative trends in the Skagerrak Sea
Test 8 CSI023	Yearly summer mean and ocean basins (Figure 2.17)	Ocean colour trend signs are generally similar to the ones estimated from in-situ. See Test 7 for comments.

Table 2.7. Validation table, the left column lists the variable that is validated, the right column describes the type of spatial and/or temporal aggregation that is performed.

Results of ocean colour validation are presented in paragraph 2.4.3.3.

c) Chl-a areas

The Chl-a areas have been identified in the Mediterranean Sea (66 *Chl-a areas*), in the Black Sea (5 *Chl-a areas*) and in the Marmara Sea (1 *Chl-a area*). Chl-a areas have been defined using the information on the Rived Basin Districts (RBD) and Countries political border when RBD were not defined. Moreover 18 ocean sub-basins have been identified in the Mediterranean and used to identify the *Chl-a areas*. Within each Chl-a area two sub-areas are defined: the coastal one from the coast to 30 meter depth and the off-shore one from 30 meter to 200 meter depth. Each sub-area has been painted with different colours. *Chl-a areas* are presented in Figure 2.3.

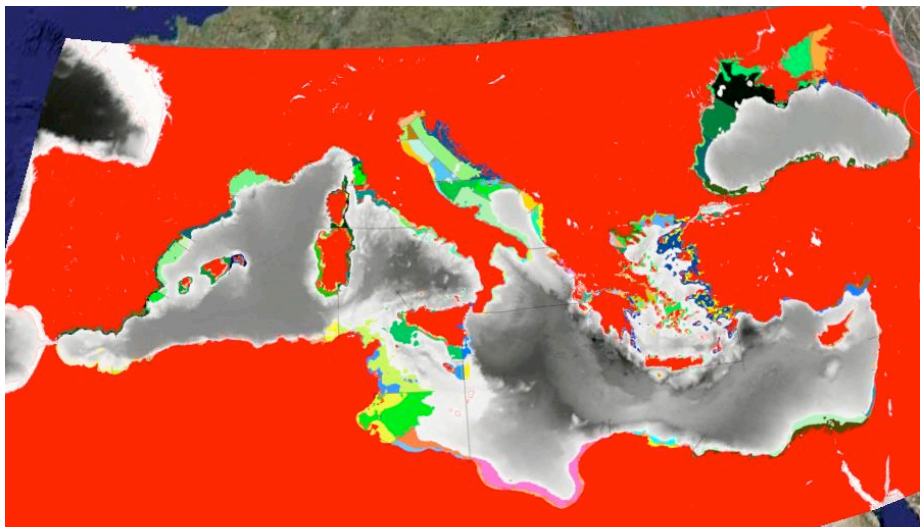


Figure 2.3. *Chl-a areas* for the Mediterranean Sea and Black Sea. Each *Chl-a area* is defined by the black lines perpendicular to the coastline. Within each *Chl-a area* two sub-areas are defined: the coastal one from the coast to 30 meter depth (IN) and the off-shore one from 30 meter to 200 meter depth (OFF). Each sub-area is finally identified has been painted with different colours.

Areas have not been defined yet in the northern European Seas because the ocean colour dataset for the used for the Northern European Seas is at a lower horizontal resolution (9km) than the one used for the Mediterranean and Black Sea (1km). Chl-a areas will be defined for the northern European Seas as soon as the regional higher resolution products will be available (early 2010).

2.4.3.3. *Results and discussion*

a) Interpretation of validation

The comparison between in-situ products and trends and the ocean colour products and trends presented in this paragraph and shows that the global ocean colour algorithm seems to overestimate Chl-a concentration but performs better if used to estimate trends; in fact, trends estimated by ocean

colour products show similar slope and sign when compared with trends estimated by in-situ (Figures 2.14 and Figure 2.15).

Figure 2.4 presents the comparison of summer period (May-September) Chl-a in situ concentration (x axis) with the ocean colour SeaWIFS Chl-a concentration (y axis) for all available stations in the European Seas.

T1 shows that summer mean ocean colour and Chl-a concentration comparison have good correlation ($R^2=0.6$) if the analysis is performed for all the available stations in the European Seas (Figure 2.4) but when the analysis is done at basin scale the correlation decreases (Figures 2.5 and 2.6). This good result for the comparison at European level is expected because of the wide range of values observed on a European scale.

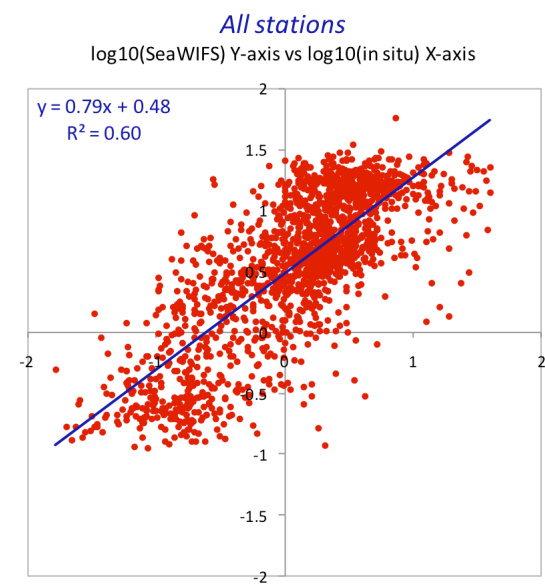


Figure 2.4. Summer period (May September) log10 Chl-a in situ concentration (x axis) with the ocean colour SeaWIFS log10 Chl-a concentration (y axis) for all defined stations in the European Seas.

Figure 2.5 presents the comparison of summer period (May September) Chl-a in situ concentration (x axis) with the ocean colour SeaWIFS Chl-a concentration (y axis) for the Mediterranean Sea.

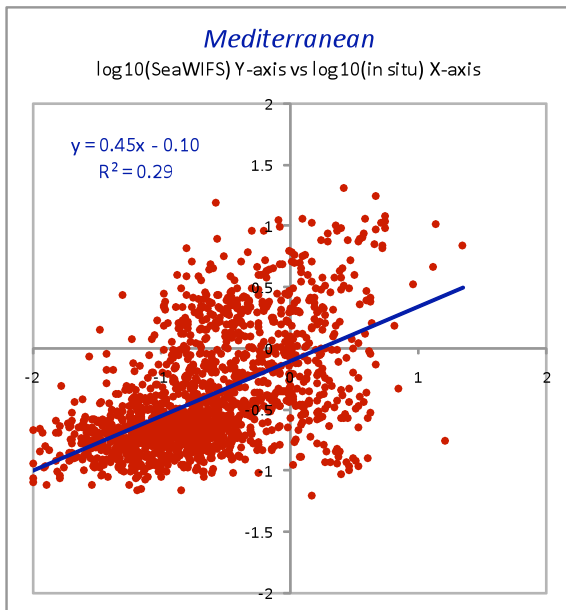


Figure 2.5. Summer period (May September) log10 Chl-a in situ concentration (x axis) with the ocean colour SeaWIFS log10 Chl-a concentration (y axis) for all defined stations in the Mediterranean Sea.

Figure 2.6 presents the comparison of summer period (May September) Chl-a in situ concentration (x axis) with the ocean colour SeaWIFS Chl-a concentration (y axis) for the Baltic Sea.

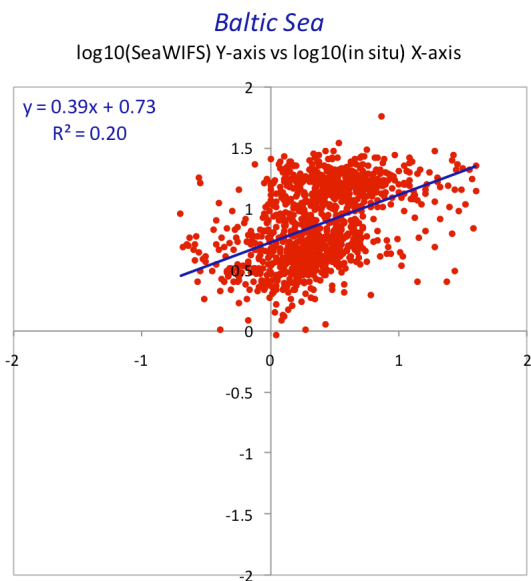


Figure 2.6. Summer period (May September) log10 Chl-a in situ concentration (x axis) with the ocean colour SeaWIFS log10 Chl-a concentration (y axis) for all defined stations in the Baltic Sea.

A possible methodology for validating the ocean colour versus the in-situ data is to present and compare over a certain years the data over European Seas as it is done in Figure 2.7 for year 2005. This approach for comparison is extensively used at EEA since is a very synthetic and easy to communicate. This analysis reveals that ocean colour products overestimate the in-situ Chl-a concentrations in the northern European seas.

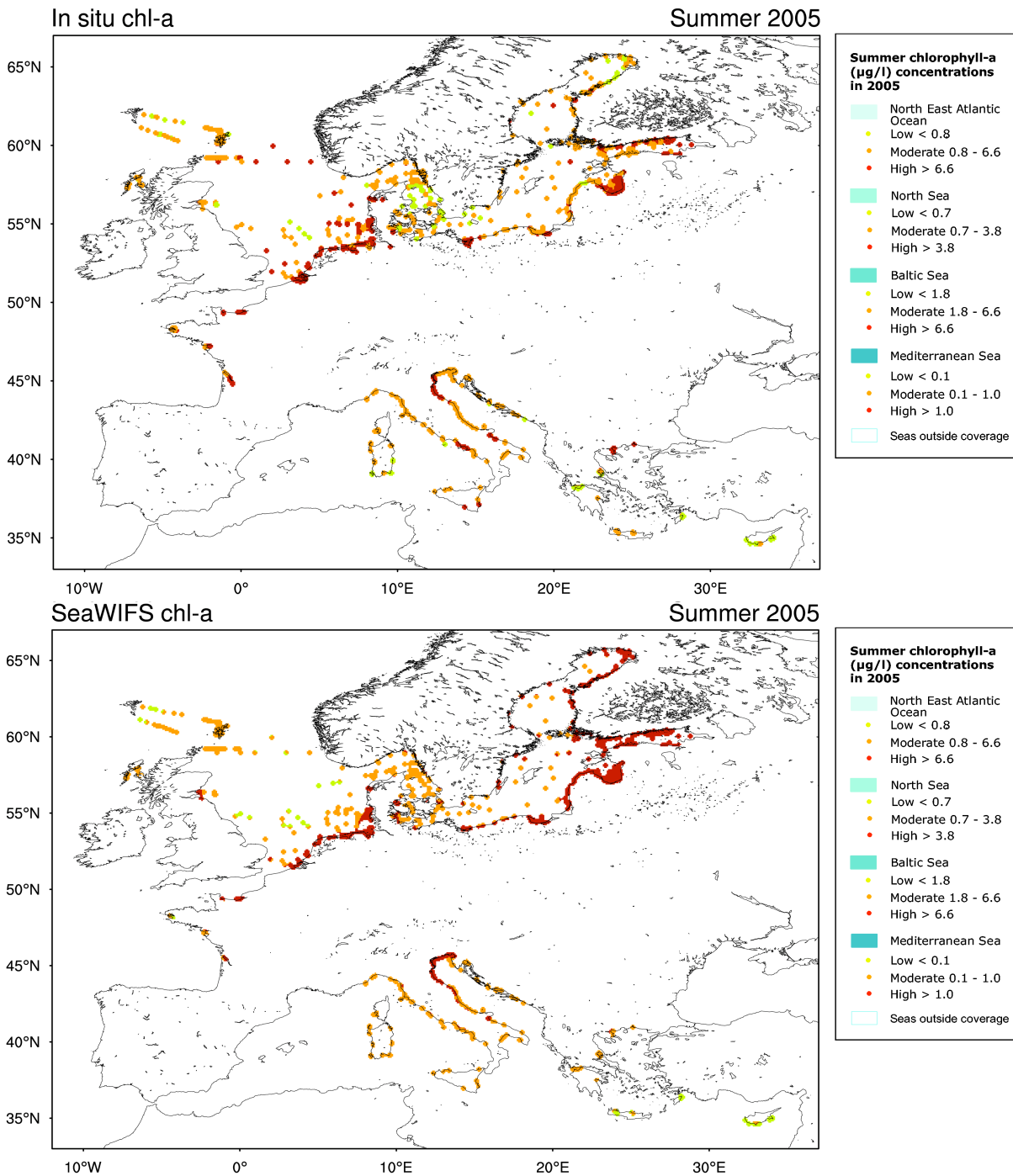


Figure 2.7. Chl-a concentration as estimated by in situ (upper panel) and ocean colour (lower panel) for summer period of year 2005.

Yearly summer mean extracted from in situ data (in this comparison all corresponding in situ data are included, without taking into account the length of timeseries) are compared with trends extracted from ocean colour products, also regression line of data time series is presented. The analysis is presented for the Pan-European dataset of ocean colour and is performed for each sea. The Mediterranean Sea trends are presented in Figure 2.8.

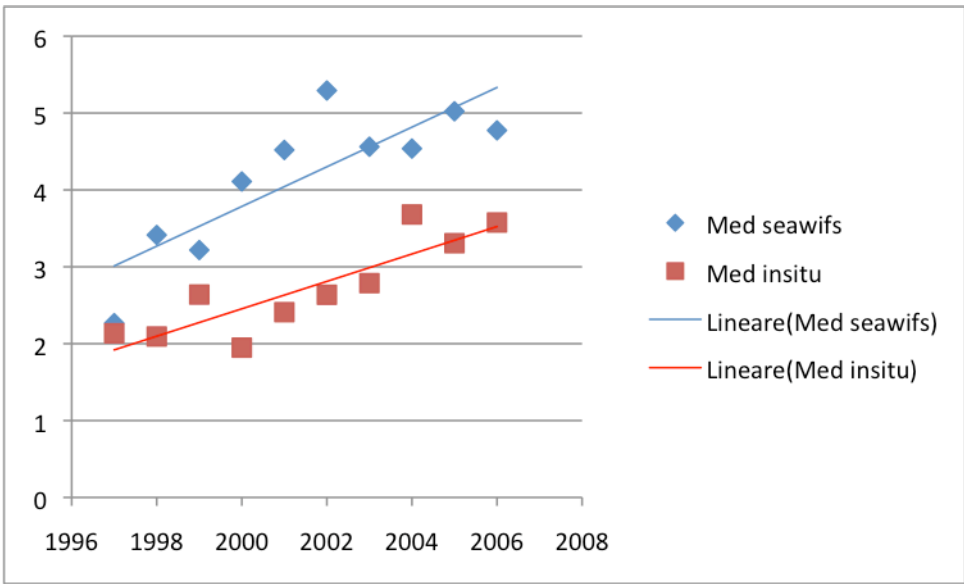


Figure 2.8. Mediterranean Sea summer annual mean and related regression line for both in situ (red, $b = 0,2$ $R^2 = 0,8$) and ocean colour SeaWIFS (blue, $b = 0,3$ $R^2 = 0,7$) data. To perform the comparison only SeaWIFS data that have corresponding in situ data have been taken into account.

The Baltic Sea trends are presented in Figure 2.9.

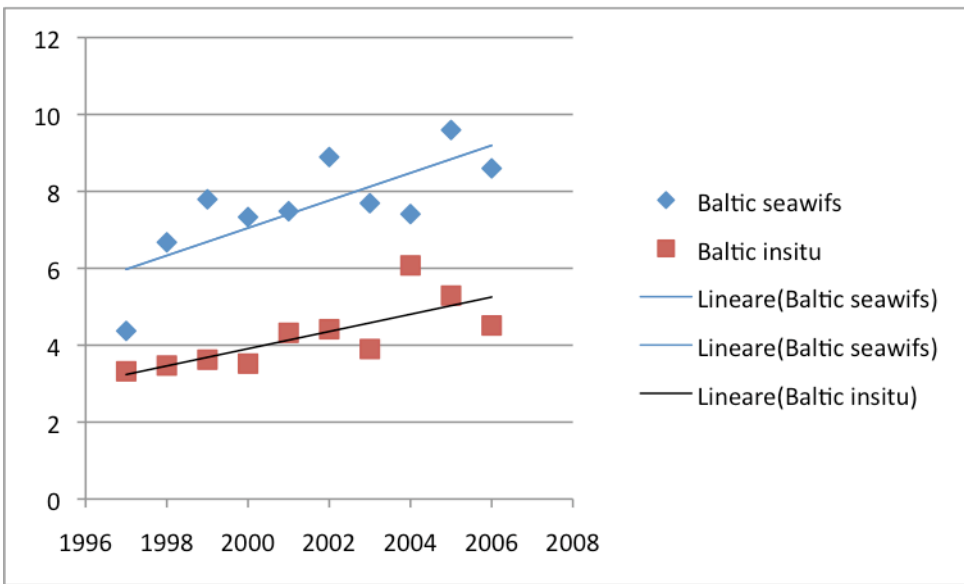


Figure 2.9. Baltic Sea summer annual mean and related regression line for both in situ (red, $b = 0,4$ $R^2 = 0,6$) and ocean colour SeaWIFS (blue, $b = 0,2$ $R^2 = 0,6$) data. To perform the comparison only SeaWIFS data that have corresponding in situ data have been taken into account.

Also the yearly summer mean, normalized by the climatological value, and related trends are compared and the results is shown in Figure 2.10 where SeaWIFS are shown in blue ($b = 0.2$ $R^2 = 0.6$) and in situ are shown in red ($b = 0.4$, $R^2 = 0.6$)

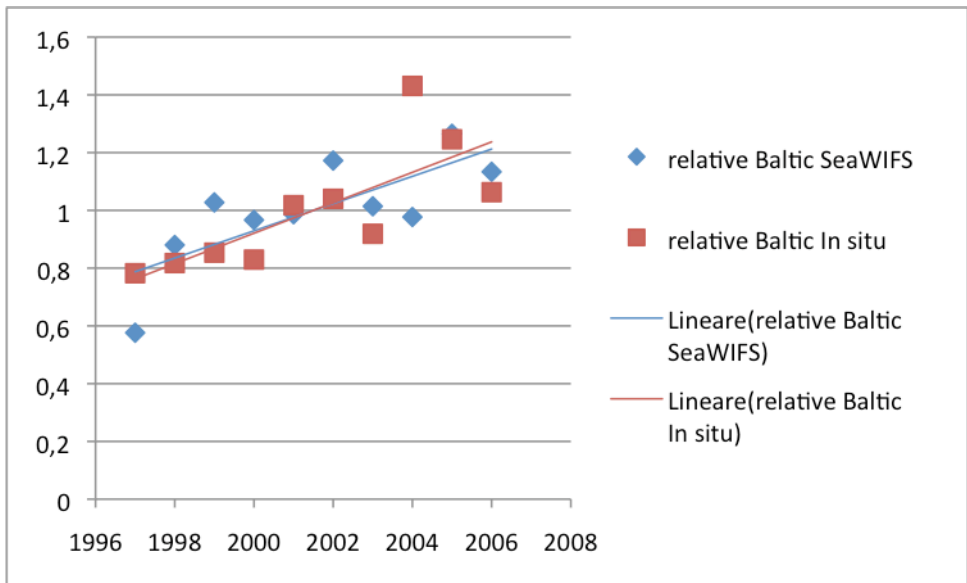


Figure 2.10. Baltic Sea summer annual normalized mean (summer yearly value divided by the summer mean of all years) and related regression line for both in situ (red, $b = 0,4$ $R^2 = 0,6$) and ocean colour SeaWIFS (blue, $b = 0,2$ $R^2 = 0,6$) data. To perform the comparison only SeaWIFS data that have corresponding in situ data have been taken into account.

The North Sea trends are presented in Figure 2.11. For the North Sea the in situ trends is positive while the one detected from SeaWIFS is negative.

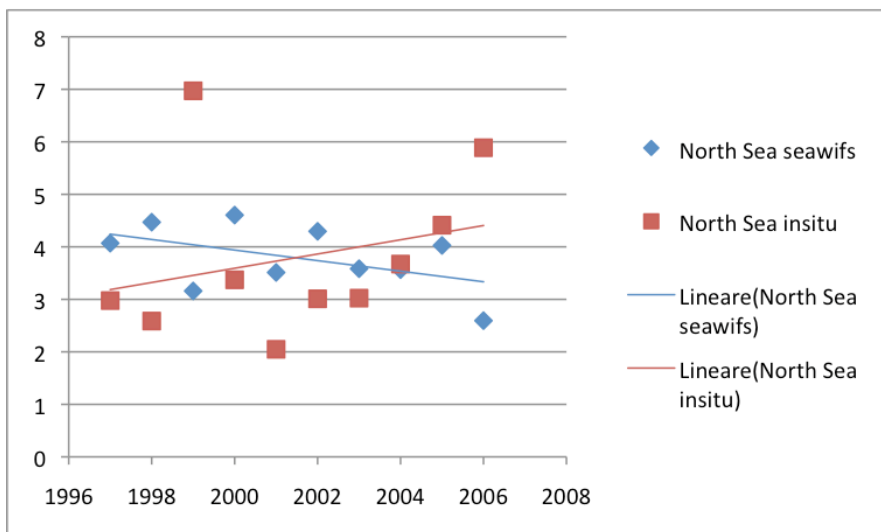


Figure 2.11 North Sea summer annual mean and related regression line for both in situ (red, $b = 0,1$ $R^2 = 0,1$) and ocean colour SeaWIFS (blue, $b = -0,1$ $R^2 = 0,2$) data. To perform the comparison only SeaWIFS data that have corresponding in situ data have been taken into account.

For a selected time period 1998-2004 also daily products of the high-resolution dataset are available and therefore the validation with in situ data is performed with a 5 days time windows instead of the monthly one. In this case data are spatially average in the *Chl-area* domain. An example of this validation is given below in Figures 2.12 and 2.13. This kind of validation is carried out at the level of each *Chl-a* areas, the example shown in Figures 2.12 and 2.13 refers to Serchio-LGS IN that is the coastal (IN) *Chl-area* of Serchio River that is included in the ocean sub domain of the Ligurian Sea.

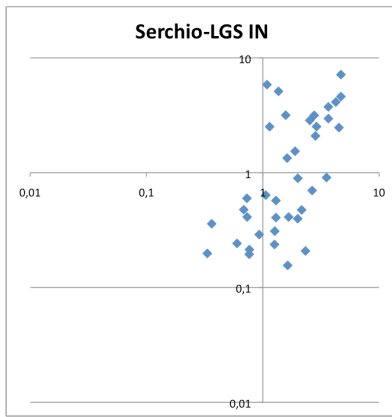


Figure 2.12 Scatter plot of in situ (x axis) versus ocean colour data (y axis) for the *Chl-a area Serchio-IN*.

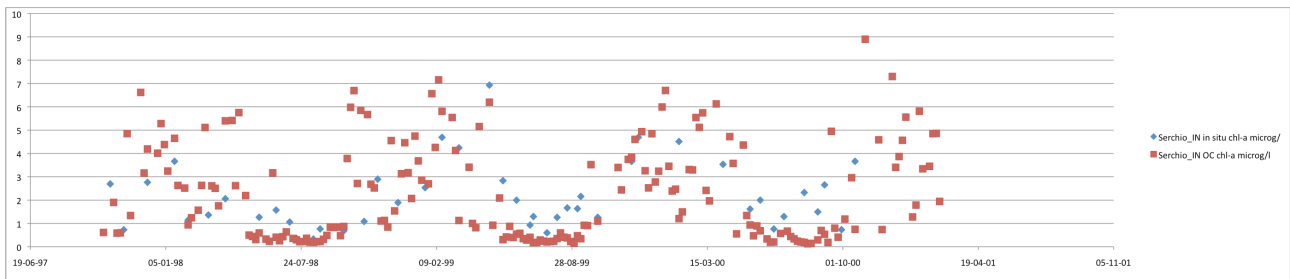
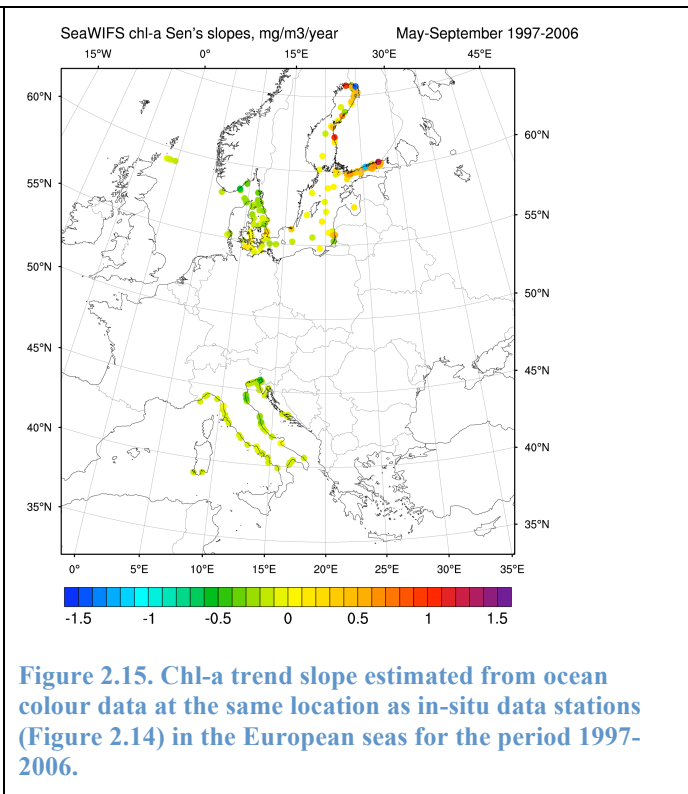
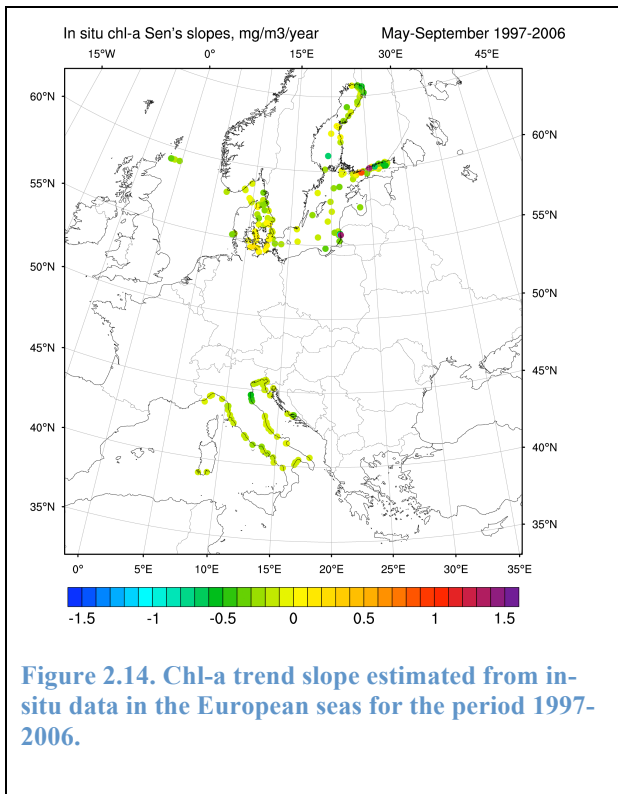


Figure 2.13 Time series (19/06/1997- 05/11/2001) of Chl-a concentration (mg/m^3) of the *Chl-a area Serchio-IN*, ocean colour data are presented in red and in situ data in blue.

The trends were extracted from in-situ and from ocean colour for the period 1997-2006. Trend detection for each time series was done with the Mann-Kendall statistics using a two-sided test with a significance level of 5%. The trend slope was calculated in Test 6 (Table 2.6) using the Sens method (Salmi *et al.*, 2002) and the spatial comparison of these trends is shown in Figures 2.14 and 2.15. Trends of ocean colour are similar to in-situ estimated trends in several region such as the Italian seas, Kattegat Sea and Southern Baltic Sea while ocean colour products are seems to overestimate positive trends in the northern Baltic Sea.

Tests 7 and 8 compared trends signs, results are presented in Figure 2.17 trends signs of ocean colour are similar to in-situ estimated trends but ocean colour products are not able to detect negative trends in the Tyrrhenian Sea, and seems to overestimate positive trends in the southern Baltic Sea while overestimating negative trends in the Skagerrak Sea.



In Figure 2.16 present quantitative estimation of the difference between ocean colour and in situ trends presented separately in Figure 2.14 and 2.15. The table 2.7 present the methodology in which differences in trends signs (positive, negative and no significant trend) between ocean colour and in situ have been estimated and then displayed in the map in Figure 2.16. In situ trends presented in Figure 2.14 have been compared to ocean colour trends presented in Figure 2.15, colour have been associated to the differences in trend significant signs as it is presented in table 2.7: i.e. if a station have positive trends in-situ map and no trend in the ocean colour map it will be represented in blue in Figure 2.16.

		Ocean colour		
		<i>Significant positive trend</i>	<i>Not significant Trend</i>	<i>Significant Negative Trend</i>
In Situ	<i>Significant positive trend</i>	Green	Blue	X
	<i>Not significant Trend</i>	Red	Green	Blue
	<i>Significant Negative Trend</i>	X	Red	Green

Table 2.8. Schema used to estimate and display differences between in situ and ocean colour trends of Figure 2.14 and Figure 2.15 respectively. Green colour in Figure 2.16 means that there is no difference between the sign of trends estimated by ocean colours and the ones estimated by in situ; Blue colour in Figure 2.17 means that a significant positive in situ trend is estimated to be a not significant trend by ocean colour; red colour in Figure 2.16 means that a not significant in situ trend in Figure 2.14 is estimated to be a positive significant trend by ocean colour in Figure 2.15.

SeaWiFS vs in situ trends difference, May-September 1997-2006

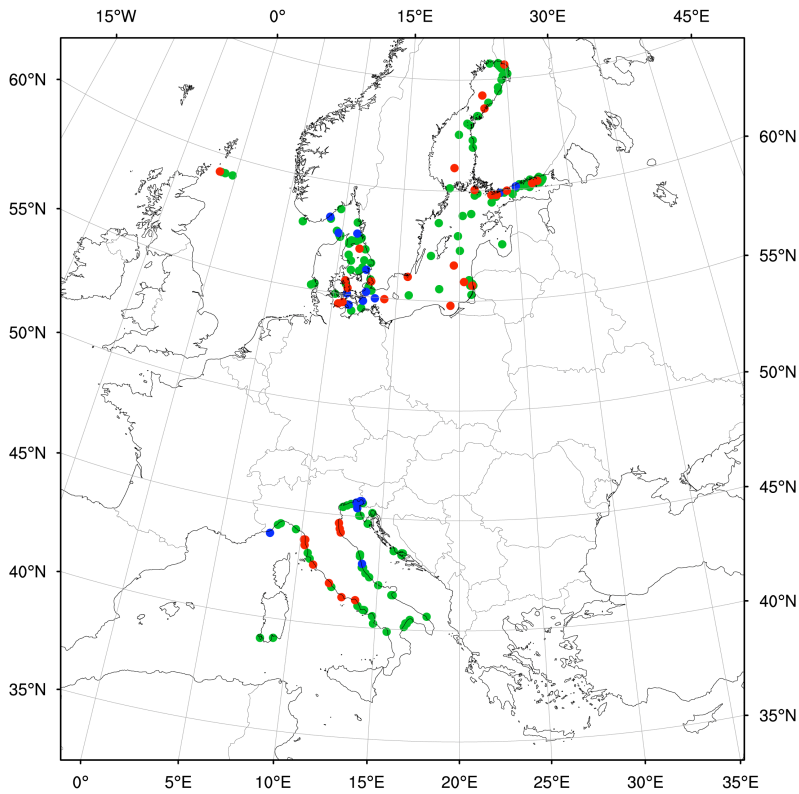


Figure 2.16. Difference in trends extracted from in-situ and trends extracted from SeaWiFS. Colours are described in table 2.7.

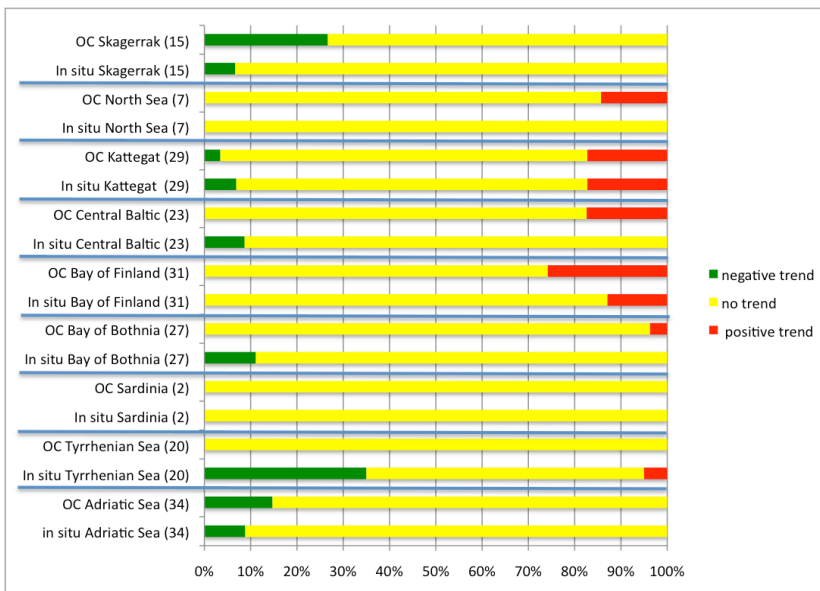


Figure 2.17. Station-wise trends in Chl-a concentrations at stations, expressed in % of stations showing statistically significant change, within the years 1997-2006. For each basin the first row indicates the trends estimates by ocean colour products (OC) and the second row indicates the trends estimates from in-situ observation. Numbers in parentheses indicates number of in-situ stations included in the analysis for each basin that corresponds to the ocean colour pixels used.

b) Products

The ocean colour products provided are:

- A summer (May-September) mean of Chl-a concentration (mg/m^3) for the period 1998-2007 (Figure 2.18).
- *Pan-European trends* of Chl-a based on a global SeaWIFS dataset for the period 1998-2007 (Figures 2.19 and 2.20).
- Mediterranean and Black Sea trends for each *Chl-a area* (Figure 2.22).

Chl-a summer climatology

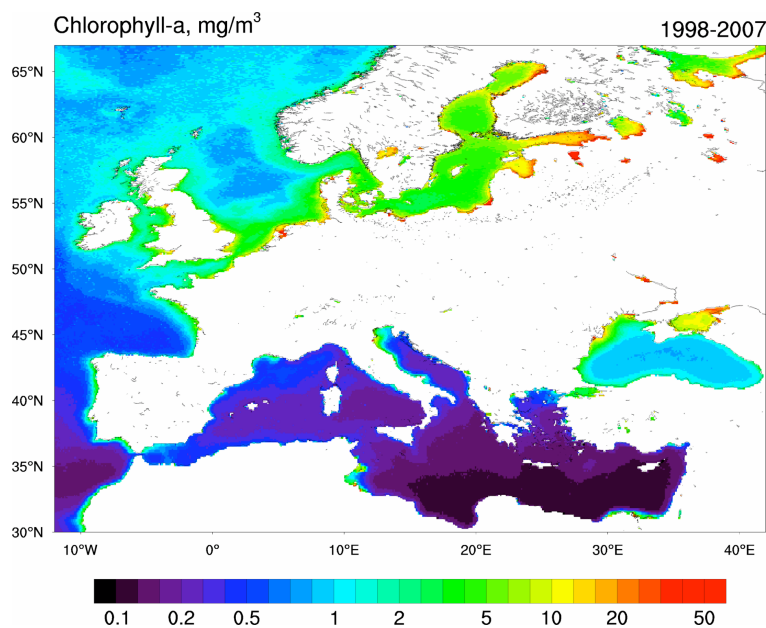


Figure 2.18. Summer (May-September) mean of Chl-a concentration (mg/m^3) for the period 1998-2007.

Two different way of presenting CSI023 (+) have been defined:

1. *Pan-European trends* of Chl-a based on a global SeaWIFS dataset for the period 1998-2007. The methodology for calculating pan-European trends is described in a) below.
2. Mediterranean and Black Sea trends for each *Chl-a area* (*Chl-a area trends*) for the period 1998-2008 based on high resolution (1km) SeaWIFS dataset. The methodology for calculating Mediterranean and Black Sea trends is described in b) below.

a) *Pan-European trends*:

1. For each pixel a yearly time series of summer mean⁵ of Chl-a concentration has been calculated for the period 1998-2007 (10 years) (mg/m^3)
2. Trend value ($(\text{mg}/\text{m}^3)/\text{year}$) for each Chl-a time series has been calculated as following:

$$Y = \text{Chl-a summer mean}^2 \text{ concentration } (\text{mg}/\text{m}^3)$$

⁵ June to September for stations north of 59 degrees in the Baltic Sea (Gulf of Bothnia and Gulf of Finland) and from May to September for all other stations

X=year

Tr=trend

$$Tr = \frac{\overline{xy} - \overline{x}\overline{y}}{\overline{x^2} - \overline{x}^2}$$

3. A reference field, also called climatology, is calculated as the average of all the 1998-2007 summer periods (May-September) Chl-a concentrations (mg/m^3). Climatology is expressed in terms of mg/m^3 .
4. The trend (Tr) is normalized by the reference layer (see 3 above) and is called then Relative Trend ($RelTr$) being calculated as following:

$$RelTr = \frac{Tr}{\overline{Y}}$$

Where \overline{Y} is the average of summer Chl-a concentration over the time frame 1998-2007.

RelTr is therefore a % of change of Chl-a over the period 1998-2007.

5. Mann-Kendal statistics are applied to each pixel Chl-a concentration time series to identify statistical significant trend at a 95% confidence level.

b) *Chl-a areas trends*:

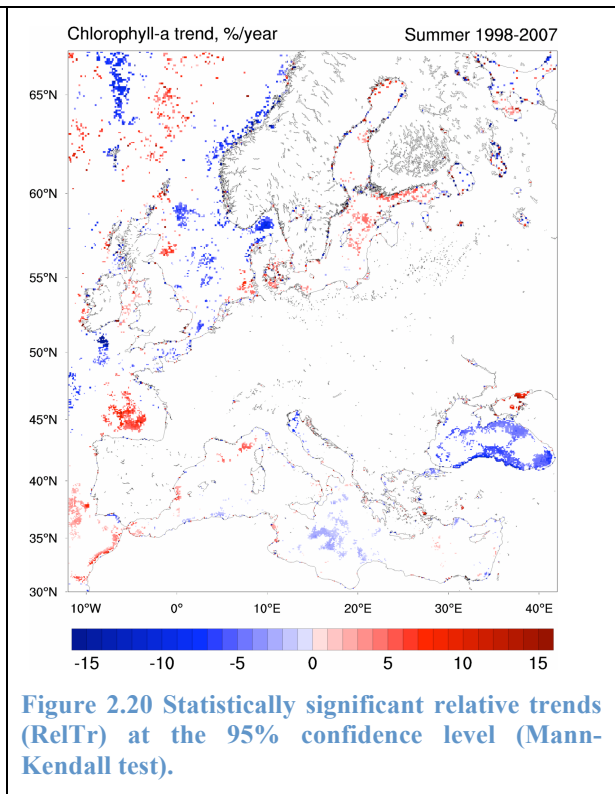
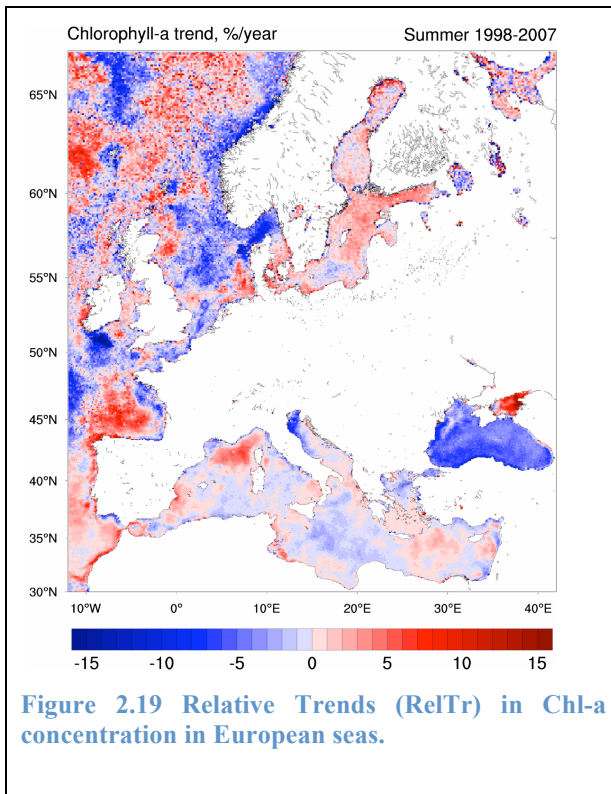
1. For each pixel data are aggregated in the yearly summer (May-September) mean.
2. For each pixel a timeseries of summer Chl-a concentration has been calculated for the period 1998-2008 (11 years)
3. Trend detection for each pixel time series was done with Mann-Kendall statistics as in CSI023
4. Results are presented in terms of percentage of positive, negative significant pixels and no-trend for each of the Chl-a areas over the period 1998-2008

Below we present the analysis of CSI023 (+) in terms of *pan-European trends* and *Chl-a areas trends*.

1) Pan European trends:

Trends of Chl-a over the period 1998-2007 are presented in Figures 2.19 and 2.20. Trends in Figure 2.19 are estimated as explained above in the statistical methods section. Significant trends in Figure 2.20 are detected through the Mann-Kendall method.

Space observations of Chl-a show a large area with decreasing Chl-a concentrations in the Black Sea, in the Northern Adriatic Sea, and in the Skagerrak, whereas a large area with increasing trends is observed in the Bay of Biscay and in the Baltic Sea (Figures 2.19 and 2.20).



2) Chl-a areas trends

The Chl-a trends are calculated for each Chl-a area of the Mediterranean, Sea of Marmara and Black Sea. Figure 2.21 presents percentage of positive, negative significant pixels and no-trend for some of the *Chl-a areas* in the Mediterranean Sea 1998-2008.

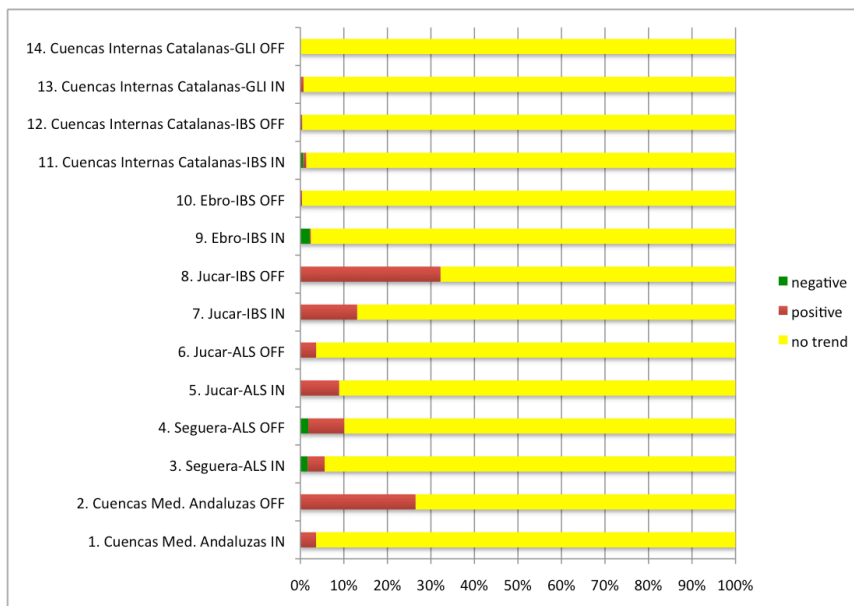


Figure 2.21: Trends in mean summer Chl-a concentrations in some Mediterranean Chl-a areas in 1998-2008: for each Chl-a areas the red bars indicate the percentage of pixels with Chl-a increasing significant trends, the green bars indicate the percentage of pixels with Chl-a decreasing significant trends, the yellow bars indicate the percentage of pixels that does not show any significant trend.

2.4.4. Coastal water extension indicator derived from the Chl-a SDTE

The coastal water indicator has been developed for the EEA to describe marine waters influenced by river run-off and terrestrial inputs. The indicator is based on the Case 1 and Case 2 flags of ocean colour products as explained below. Case 2 waters are defined as water with optical properties characteristic of inorganic particles in suspension and yellow substances in addition to phytoplankton. Inorganic material and yellow substances originate from land and for this reason Case 2 water can be interpreted as coastal water visibly influenced by river run-off.

2.4.4.1. Dataset used to calculate the indicator

The data used for this indicator are the flags associated with the MODIS dataset elaborated by CNR-ISAC in Rome. The data are processed using the MEDHOC4 Mediterranean regional algorithm (Santoleri, 2008). The indicator is based on the analysis of daily Case 2 water products. The products used are the one produced by CNR-ISAC that retrieves MODIS data in the Southern European seas; in this case specifically, they extract the Case 2 water flags. The Case 2 water flag is a file that contains for each grid point the information whether the grid point has the Case 2 water characteristics, or not. Data provided by CNR-ISAC are further processed by INGV in Bologna.

2.4.4.2. Methods:

The coastal water indicator is produced by estimating the frequency (days over a certain 3 month period) of Case 2 waters: how many days a certain area (1x1 km) has Case 2 characteristics over a certain period of time (3 months). Measurements of water-leaving radiance through satellite radiometers are not possible when clouds are present and therefore, if the number of cloudy days over the 90-day period is higher than 95 the pixels are masked. The Sea of Azov has been masked because it is a very shallow sea (maximum depth around 15 metres) and ocean colour products are probably affected by bottom reflectance problems. The maps are calculated for different years and then operationally every 3 months for each season divided as following: winter: J.F.M., spring: A.M.J., summer J.A.S., autumn: O.N.D.

The presence of CASE 2 water is counted for each grid point and then the frequency over a certain season is calculated following the method proposed in Bignami et al (2007). The map obtained is masked and the grid points where the frequency is lower than 20% are masked white.

2.4.4.3. Results

The indicator is presented as a map showing marine waters influenced by river run-off and terrestrial inputs, also referred to as CASE 2 waters (Figures 2.22 and 2.23).

Figure 2.22 (upper panel) presents the indicator for winter 2009 (January-March) and highlights the influence of coastal waters and their extension toward the open ocean. River plumes (Danube, Po, Rhone, Gironde estuary and Nile) are evident and affect vast areas of the open ocean and of the surrounding coastal zones. Moreover, it is evident that the river plumes do not spread homogeneously but are affected by ocean currents: in the case of the Rhone, westward currents transport the plumes in that direction and similarly the Po plume is transported south.

Figure 2.23 (lower panel) presents the indicator for summer 2009 (July-Sept). The indicator highlights the influence of coastal waters and their extension toward the open ocean. Coastal water extension is limited in summer time. River plumes are visible only for the Po, Nile and Danube and this last is the only one affecting vast areas of the surrounding northeast coastal zones.

By comparing the indicators during the two seasons (winter and summer 2009) it is evident that there is a seasonal variability in the extension of open ocean waters influenced by the river run-off and that this influence is larger in the winter period.

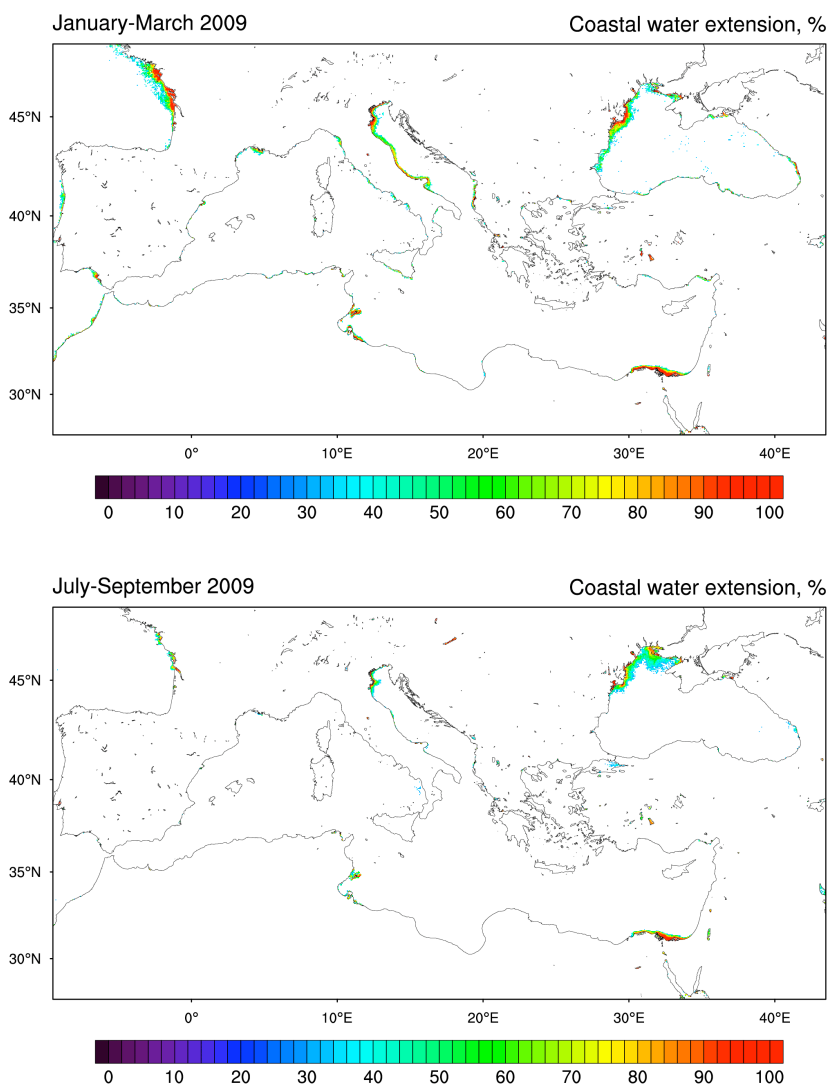


Figure 2.22. Winter 2009 (JFM), upper panel and Summer 2009 (JAS), lower panel, of 'Coastal water indicator: Marine waters influenced by river run-off and terrestrial inputs' indicator in souther European seas.

The indicator is calculated for each season and is distributed by the EEA on the Water Information System for Europe (WISE) at the following link:

<http://www.eea.europa.eu/themes/water/mapviewers/caseII>

2.5. Conclusions

This chapter has demonstrated how to define and implement several indicators for climate change state assessment and for the state of the environment assessment. Indicators have played and will continue to play a vital part in focusing and illuminating the significance of environmental change and the progress towards sustainable development. Some of the key SDTEs produced from OO services are considered mature for contribution to the development of indicator reporting as demonstrated in this chapter. Temperature and Chl-a SDTEs have been analysed and the indicators that can be derived from these SDTEs have been identified and developed.

The Temperature SDTE is a mature and multiple-source dataset in OO (satellite, in-situ measurements and models). SST from OO SDTE products allows a high frequency and complete spatial coverage for the Global Ocean and the regional seas. In-situ surface data are of large importance to validate satellite data and to increase the accuracy of the combined satellite and in-situ dataset.

Different indicators can be derived from the temperature SDTE. A first set is related to SST where the longest time series are available (1871-present). The inclusion of regional high-resolution satellite datasets for several European seas started with the 2008 EEA Climate Change report and has continued with the inclusion of these indicators in the EEA State of the Environment Report of 2010. Additional indicators, not presented in this work, may be developed that consider the whole water column temperature and could be indicative of long term effects and extreme events. The latter are very relevant for ecosystems dynamics and possible stresses (real time SST anomaly maps with time scales from daily to monthly, annual basin average Heat Content (HC) anomalies from approx. 1985-present, HC linear trends and maps of the spatial distribution of HC linear trends from 1985-present, real-time temperature anomaly profiles in the water column, mixed layer depth anomalies time series).

The Chl-a SDTE appears the most mature and two indicators have been developed: Chl-a trends and coastal water extension. The OO Chl-a SDTE, deduced from satellite data, has been shown to be able to contribute to the further development of the CSI023 Chl-a indicator, improving its

representativeness for European coastal waters. It is recognized that the study of the different morphological and hydrological structure of European regional areas needs to be further improved, especially in the northern European seas, identifying shelf, coastal and deep ocean water areas and classifying them into ‘*Chl-a areas*’ as has been done for the Mediterranean and Black Seas.

Much effort has been made to validate the Chl-a trend concentrations estimated through remote sensing with the in-situ ones. The comparison presented shows that the global ocean colour algorithm seems to overestimate Chl-a concentration but performs better if used to estimate trends; in fact, trends estimated by ocean colour products show similar slope and sign when compared with trends estimated by in-situ (Figures 2.14 and 2.15). The regional daily dataset, Mediterranean CNR-SeaWiFS, used in the Mediterranean Sea, seems to show a good comparison with in-situ data (Figures 12 and 13) but further investigations need to be performed.

The Chl-a trend indicator has been included in the 2010 EEA State of the Environment Report (<http://soer2010.ew.eea.europa.eu/>) and shows a large area with decreasing Chlorophyll-a concentrations in the Black Sea, in the Northern Adriatic Sea, and in the Skagerrak, whereas a large area with increasing trends is observed in the Bay of Biscay and in the Baltic Sea

The analysis has also revealed the need for regional ocean colour products to be available to develop support of the EEA indicator and that there is potential in a long-term trend analysis based on ocean colour because large-scale and in some cases even regional-scale changes appear to be captured by the satellite images. In order to build confidence in this analysis, it is however clear that it needs to be based on the best possible regional products.

A preliminary implementation of the indicator showing marine waters influenced by river run-off and terrestrial inputs, also referred to as Case 2 waters (Figures 2.22) has been presented. The indicator has been thought up for the EEA to present a qualitative estimation of the influence of river and terrestrial inputs in the marine domain and is able to highlight the seasonal variability in the extension of open ocean waters influenced by the river run-off, this influence is larger in the winter period. The indicator is calculated for each season and is distributed by EEA on the Water Information System for Europe (WISE).

After the work of definition and development of the indicators the objective is to move towards an operational phase in which indicators providers are link with a formal and direct contact with the EEA.

3. Oil spill accidents and illegal discharges

This chapter is composed of two parts detailing two different cases experienced in the last four years in the Mediterranean Sea in the field of marine oil pollution monitoring and forecasting. Section 3.1 describes the hindcast of oil spill pollution during the Lebanon Crisis that occurred in July-August 2006, and Section 3.2 present the MOON-REMPEC (Mediterranean Operational Oceanography Network-Regional Marine Pollution Emergency Response Centre for the Mediterranean Sea) agreement and the ERO (Emergency Response Office) exercise carried out in October 2009 as a contribution to the OSCAR-MED (Opération de Surveillance Cordonnée Aérienne des Rejets en Méditerranée) operation organized by REMPEC.

3.1. Hindcast of Oil Spill Pollution during the Lebanon Crisis, July-August 2006

3.1.1. Summary

The Mediterranean Operational Oceanography Network (MOON) provides near-real-time information on oil spill detection and predictions that have been used during the Lebanese oil pollution crisis in summer 2006. A MOON decision support system for oil spill monitoring and prediction comprising ocean colour satellite and SAR images, ocean current forecast (MFS-Mediterranean Forecasting System and CYCOFOS-CYprus Coastal Ocean Forecasting & Observing System) and the MEDSLIK oil spill model has been developed. The oil spill predictions obtained with MEDSLIK coupled to the CYCOFOS high-resolution ocean fields are compared with the oil spill predictions obtained using the lower resolution MFS hydrodynamics and both are validated against satellite observations. The predicted beached oil quantities along the Lebanese and Syrian coasts are compared with the in-situ observations.

It is found that both CYCOFOS and MFS are capable to simulate the northward movement of the oil, with the higher resolution CYCOFOS predictions being in better agreement with satellite observations. Among the free MEDSLIK parameters tested in the sensitivity experiments there are the wind corrections (wind factor and angle) and the Eulerian currents fields depth used in the Lagrangian oil spill particle model. Among these the drift factor appeared the most relevant in order to improve the quality of the results suggesting that operational models such as MFS and CYCOFOS still lack adequate resolution and physical process parametrization at the air-sea interface. The oil moved from Lat 33°40'N Lon 35°25'E northward toward Syria to reach in 8 days the Lebanese/Syrian border (Lat 34° 38'N Lon 35° 58'E) and Tartus (Lat 34° 52'N Lon 35° 54'E); in agreement with satellite and in situ data.

3.1.2. Introduction

Accidental and illegal marine pollution in the Mediterranean Sea constitutes a major threat for the marine environment. Previous incidents in the Mediterranean Sea (i.e., Haven tanker, Ligurian Sea, 1991) and in the European Seas (i.e., Prestige tanker, Galicia, Spain 2002) documented the consequent environmental and economic damages (Loureiro et al., 2009) to fishery, the tourism industry and the coastal marine ecosystems. Oil pollution discharges from ships in the Mediterranean have been described in the past to be significant (Pavlakis *et al.*, 2001) and a cause of environmental degradation for the Mediterranean Sea. In order to prevent the high impact of oil spill accidental releases it is necessary to use computer aided support system based on operational oceanography real time ocean forecasts coupled with satellite images and oil spill models.

Operational Oceanography in the Mediterranean Sea was established in 2003 by a Mediterranean Operational Oceanography Network (MOON), which offered real time services consisting of a set of Core Services-CS and Downstream Services-DS. The CS deliver generic, all-purpose products from observations and models while the DS use CS products to formulate customized services for specific applications. One such DS service is the so-called decision support system for oil spill detection and forecasting which will be described in this chapter. It consists of integrated satellite data and ocean forecasting systems, MFS⁶ and CYCOFOS⁷, coupled with MEDSLIK oil spill model (Lardner et al, 1998 and 2006). The satellite component consists of the integration of the data received from recent generation spectroradiometer and radar satellite sensors such as MODIS (on board AQUA, since 2002 and TERRA, since 2000) and ASAR (on board ENVISAT, since 2002) making it possible to monitor, on daily basis, the evolution of the oil pollution if needed. Remote sensing can provide substantial support to routine surveillance in the open ocean and coastal areas and has the advantage of being able to observe oil spill events in remote and often inaccessible areas. Moreover it can provide information on the rate and direction of oil movement through multi-temporal imaging.

In this work we illustrate the application of the MOON oil spill decision support system to the largest oil spill release accident in the Eastern Mediterranean, the Lebanese oil pollution crisis occurred in mid-July 2006. The amount of oil released is considered the largest volume of oil ever dispersed in Eastern Mediterranean waters.

This work aims to demonstrate the strengths and weaknesses of the operational oil spill monitoring and forecasting system available today in the Mediterranean Sea. While CYCOFOS was run in real

⁶ <http://gnoo.bo.ingv.it/mfs>

⁷ <http://www.oceanography.ucy.ac.cy/cycofos/forecast.html>

time, the MFS simulations have been carried out in delayed mode. In this work MFS simulations will be compared with the CYCOFOS simulations and with satellite images from MODIS and ASAR. The results from the sensitivity experiments (using different wind parameters and current depths) are presented. The work is organized as follows: section 3.1.3 describes the remote sensing for oil spill monitoring, section 3.1.4 the forecasting model, section 3.1.5 the hindcast experiments of the Lebanon crisis event, section 3.1.6 the sensitivity experiments and finally section 3.1.7 concludes the chapter.

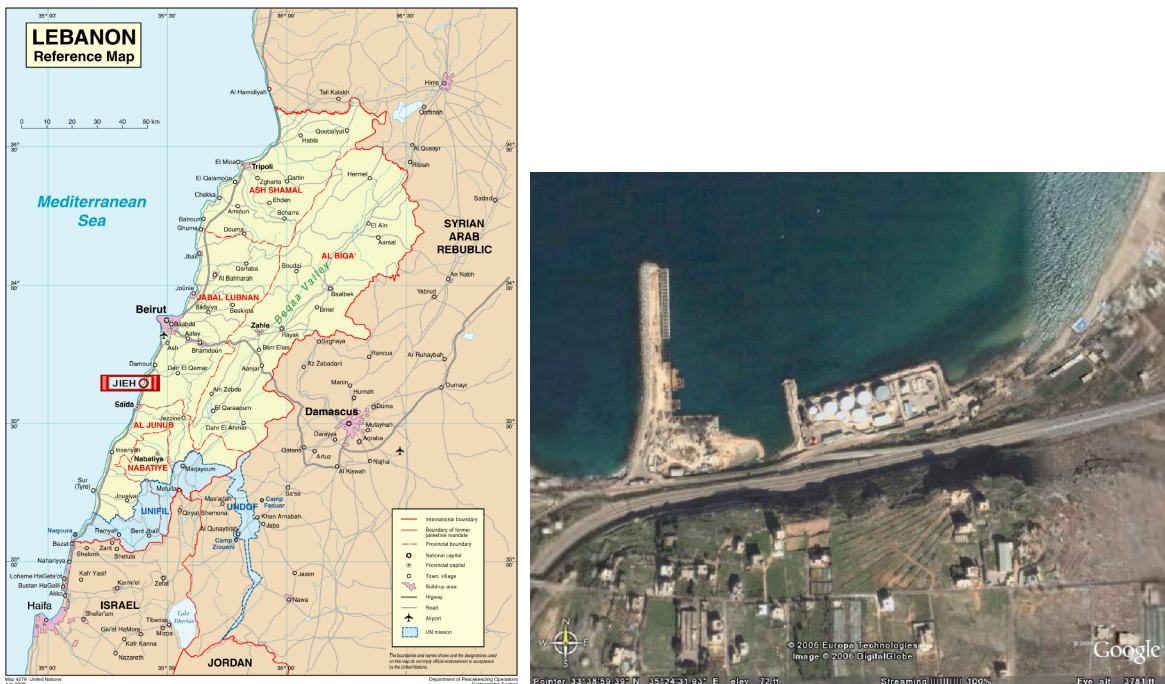


Figure 3.1. (a) Jieh geographical position; (b) on-shore position of the Jieh power station taken from Google Earth before the crisis.

3.1.3. Remote sensing for oil spill monitoring

Oil spills floating on the sea surface can be detected by Synthetic Aperture Radar (SAR) mounted on satellites (Fingas and Brown, 1997 and Fiscella *et al.*, 2000). Oil spills appear as darker areas due to the absence of short gravity and capillary waves which normally backscatter the radar signal measured by SAR. Even though there are some limitations in the use of SAR data for oil spill detection at very low (<3 m/s) and high wind speed (>25 m/s) conditions, the use of SAR is a mature tool for oil spill monitoring. The main limitations in the use of SAR are due to the long revisit time and limited swath width of the sensors aboard of currently available satellite missions (ERS-2, ENVISAT and RADARSAT), which cannot guarantee seamless daily coverage. Table 3.1 gives an overview of the swath widths and revisit times of the SAR satellite instruments aboard the abovementioned satellite platforms.

Missions	Instruments	Type of measurement	Max swath width	Revisit time
ERS-2	SAR	Roughness	100km	35 days
RADARSAT-2	SAR	Roughness	500km	24 days ⁸
ENVISAT	ASAR	Roughness	400km	35 days ⁹
ENVISAT	MERIS	Colour	1150km	3 days
TERRA and AQUA	MODIS	Colour	2330km	2 days

Table 3.1. Overview of the swath widths and revisit times of the SAR satellite instruments aboard ERS-2, RADARSAT and ENVISAT satellite platforms and of MODIS instrument aboard TERRA and AQUA satellites.

Remote sensing devices for oil spill detection include infrared video and photography, thermal infrared imaging, airborne laser fluorosensors; airborne and space-borne optical sensors can complement SAR and contribute to implement cost effective and reliable monitoring systems (Jha, 2008). Visible or optical sensors do not guarantee all-time, all-weather coverage, and usually suffer from reduced resolution capabilities compared to SAR; on the other hand, they allow monitoring of wider areas (at lower resolution).

Oil at the sea surface has different reflectance than water in the visible region of the electromagnetic spectrum, the difference being positive or negative, depending on illumination-view angles, i.e. the solar and satellite azimuth and zenith angles of a given image pixel. Positive differences, i.e. positive oil-water contrast, usually occur when an oil spill is in a high glint region of the image, i.e. in approximately mirror-like reflection conditions. Recent optical modelling (e.g. Otremba and Piskozub, 2001, 2004) has described the variability of such contrast with changes in illumination-view situations, film thickness and oil type, the main conclusion being that an oil film can generally be detected using VIS/IR sensors (see an application in Hu *et al.*, 2003). The medium-resolution of MODIS (250 m; <http://modis.gsfc.nasa.gov>) and MERIS (300 m; <http://envisat.esa.int/instruments/meris/>) channels show great potential for daily monitoring of the oil because of their unprecedented synoptic and repetitive coverage (see also Adamo, 2007, Shi *et al.*, 2007 and Lotliker Aneesh, 2008). In this work we show the potential capability of the synergic use of active and passive sensors to monitor the Lebanon oil spill incident. MODIS and ASAR imagery will be used in comparison with model results to assess model simulation performance.

MODIS daily images from the AQUA and TERRA satellites have been processed from 13 July to 27 August 2006 for a total number of 72 scenes. ASAR satellite images have been processed from 21 July to 27 August 2006 for a total number of 8 scenes. MODIS images are downloaded at a Level 0 format, which consists of raw data received from the satellite in standard binary form.

⁸ <http://www.radarsat2.info/about/mission.asp> - selective looking can reduce the revisit time.

⁹ <http://envisat.esa.int/handbooks/asar/CNTR1-1-4.htm>

After being processed to a Level 1B format for 36 spectral channels (<http://oceancolor.gsfc.nasa.gov>), 7 spectral bands of the Visible and near-infrared spectrum are then extracted and some re-sampled at the spatial resolution of 250 m, two bands being already at 250 m resolution while the others are still at 500 m.

All seven bands are then graphically displayed as a color-coded reflectance image, using IDL ENVI; contrast stretching is performed to enhance local contrast in sections of the image containing oil slicks. Also, ENVI is used to compute band ratios (e.g. 645 nm and 859 nm L1B images) in order to further highlight oil slicks. The best band ratio is chosen by trial and error, maximizing oil-water contrast, according to the illumination-view conditions (glint or no-glint situation). Oil features are then manually digitized on these maximum contrast images using the ENVI Region Of Interest (ROI) tool and each oil slick ROI is saved to a text file containing pixel latitude, longitude and reflectance in the various bands. This information is then used to extract oil slick spectral properties, statistics for classification, masking, etc.

Processed ASAR images were kindly provided by Telespazio SpA (<http://www.telespazio.it>). The analysis of the entire time series of ASAR and MODIS data for the Lebanon oil pollution incident reveals that during the 43 monitored days, MODIS with its daily coverage provided useful information on the evolution of the oil spill for 24 days, while ASAR, because of its spatial and temporal coverage, only contributed 8 days of observations.

It is therefore of great importance to integrate the information from these two sensors in order to perform a monitoring activity at the space and time coverage required by the users.

3.1.4. The oil spill forecasting systems

The oil spill model used in this work is MEDSLIK (Lardner, 1998 and Lardner et al 2006). MEDSLIK consists of a drifting model with a representation of transformation processes to simulate the fate and dispersal of oil slicks. The spill is subdivided into a large number (up to 100,000) of Lagrangian parcels of equal size.

The oil parcel drift is given by two effects: a deterministic advection by the water currents and a turbulent diffusive process. In finite difference form, each "i" oil parcel position in space (x_i , y_i , z_i) and time is written as:

$$\begin{aligned} x_i(t + \tau) &= x_i(t) + \left\{ u(x_i, y_i, z_i, t) + \alpha(W_x(x_i, y_i, t) \cos \beta + W_y(x_i, y_i, t) \sin \beta) \right\} \tau + \Delta x_i^{(d)} \\ y_i(t + \tau) &= y_i(t) + \left\{ v(x_i, y_i, z_i, t) + \alpha(-W_x(x_i, y_i, t) \sin \beta + W_y(x_i, y_i, t) \cos \beta) \right\} \tau + \Delta y_i^{(d)} \\ z_i(t + \tau) &= z_i(t) + \Delta z_i^{(d)} \end{aligned} \quad (1)$$

where:

- $x(t + \tau), (t + \tau), z(t + \tau)$ is the position of the parcel at time $(t + \tau)$;

- $u(x_i, y_i, z_i, t)$ and $v(x_i, y_i, z_i, t)$ are the zonal and meridional water velocity components provided by the hydrodynamic model (MFS or CYCOFOS);
- W_x and W_y the surface wind vector zonal and meridional components respectively;
- α and β are the so-called drift factor and drift angle;
- τ is the integration time step;
- $\Delta x^{(d)}, \Delta y^{(d)}, \Delta z^{(d)}$ are the turbulent diffusion terms written for a random walk motion (Ahlstrom, 1975 and Hunter, 1987):

$$\begin{aligned}
\Delta x_i^{(d)} &= [2r - 1] \sqrt{6k_h \tau} \\
\Delta y_i^{(d)} &= [2r - 1] \sqrt{6k_h \tau} \\
\Delta z_i^{(d)} &= [2r - 1] \sqrt{6k_v \tau}
\end{aligned} \tag{2}$$

where:

- K_h and K_v are horizontal and vertical diffusivities chosen in our case to be constant and equal to $K_h = 2 \text{ m}^2/\text{s}$ and $K_v = 0.01 \text{ m}^2/\text{s}$;
- r is a random value between 0 and 1.

The terms between parentheses in (1) are the deterministic components of the parcel movement and they consider the water current velocities from the hydrodynamic model and a correction factor due to unresolved but deterministic processes. These are parameterized in terms of the wind drift factor and the wind drift angle. These correction factors were interpreted in different ways in the literature of the past thirty years. Initially, this correction factor was chosen to account for unresolved Ekman currents at the surface since numerical models of water currents were coarse and inaccurate. The water currents used in the eighties and before were mainly climatological and deduced from observations, i.e., they were approximately equal to the subsurface geostrophic currents. There was considerable dispute among modellers as to the best choices for the values of the drift factor and angle for Ekman currents, most models using a value of around 3% for the former and a value between 0° and 25° for the latter (Reed *et al.*, 1994 and Al-Rabeh, 1994).

With the advent of operational oceanography (Pinardi *et al.*, 2003) and accurate operational circulation models, Ekman processes are resolved and they are already included in the water current velocity (the terms with $u(x_i, y_i, z_i, t)$ and $v(x_i, y_i, z_i, t)$ in equation (1)).

However in this work we will make the more traditional assumption adopted for the wind drift and angle using the water velocity field at a depth of 30 m. The choice of 30 m is corresponding to the Ekman layer e-folding depth, which for the Mediterranean Sea is generally between 10 and 30 m. Such an estimate is calculated using the scaling formula:

$$\delta_E = \sqrt{\frac{K_v}{f}} \quad (3)$$

(Pond and Pickard, 1983) where f is the Coriolis parameter between 30 and 40 N. K_v is the vertical eddy coefficient for momentum that is normally variable between 10^{-2} and $10^{-1} \text{ m}^2 \text{ sec}^{-1}$ near the surface. A depth of 30 m is therefore considered an average depth at which the effects of surface Ekman wind drift are significantly reduced. By using the water velocity at 30 m the effects of Ekman drift velocities can be safely added. If a current forecasting model is sufficiently fine to resolve the Ekman dynamics the best choice should be to set the drift factor to zero and to use the water surface flow from the eulerian model.

The wind correction factor can still be used to account for missing processes at the air-sea interface such as wind waves induced currents. The Stokes drift is in fact proportional to wind speed, i.e., wind drift angle equal to zero (Rascle and Ardhuin 2005 and Ardhuin et al, 2009). Several other deterministic corrections could be considered but in this work we have used only the traditional wind drift factor (3%) with water currents at 30 meters, with wind drift angle equal to 0° (Reed *et al.*, 1994 and Al-Rabeh, 1994) and an overall wind drift factor of 1.2% with zero angle related to wave effects on the surface currents (Rascle and Ardhuin, 2005 and Ardhuin et al, 2009).

MEDSLIK includes fate processes such as evaporation of the lighter oil fractions, mixing into the water column by wave action, emulsification and beaching on the coast (Mackay and Paterson, 1980 and Mackay and Leinonen, 1977). The viscosity and density change of the oil are computed according to the amount of emulsification and evaporation of the oil itself. Input data for the model are: oil spill start date and time, duration, location, oil type and volume. The output is given in terms of oil parcels trajectories and their corresponding oil properties (i.e., evaporated and emulsified oil percentage, surface and dispersed in the water column).

MFS (Pinaridi *et al.*, 2003) produces daily mean analyses (combination of model and observations) on a weekly basis and daily mean or hourly mean 10-day forecasts on a daily basis. The system consists of a numerical model (Tonani *et al.*, 2008) and a data assimilation scheme (3DVAR) (Dobricic and Pinaridi, 2008) capable of assimilating all the available satellite and in situ data. MFS horizontal resolution is $1/16^\circ \times 1/16^\circ$, approximately 6 km. MFS is forced by atmospheric forcing produced by the European Center for Medium range Weather Forecast-ECMWF analyses and forecasts (ECMWF, 2005) at $0.5^\circ \times 0.5^\circ$ degrees and 6 hours resolution. The MFS analyses and

forecasts are compared once a week with observations, providing the quality control and assessment of the products. This continuous evaluation of the system performance and the data assimilation make operational oceanography of the last ten years a real step forward with respect to the modelling systems of the last decades.

The MFS products are used by the nested ALERMO sub-regional forecasting system (Sofianos *et al.*, 2006) and then ALERMO output is used as boundary and initial conditions for the nested CYCOFOS high-resolution forecasting system. The CYCOFOS high-resolution model (Zodiatis *et al.*, 2003) covers an area of the NE Levantine Basin in the Eastern Mediterranean (31° 30'E – 36° 13'E and 33° 30'N – 36° 55'N). CYCOFOS horizontal resolution is 1/60°x1/60° degrees, approximately 1,5 km. CYCOFOS is forced by atmospheric forcing produced by SKIRON (Kallos, 1997 and Papadopoulos *et al.*, 2002). CYCOFOS produces 6-hourly mean forecasts for the next 5 days on a daily basis. The CYCOFOS ocean forecasts received extensive validation and inter-comparison with the parent models and with remote and in-situ observations (Zodiatis *et al.*, 2008).

3.1.5. Hindcast experiments of the Lebanon oil pollution event

The spill occurred in mid-July 2006 from the Jieh power plant, which is located 30 km south of Beirut (Figure 3.1). It is now believed that the spill occurred as the result of two bombing raids, in the mornings of 13 and 15 July, as reported by different press releases. The available MODIS image shows the smoke plumes from the Jieh Power plant on 16 July 2006 at 8:30 GMT (Figure 3.2), while in the MODIS image dated 15 July (11:00 GMT) no smoke is visible (not shown). There is therefore the possibility that the bombing event occurred on 13 July but the power plant started to burn only on 16 July. This lack of information causes uncertainties about the starting day of the spill and the duration of the spill is uncertain. The amount of oil spilled was variously reported as being between 15000 and 20000 tons. As far as the type of oil is concerned, according to UNEP information (UNEP, 2007) the oil contained in the tanks was heavy IFP-number 6 fuel¹⁰, which has the following key properties:

- High viscosity, or resistance to flow, resulting in low mobility of the oil;
- High density (950-1030 kg/m³);
- Tendency to break up into tar balls and sink to the bottom when released into water; and
- Low volatility, leading to low fuel evaporation.

¹⁰ Information on n.6 fuel oil at http://en.wikipedia.org/wiki/Fuel_oil



Figure 3.2. MODIS AQUA image on 16 July (08:30 GMT): a black smoke plume is visible and bombing has occurred.

The spill has been modelled as being a continuous leakage of oil over a period of 144 hrs or 6 days starting from 13 July 2006 with a total mass of oil (18770 tons) representing the total mass of oil released in this time.

The hindcast experiments have been carried out using MEDSLIK coupled with CYCOFOS and MFS. The water current fields for 16 July 2006 from CYCOFOS (Figure 3.3) showed a northerly flow, parallel to the coasts of Lebanon and Syria with flow velocities in 20-30 cm/s range. This flow eventually turns westward to form the Asia Minor current in the Cilician Basin. This flow regime is close to the climatological flow regime known for this region (Pinardi et al, 2006). The departure from a northerly flowing current along the Lebanese and Syrian coasts has also been registered but on a more episodic way (Brenner et al., 2003).



Figure 3.3. Surface current field for the day 16 July 2006 at 12:00 from CYCOFOS forecasting system, dark arrows represent current directions and intensity in cm/s.

These features persisted for the next two months apart from the occasional development of small eddies in the lee of the various headlands. In the gulf of Beirut a detachment of the currents from the coasts and the formation of a stagnation-like circulation are noticed, which might be interpreted as an anticyclonic eddy localized in the Gulf. However the model resolution does not allow the complete reconstruction of this flow field. Sea surface temperature in the same period from CYCOFOS (Figure 3.4) and along the affected coastal areas was as high as 30°C. The high frequency SKIRON wind forecast (Figure 3.5) showed winds varying in direction between South-easterly to North-easterly. This wind pattern remained steady for most of the months of July and August 2006, the wind strength varying generally between 2 and 7 m/s.

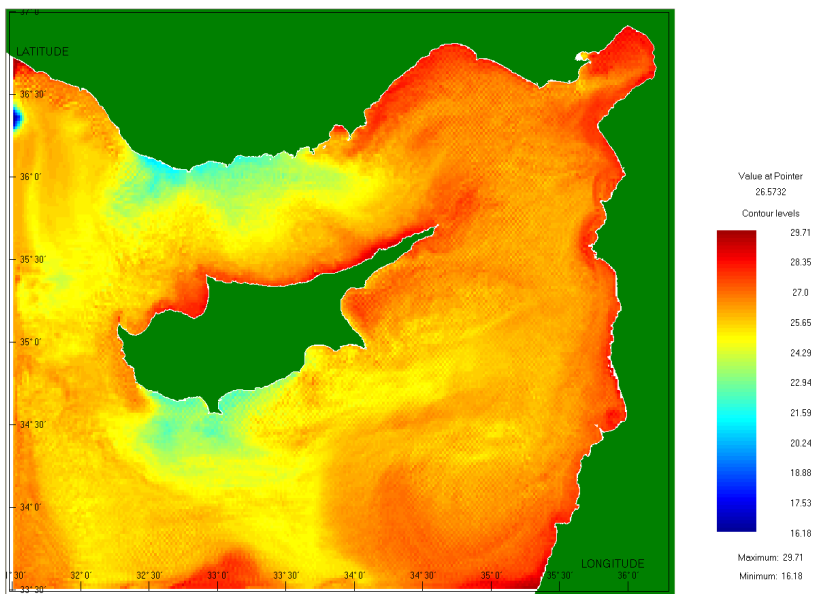


Figure 3.4. CYCOFOS surface temperature fields for the day 15 July 2006.

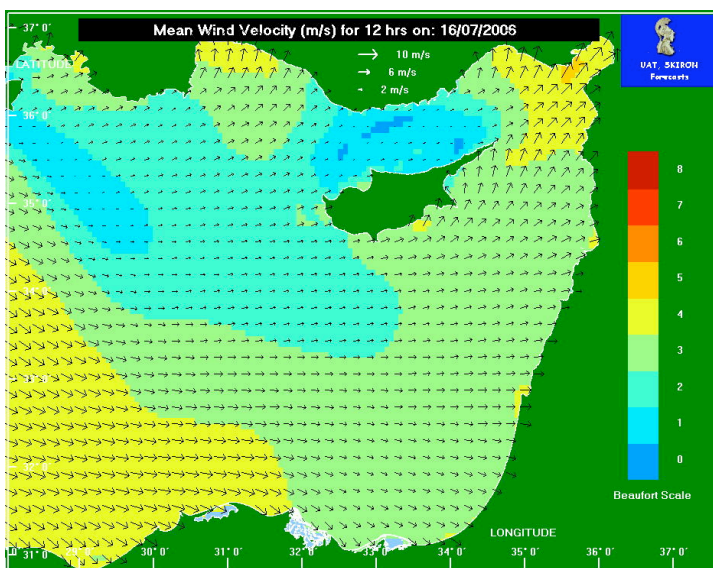


Figure 3.5. Mean wind velocity field for the day 16 July 2006 at 12:00 from the SKIRON forecasting system, dark arrows represent wind directions and intensity in m/s. Wind intensity is also shown in colour scale in the background.

During the first day of spill the northward currents are present (Figure 3.3) while the flow field of 14 July 2006 in front of the power plant appears weaker and unstable (not shown). In the following days the northward current flow in front and north of the Jieh power plant sets up steady, and the clockwise eddy in the gulf of Beirut seems to be stable. The northward current returns closer to the coast north of the Gulf of Beirut, and strengthens, while in front of the Jieh power plant the currents weakens during the 21-22-23 July 2006 (Figure 3.6). The flow intensity along the coast north of Beirut seems to decrease around 27 July 2006 and to increase again during the end of the July. The northward direction and intensity of the flow along the coast seem steady in the first half of August 2006.



Figure 3.6. Surface currents field for the day 23 July 2006 at 12:00 from CYCOFOS forecasting system, dark arrows represent current directions and intensity in cm/s.

3.1.6. The reference experiments

The hindcast experiments of this study are reported in Table 2. The experiments have been designed to test the impact of water currents from MFS and CYCOFOS, the wind factor and angle parameters and the depth of the water currents considered. In experiments 1 and 2, water currents are taken at 30 m depth and wind parameter is fixed at 3%. In experiments 3 and 4, water currents are taken at surface and the wind parameter is fixed at 0%. In experiments 5 and 6, water currents are taken at surface and the wind parameter is fixed at 1,2%.

	Experiment 1	Experiment 2	Experiment 3	Experiment 4	Experiment 5	Experiment 6
Current field	CYCOFOS (6- hourly forecast)	MFS (1- hourly mean forecast)	CYCOFOS (6- hourly forecast)	MFS (1- hourly mean forecast)	CYCOFOS (6- hourly forecast)	MFS (1- hourly mean forecast)
Wind field	SKIRON (1-hourly forecast)	ECMWF 6- hourly mean forecast)	SKIRON (1-hourly forecast)	ECMWF 6- hourly mean forecast)	SKIRON (1-hourly forecast)	ECMWF 6- hourly mean forecast)
Spill position	33°40'N 35°24.75'E	33°41'N 35°10 'E	33°40'N 35°24.75'E	33°41'N 35°10'E	33°40'N 35°24.75'E	33°41'N 35°10 'E
Start spill date	13/07/2006 08:00	13/07/2006 08:00	13/07/2006 08:00	13/07/2006 08:00	13/07/2006 08:00	13/07/2006 08:00
Spill duration	144 hr	144 hr	144 hr	144 hr	144 hr	144 hr
Total mass of spill	18770 tons	18770 tons	18770 tons	18770 tons	18770 tons	18770 tons
Type of oil	API=20	API=20	API=20	API=20	API=20	API=20
Wind correction factor	3%	3%	0	0	1.2%	1.2%
Wind angle factor	0	0	0	0	0	0
Current depth	30 m	30 m	surface	surface	surface	surface
Number of particle released	90000	90000	90000	90000	90000	90000

Table 3.2. model runs and sensitivity experiments summary table. Experiments 1 and 2 are the ones where the hydrodynamics models MFS and CYCOFOS and the oil spill model MEDSLIK are used in the basic configuration. Experiments 3, 4, 5 and 6 evaluate the responses of MFS to a change in the wind parameters and to the current transfer depth.

Experiment 1 has been run also in real time during the actual oil spill accident. Comparisons of oil slick position and extension detected by satellite images (MODIS and ASAR) and simulated oil at sea from experiment 1, using CYCOFOS, and experiment 6, using MFS, are presented in the figures from 7 to 11. Oil slick regions digitized from MODIS images are shown in green so as to be more easily compared with the model simulations.

The first comparison between satellite images and model outputs is given in Figure 3.7 for 19 July, when the MODIS AQUA image (2006 10:35, 19 July) shows that the smoke plume (blue) is still rising from the power plant and the oil (yellow-brown) has reached the Gulf of Beirut and Byblos. Both the CYCOFOS (Figure 3.7 b) and MFS (Figure 3.7 c) simulations showed that the spilled oil was transported northward: CYCOFOS forecasted the oil offshore the Gulf of Beirut, quite similarly to the pattern of the oil spill as seen from the satellite image. The MFS simulation shows the oil offshore the Gulf of Beirut and off Byblos, in agreement with the satellite observations but maybe too far offshore.

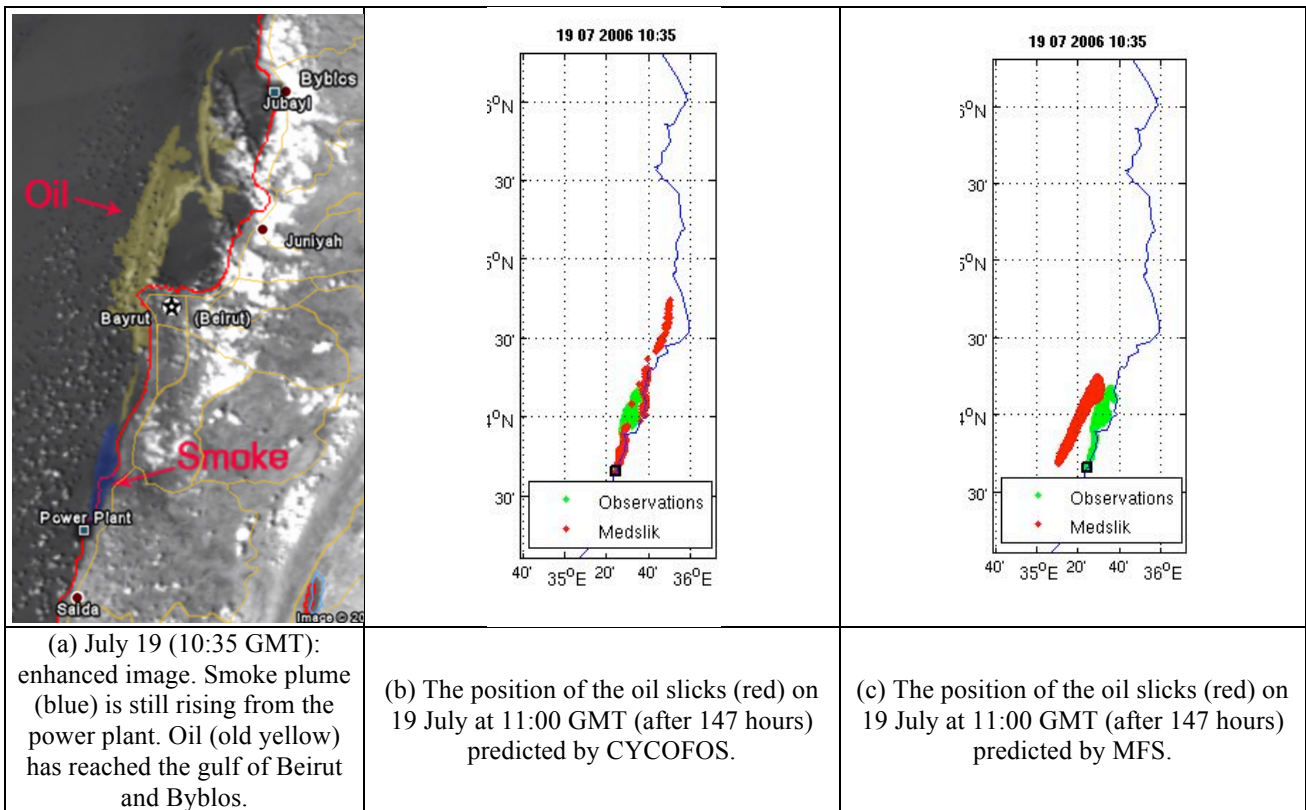


Figure 3.7. Panel (a) shows the MODIS AQUA image of 19 July 2006 at 10:35 GMT. Panel (b) shows the position of the oil slick on 19 July at 11:00 GMT (after 147 hours) as predicted by CYCOFOS. Panel (c) shows the position of the oil slick on 19 July 2006 at 11:00 GMT (after 147 hours) as predicted by MFS.

The first comparison between satellite images and model outputs is given in Figure 3.7 for 19 July, when the MODIS AQUA image (2006 10:35, 19 July) shows that the smoke plume (blue) is still rising from the power plant and the oil (yellow-brown) has reached the Gulf of Beirut and Byblos. Both the CYCOFOS (Figure 3.7 b) and MFS (Figure 3.7 c) simulations showed that the spilled oil was transported northward: CYCOFOS forecasted the oil offshore the Gulf of Beirut, quite similarly to the pattern of the oil spill as seen from the satellite image. The MFS simulation shows the oil offshore the Gulf of Beirut and off Byblos, in agreement with the satellite observations but maybe too far offshore.

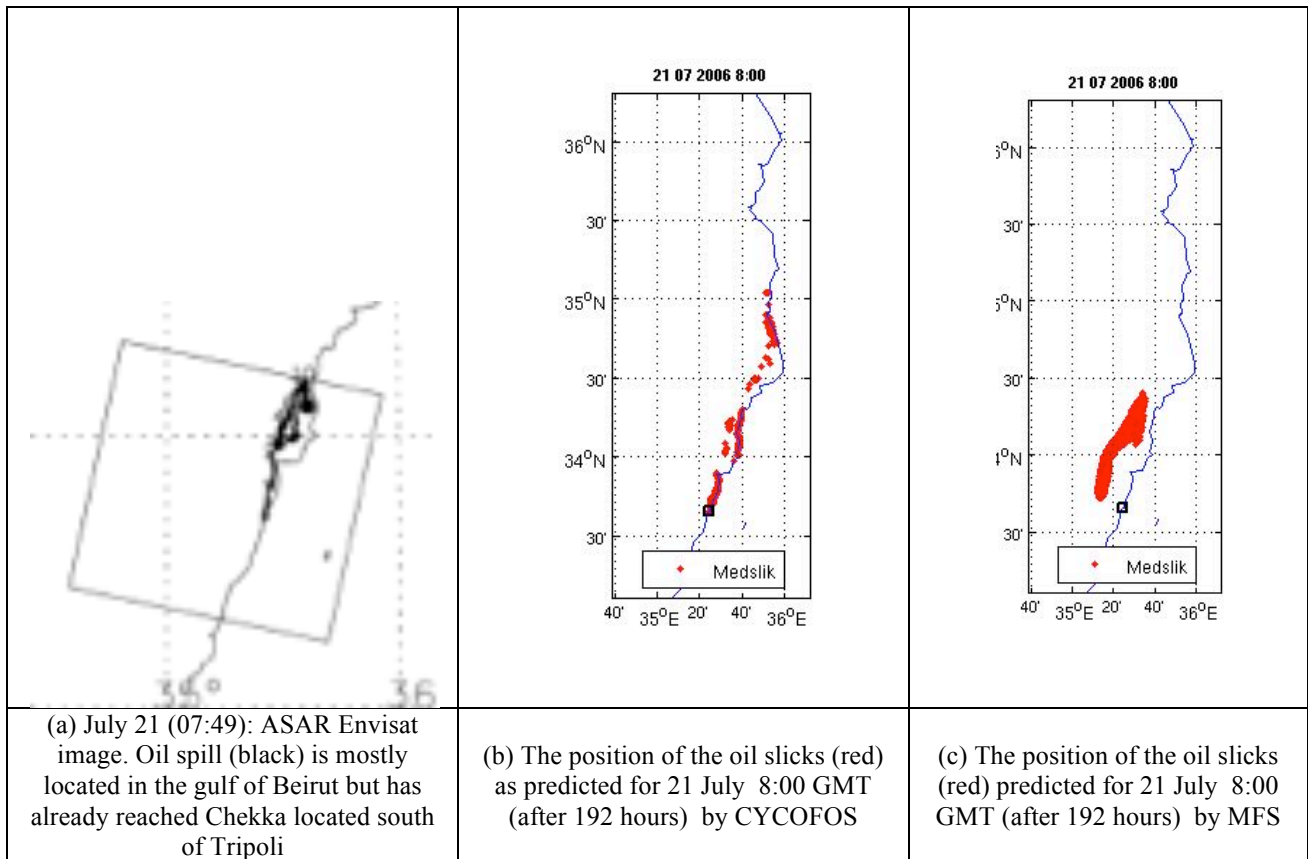


Figure 3.8. Panel (a) shows the ASAR ENVISAT image for day 21. The ASAR image is compared with the position of the oil slick predicted by CYCOFOS (panel b) and by MFS (panel c).

On 21 July an ASAR image (Figure 3.8 a) was available showing the oil in the Gulf of Beirut reaching Byblos. The CYCOFOS predictions (Figure 3.8 b) progressive transport of the oil northward, reproducing well the pattern of the oil in the Gulf of Beirut and north of Tripoli. MFS predictions (Figure 3.8 c) also show a northward displacement of the slick but seem to overestimate the oil in the Gulf of Beirut and continue to show an unrealistic offshore extension of the slick due to the offshore starting position and the coarse model resolution.

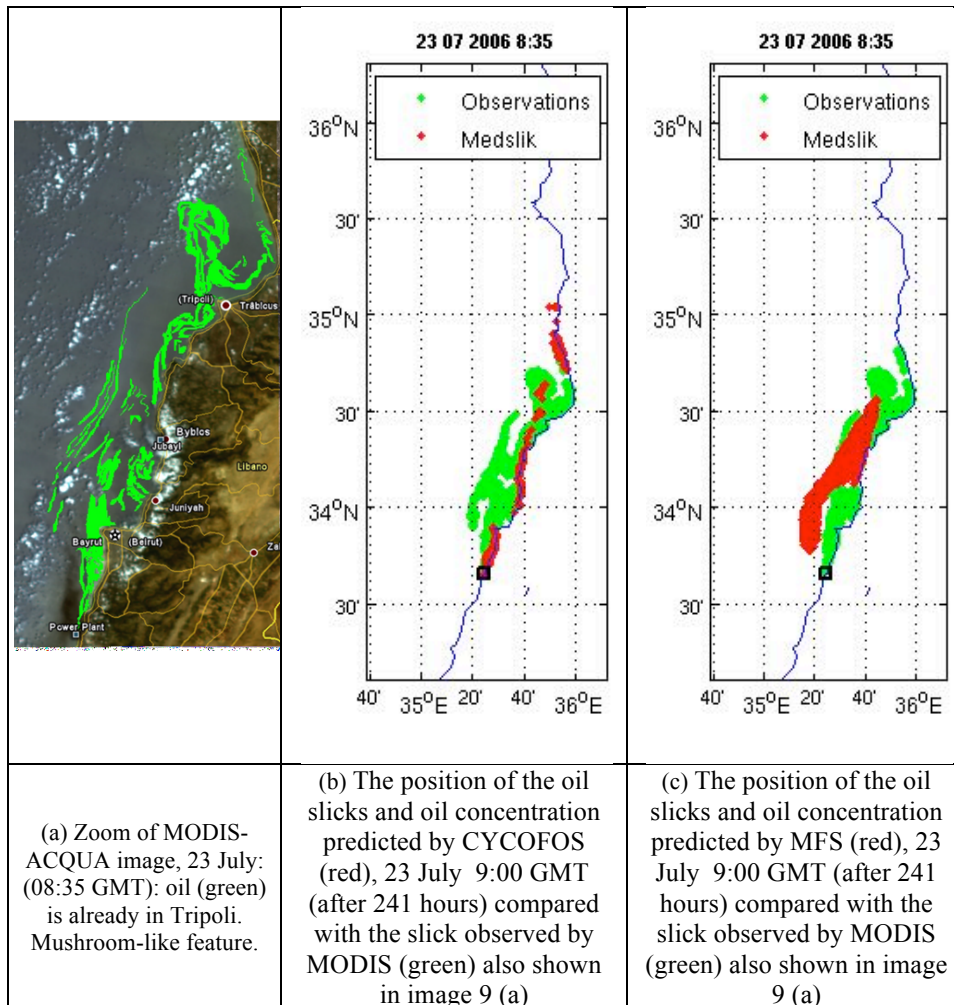


Figure 3.9. Panel (a) shows the MODIS AQUA image of 23 July 2006, 8:35 GMT. Positions of the observed slicks (panel a) are compared with the positions predicted by CYCOFOS (panel b) and by MFS (panel c).

On 23 July the satellite image (Figure 3.9 a) shows the oil spill in the Gulf of Tripoli well simulated by the CYCOFOS hindcast (Figure 3.9 b) which however seems to underestimate the offshore extension of the oil slick and overestimate the northward extension of the slick. However the northernmost part of the coast is not covered by satellite images due to clouds. The offshore part of the slick is well reproduced by MFS except in the southern part (Figure 3.9 c) and the MFS seems to underestimate the northernmost extension of the slick.

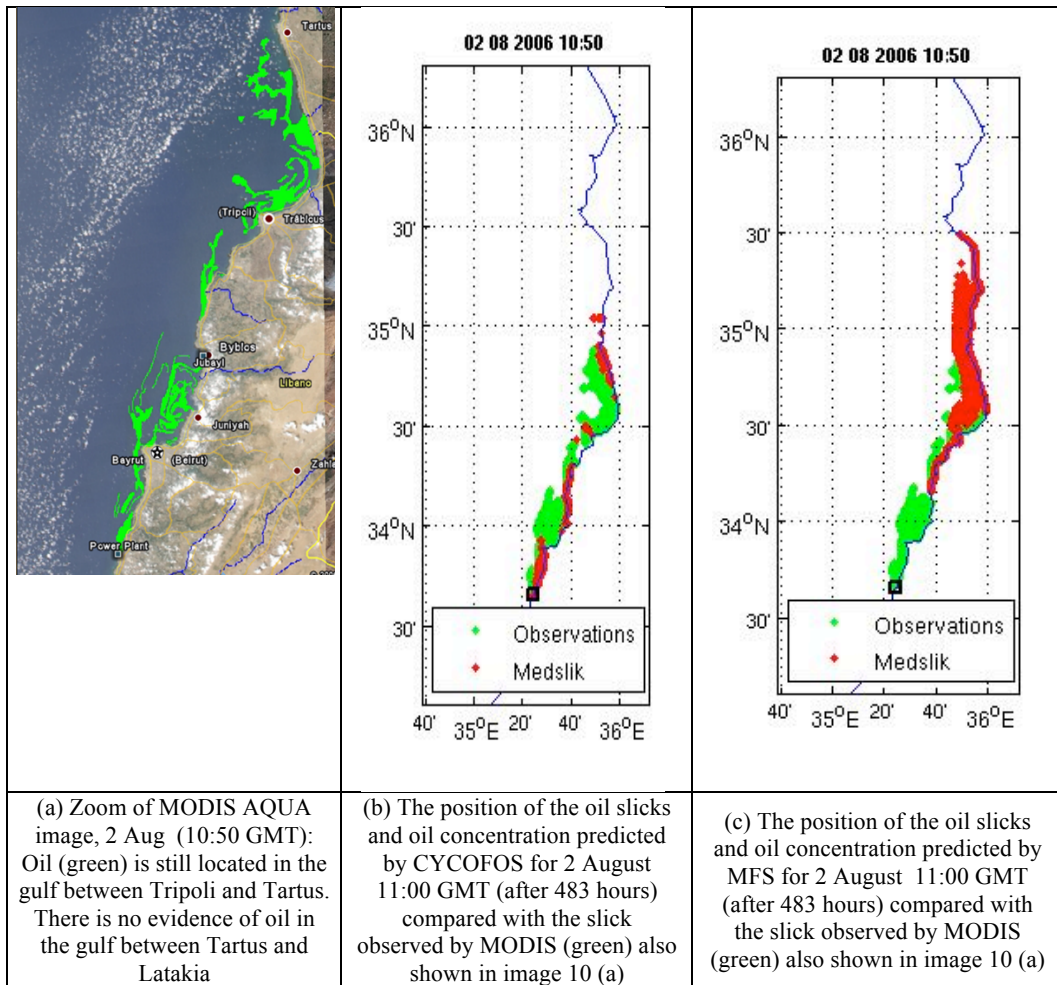


Figure 3.10. Panel (a) shows the MODIS AQUA images of August 2, 2006, 10:50 GMT . Positions of the observed slicks (panel a) are compared with the predicted positions by CYCOFOS (panel b) and by MFS (panel c).

The oil continues to move northward and the comparison, on 2 August (Figure 3.10 a) shows that the oil spill has reached Tartus. The CYCOFOS prediction (Figure 3.10 b) shows a good agreement with the satellite image, the model seems still to underestimate the offshore extension of the slick in the Gulf of Tartus and in the Gulf of Beirut; the MFS prediction (Figure 3.10 c) is in good agreement with the satellite observation in the Gulf of Tartus but the model underestimates the oil in the Gulf of Beirut and overestimates the northernmost extension of the observed slick.

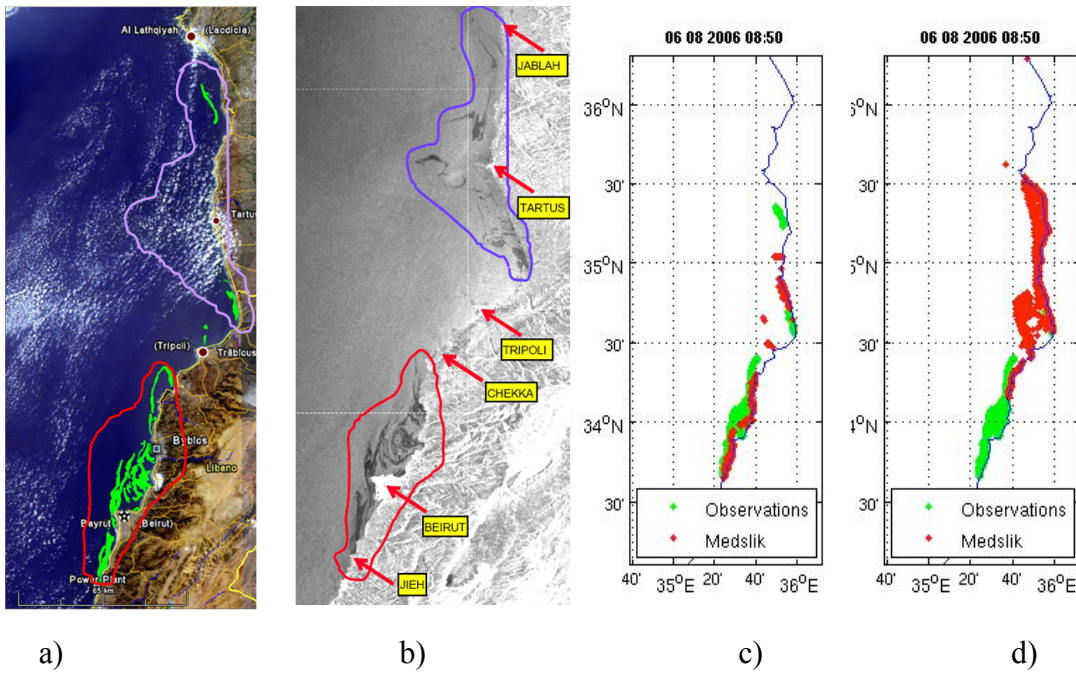


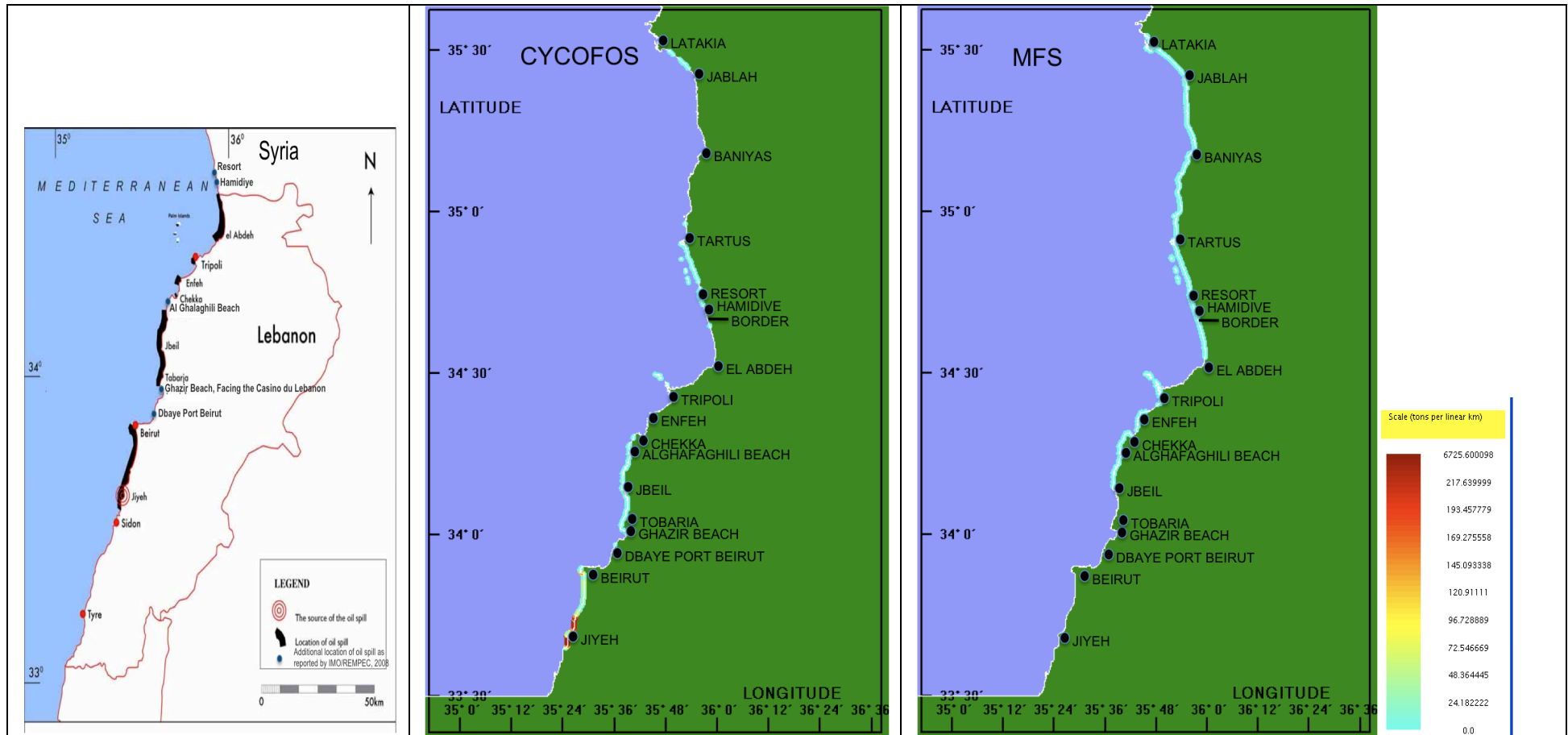
Figure 3.11. 6 August 2006 comparison between: a) MODIS TERRA image at 8:50 GMT; b) ASAR image at 7:51 GMT courtesy of ESA and JRC; c) position of the oil slicks predicted by CYCOFOS on 6 August 9:00. GMT (after 576 hours) and d) position of the oil slicks predicted by MFS on 6 August 9:00. GMT (after 576 hours)

On 6 August an ASAR image is also available (7:51 GMT). In Figure 3.11 we present both the MODIS TERRA 8:50 GMT image (Figure 3.11 a) and the ASAR image at 7:51 GMT (Figure 3.11 b). The MODIS-ASAR comparison highlights that the method used for detecting oil spill in the visible bands of MODIS works well. In fact, the slick patch (green) localized in the Beirut area shows a pattern that matches the one retrieved in the ASAR image. However, in the portion of sea close to Tartus, clouds preclude the detection of the oil slick by the visible sensor, while slicks are present in the ASAR picture. Nevertheless, it is possible to detect the presence of a slick in a partially cloud-free area south of Latakia in the MODIS picture. The importance of the integration of the information from the two satellite datasets is obvious: in clear sky conditions MODIS can monitor an area of interest twice a day, resolving the temporal evolution of the event while ASAR validates the MODIS image and provides information in cloudy areas. The CYCOFOS prediction reproduces well the evolution of the oil slick apart from underestimation of the northernmost extension of the slick. The MFS prediction underestimates the oil in the Gulf of Beirut but reproduces well the oil detected south of Tartus in the ASAR image. MFS overestimates the northernmost component of the slick.

Oil on the Lebanese coastline was observed and reported by the Green Line Association (GLA, 2006), by the Experts Working Group for Lebanon in 2006 (EWGL, 2008) and by World Bank report (World Bank, 2007). Figure 3.12 presents the areas of the Lebanese coast that have been reported to be impacted by oil pollution. The observations of oil on the Syrian coast are few;

according to the declarations of Syrian Government representatives, a first ‘wave’ of oil arrived on the coast on 26 July, a second ‘wave’ arrived on 2 August (IMO/REMPEC and Joint UNEP/OCHA, 2006). According to the Expert mission in Syria (REMPEC, 2006 and Amato and Alcaro, 2006) oil residues affected beaches along the coast of Syria from the Lebanese border to Baniyas, 50 km north of Tartus. Oil residuals, after cleaning operations had already occurred, were collected at the following locations in Syria by a delegation of international experts (IMO/REMPEC and Joint UNEP/OCHA, 2006): at the Lebanese/Syria Border (34°38’27.3”N - 035°58’22.3”E), Hamidiye (34°42’36.4”N - 035°56’38.2”E) and Resort (34°44’37.4”N - 035°55’54.1”E). The latter location was, according to the Syrian Authorities, the northernmost area where oil pollution could be visually detected. Out of the three Syrian sites visited, this beach appears the least affected by oil residues (IMO/REMPEC and Joint UNEP/OCHA, 2006).

The CYCOFOS simulation showed oil deposition on the coast (Figure 3.12 b) extending northward and southward of Jieh. North of Jieh the oil at the coast is simulated up to Beirut in agreement with the observations. The MFS simulation (Figure 3.12 c) does not show oil at the coast south of Jbeil, which is not in agreement with the observations (Figure 3.12 a) that show oil at the coast south of Jbeil (from Jiyeh to Beirut and from Ghazir to Jbeil). Observations show oil on the coast from Ghazir Beach to a position south of Chekka, these observations are very well reproduced by CYCOFOS and MFS (only for the part north of Jbeil). Between Chekka and Tripoli oil is observed only at Enfeh and south of Tripoli, MFS simulation overestimates these observations while CYCOFOS seems to underestimate them. The beached observed between El Abdeh and the Lebanese/Syrian border is reproduced by MFS, which seems to overestimate the oil north of Resort location along the Syrian coast. The CYCOFOS simulation results (Figure 3.12 b) underestimate the oil observed between Abdeh and the Border while reproduce the observation in Hamidive and Resort but overestimate the oil north of Resort. CYCOFOS shows small amount of oil south of Latakia where the model forecast oil on the coast but no clear observation was reported, while MFS strongly overestimates the oil in this part of the Syrian coast.



a) b) c)

Figure 3.12: Panel a shows the oil as observed along the Lebanese coastline by the Green Line association (GLA, 2006) integrated with the observations reported by the Experts Working Group for Lebanon in 2006 (EWGL, 2008). Panel b and c present the oil at the coast (Tons per linear km) on 6 August 2006 simulated by CYCOFOS (Experiment 1) and MFS (Experiment 6) respectively, the color palette is the same for both panel b and c.

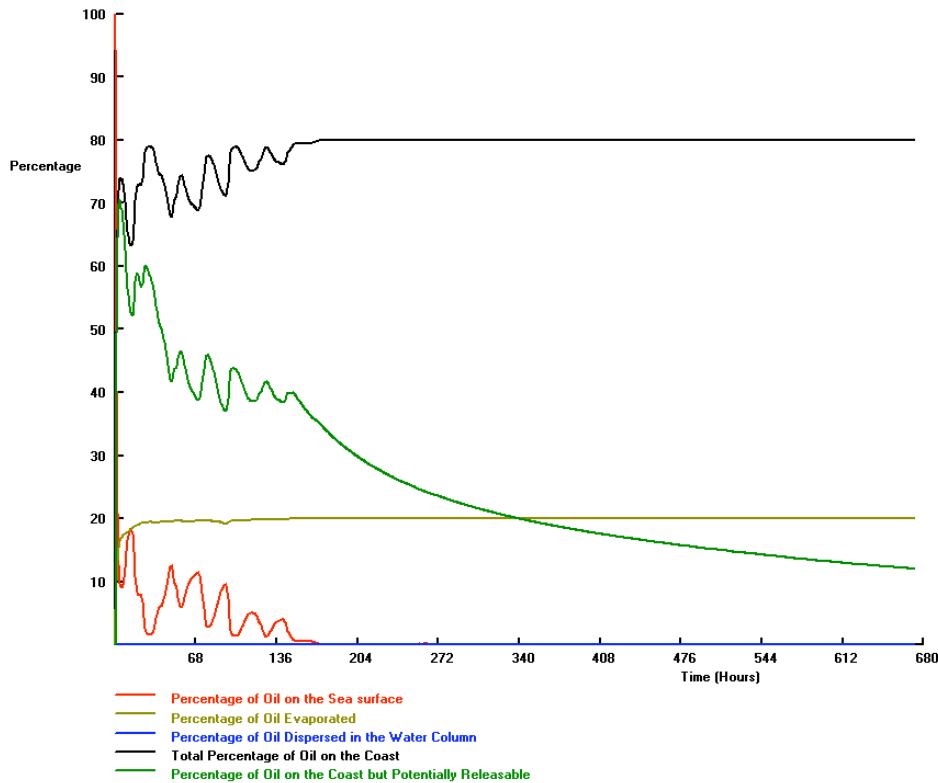


Figure 3.13. Fate parameters simulated by CYCOFOS (Experiment 1) from 13 July 2006 to 6 August 2006.

The CYCOFOS simulation shows that the percentage of oil on the surface decreases as the percentage of oil on the coast increases (Figure 3.13), as expected. The rate of absorption of oil onto the coast decreases as the existing coastal loading becomes larger; this implies that greater amounts of oil are available for re-entering the sea when the winds and currents are offshore. In less than 2 days of the start of the incident, due to the high SST (Figure 3.4), evaporation was high and a little less than 20% of the original oil had evaporated (Figure 3.13). The oil fate graphs show that after 28 days (672 hours) 80% of the oil is on the coast as before, but about 10% of that is still free to move back to the sea. The model predicted that after 8 days (192 hours) less than 1% of the original oil was dispersed into the water column and less than 1% remained on the surface.

3.1.7. Sensitivity Experiments

The sensitivity experiments have been designed to test the impact of using water currents from MFS and CYCOFOS, the wind factor and angle parameters and thus the depth of the currents considered. The sensitivity experiments results are synthesized in Figure 3.14 for 23 July 2006. The simulations from CYCOFOS are presented in panels a, b and c while panels d, e and f show the comparison with the simulation by MFS.

Experiment 1 clearly reproduces well the northward and coastal extension of the oil slick but it underestimates the offshore extension. Experiments 3 (Figure 3.14 b) and 5 (Figure 3.14 c), carried

out with surface currents and Stokes drift parametrization, underestimate the oil slick northward extension. This clearly shows a difficulty of the CYCOFOS system to properly model the Ekman transport probably due to sigma layers displacement.

Figure 3.14 shows also the MFS simulation results which overall seem to be less sensitive to the model parametrization tested in the present work. MFS simulation number 7 seems to be the most appropriate. We conclude that MFS is lacking the correct current amplitude because of the coarse resolution but it resolves well the Ekman flow.

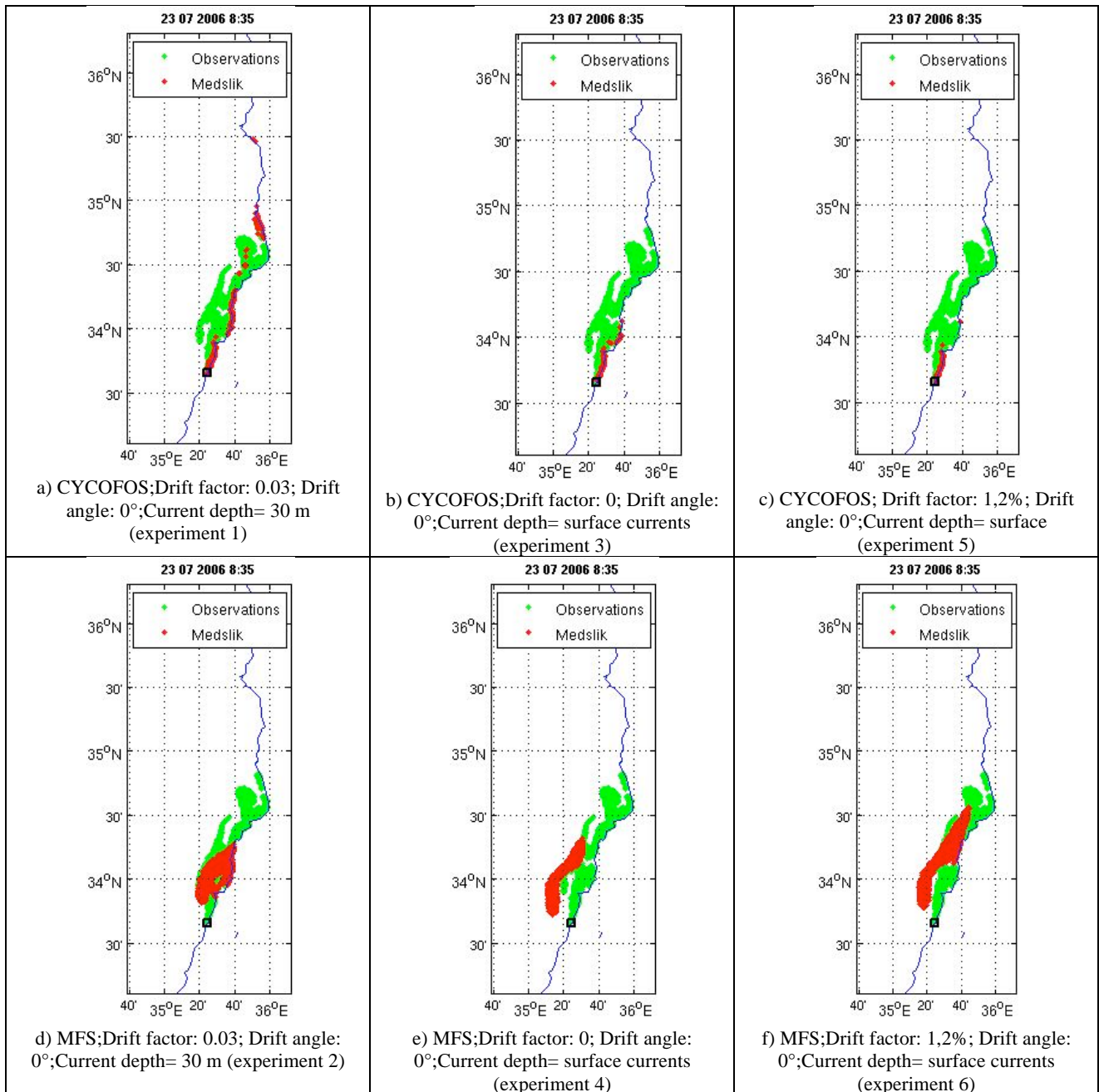


Figure 3.14. Comparison for 23 July 2006 between MFS and CYCOFOS simulations (red) with different wind parameters and different current depth and the oil slick extension as resulting from the MODIS TERRA 8:35 GMT satellite image (green).

3.1.8. Conclusions

The Lebanon oil pollution event is the largest oil pollution incident in the Eastern Mediterranean Sea so far. The oil spill affected most of the Lebanese coast and, as it was drifting northward for over one month, reached the southern Syrian coast. At the time of the Prestige oil spill incident in 2002 only limited operational oceanographic products were available to assist the response agencies and certainly none were available at the time of the Haven oil spill incident in 1991. During the entire period of the Lebanese oil pollution crisis in July-August 2006, however, MOON was able to provide daily information on the displacement of the oil slicks.

This work shows that the technological innovation coming from operational oceanography, providing satellite images and real time forecasts on currents gives the possibility to precisely map the damage of oil spills even if very near the coasts. The satellite observing products used for oil slick detection and for validation of the MEDSLIK oil spill drift predictions were shown to be robust and capable of providing valuable operational information during this oil spill accident.

Integration of different satellite sensors (ASAR, MODIS) done during the Lebanon oil spill event is shown to be a key element in monitoring oil spill incidents properly and in a timely fashion. The integration of optical and SAR sensors aboard satellites allows to monitor oil drift evolution in space and time at unprecedented resolution. The comparison of MODIS and ASAR observations highlight (Figure 3.11) that different satellite sensors can give similar results and that these can be used to validate the models.

Sensitivity experiments to different deterministic oil spill drift factors show that best results still require ad-hoc tuning of parameters such as the current depth from the hydrodynamic model, and the wind drift factor and angle. These parameters are considered to account correctly for the Ekman drift velocities and Stokes drifts. Sensitivity experiments show that best results for a relatively coarse MFS current field are obtained when the surface currents are corrected by a Stokes drift factor (Rascle and Ardhuin, 2005 and Ardhuin et al, 2009). For CYCOFOS instead, the deterministic part of the oil drift seems to be better parameterized with 30 meter currents with a wind drift factor of 3% and wind drift angle of 0° .

Our results indicate that both MFS and CYCOFOS models coupled to MEDSLIK are capable in reproducing the timing and transport of the oil northward, along the Lebanese and Syrian coasts. This comparison also shows that the CYCOFOS currents in MEDSLIK represent better the coastal trapping of the oil. This is due to the higher horizontal resolution of the CYCOFOS forecasting system that allows to better resolve the alongshore currents and allows to place the start of the oil spill closer to the coasts, near the real oil source.

MEDSLIK predicted that after 6 days almost 80% of the original spilled oil at sea was permanently landed along the Lebanese and South Syrian coasts, 20% of the original oil was evaporated, while less than 1% of the oil remained in the sea. Coastal impact was observed to be heaviest from Jieh up to south of Beirut but also significant impacts between Beirut and Chekka and northwards in the Syrian coast were reported. It is found that MEDSLIK coupled to MFS probably overestimates the northernmost part of the slick on the Syrian coast, even though the validation of this hindcast is difficult because the quantities of oil that reached the northern Syrian shores were not clearly reported.

The operational implementation of the MEDSLIK oil spill model during the Lebanese oil pollution crisis, using the CYCOFOS and SKIRON products, made it possible to provide the ‘situation on the ground’ to EU and UN agencies and other decision makers in the region, and to assist them in drawing up an international action plan for the clean up operations in response to the biggest case of oil spill pollution in the Eastern Mediterranean so far.

3.2. The ERO exercise

3.2.1. Summary of the OSCAR-MED operation

The Coordinated Surveillance Operation in the Western Mediterranean (OSCAR-MED) was organized by the Regional Marine Pollution Emergency Response Centre for the Mediterranean Sea (REMPEC) between 12 and 16 October 2009 from the airbase of Hyères (Toulon), France, in close cooperation with the French Préfecture Maritime de la Méditerranée.

This activity represented the first attempt in the Mediterranean region to enhance operational cooperation in combating illicit discharges and was aimed not only at ensuring an extended aerial coverage but also at exchanging information on the pollution detected among the different countries and at facilitating the process for a successful prosecution of the offenders in the region.

The zone was also chosen because it is known that a high number of pollution events are detected by satellite and aerial surveillance and the coastal member states in this area are performing monitoring activities with the objective of detecting polluting slicks and possibly identifying ships discharging oil at sea, which goes against the laws on discharges of oil at sea defined in the MARPOL convention (Marpol, 1973). The operation took advantage of state-of-the-art monitoring and forecasting systems by using EMSA-CSN products (European Maritime Security Agency – CleanSeaNet), Italian, Spanish and French aerial fleets equipped with instruments for oil slick detection and the MOON (Mediterranean Operational Oceanography Network) ocean monitoring

and forecasting system to provide meteo-oceanographic forecasts and oil spill drift forecasts. MOON participation was coordinated by the MOON-REMPEC Emergency Response Office¹¹, which is the operational virtual office that coordinates the contribution of the MOON partners in the MOON-REMPEC agreement¹².

During the OSCAR-MED operation three oil spills were identified by aircraft, one oil spill was detected from CNS-EMSA service and confirmed by aircrafts and MOON-ERO provided relevant meteo-ocean forecasting information relevant to the flight missions, and the oil spill forecasting models results were in some cases validated by observations made by the surveillance aircraft. Moreover, three ships were caught red-handed, two of them while discharging mineral oil within the French Ecological Protected Zone (EPZ). The French authorities are investigating the two polluting ships.

3.2.2. Introduction

3.2.2.1. REMPEC: Combating operational discharge in the Mediterranean

The Regional Marine Pollution Emergency Response Centre for the Mediterranean Sea (REMPEC) assists the Mediterranean coastal states in ratifying, transposing, implementing and enforcing international maritime conventions related to the prevention of, preparedness for and response to, marine pollution from ships.

One of REMPEC's objectives is to combat the permanent risk from oil spill pollution in the Mediterranean Sea associated with illegal/operational discharge of oil by merchant vessels and ferries. The OSCAR-MED operation, which represents the follow-up of previous activities carried out by the Centre in the field of illicit discharges from ships, is perfectly in line with Specific Objective 6 of the Regional Strategy for the Prevention of, and Response to, Marine Pollution from Ships ('the Contracting Parties agreed to endeavour to establish, by 2010, sub-regional systems, including procedures to over-fly the waters under the jurisdiction of a neighbouring State if the Parties so agree, for surveillance of environmentally sensitive and/or high risk zones of the Mediterranean Sea') and has fully demonstrated that regional cooperation, particularly in terms of surveillance and investigation, represents a key issue for combating illicit discharges in the Mediterranean Sea.

¹¹ ERO web site: (http://www.moon-oceanforecasting.eu/index.php?option=com_content&task=view&id=86&Itemid=45)

¹² MOON-ERO agreement: http://www.moon-oceanforecasting.eu/files/REMPEC-MOON_Agr_2_10_2008.pdf

3.2.2.2. *The MOON-REMPEC agreement and the Emergency Response Office*

MOON and REMPEC established a collaboration agreement in April 2009. MOON partners and REMPEC entered into the agreement with a view to ensuring maximum coordination of the work and activities of REMPEC and MOON in respect to matters of common interest.

The agreement has the following scope of co-operation:

a) To share information and outputs of their respective activities for the purpose, and within the scope, of this agreement, subject to arrangements as may be necessary for safeguarding confidential information;

b) To utilize MOON members' expertise in the activities which are regularly carried out by REMPEC (e.g. training, organization of workshops, conferences and assistance in contingency planning);

c) To collaborate in assisting the Mediterranean coastal states, upon request, in emergency situations. In particular, relevant MOON members will provide the Centre with meteoceanographic forecasting data and oil spill drifting predictions for the affected area for prompt dissemination by REMPEC as appropriate. MOON members will further endeavour to identify and establish contact with other relevant oceanographic institutes, which could assist REMPEC during the emergency phase;

d) To collaborate in the development of projects for the prevention of operational pollution from ships in the Mediterranean region. The relevant MOON members will make available meteoceanographic data and oil spill applications (forecasting/hindcasting modelling) to enhance the possibility of identifying the polluting ship;

e) To collaborate in the development of the MOON network with a view to enhancing high resolution meteoceanographic forecasting data in areas of the Mediterranean where at present there is a lack of data; and

f) To cooperate in the development of oil risk maps for the Mediterranean region. REMPEC will contribute to fine-tuning the development of these maps through its knowledge regarding marine pollution from ships and, where possible, by providing data on the main shipping lanes in the region.

A virtual MOON Emergency Response Office (ERO) has been established to serve as the coordinating body for MOON members to receive, evaluate and disseminate information.

The ERO consists of an expert board to which MOON partners and REMPEC have each nominated one expert, and is headed by an ERO manager nominated by the board. The ERO functions as follows: in the event of an oil spill or other emergency, REMPEC will contact the ERO manager, who will compile the information and transmit it to the Expert Board via e-mail

and/or fax, as appropriate. The relevant members of the Expert Board will provide appropriate information, which the ERO manager will then relay to REMPEC.

ERO has recently participated in the REMPEC operation OSCAR-MED as described in this report. ERO provided 24h assistance producing oil spill drifting forecasts of the slicks detected by satellite and by the surveillance aircraft.

3.2.3. Area of the operation, participants and monitoring and forecasting systems used

3.2.3.1. Area of the operation.

The area identified for the OSCAR-MED operation is between Genoa and Barcelona, and is one of the three main traffic routes of commercial maritime traffic in the western Mediterranean. It is presented in Figure 3.15.

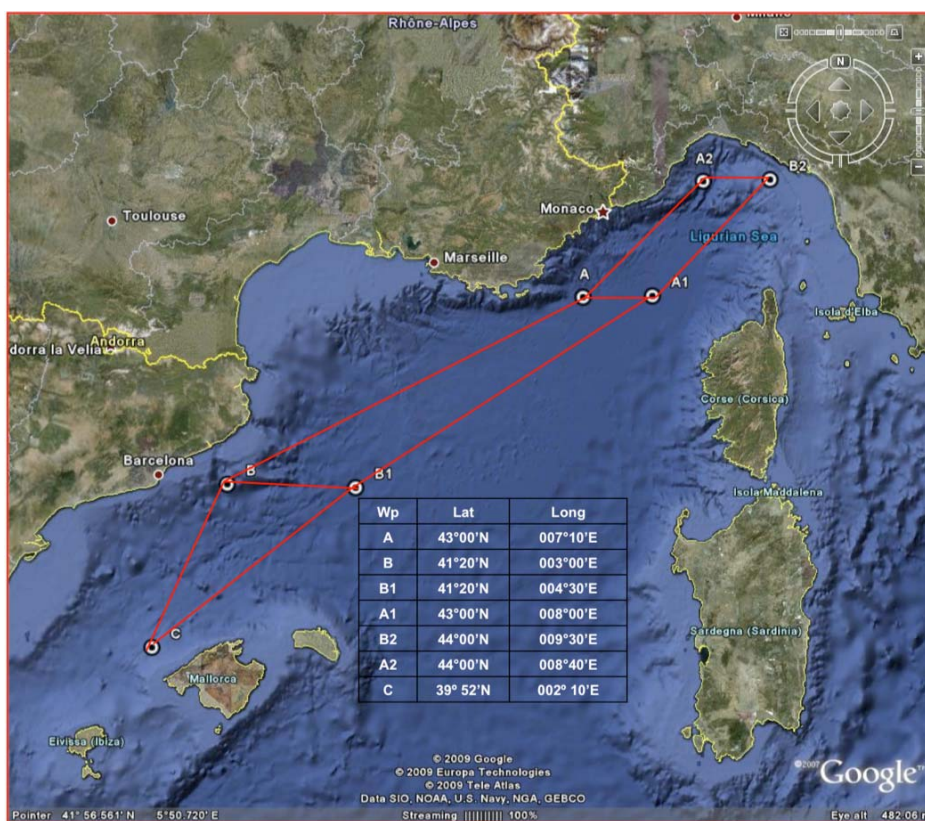


Figure 3.15. Area of OSCAR-MED operation. Wps (waypoints) define the perimeter of the operation and the red lines mark the tracks followed by the aircraft.

The general circulation of the western Mediterranean is characterized by the Liguro-Provençal current, which flows westward along the Italian and French coasts, and by the Gulf of Lion gyre. Aircraft monitored the area along the routes A/B/B1/A1, while points C and A2/B2 were flown

over only by the aircraft that had enough fuel capacity. Moreover, flight schedules were planned on the basis of operational and weather conditions.

3.2.4. Participants in the operation

The activities of MOON were coordinated by the ERO-Manager, Giovanni Coppini, and the following people from ERO participated in OSCAR-MED: Giovanni Coppini, ERO manager (INGV); Micol Ferretto, forecaster (INGV); Pierre Garreau, ocean modeller and forecaster (IFREMER). Moreover, ERO provided distributed assistance and several ERO experts following the established ERO procedures sent products to the ERO managers. The ERO experts and colleagues that contributed to the operation are: Michela De Dominicis (INGV), Nadia Pinaridi (INGV), Roberto Sorgente (CNR-IAMC), Leopoldo Fazzioli (CNR-IAMC), Rosalia Santoleri (CNR-ISAC), Gianluca Volpe (CNR-ISAC), Simone Colella (CNR-ISAC), Joaquin Tintore (CISC), Guillermo Vizoso (CSIC), George Kallos (IASA) and George Galanis (IASA).

The following people from the Italian Coast Guard participated to the operation: C.V. (CP) Giovanni GALATOLO, as Italian Project Coordinator of the operation, C.F. (CP) Vittorio PAGOTTO, Chief of the Sezione Operazioni reali, Operational Centre, and S.T.V. (CP) Debora FERIOLI, part of Sezione Impiego dei Sistemi, Operational Centre.

From France, in addition to the members of Maritime District of Toulon, Christian COSSE participated as an expert in marine pollution from French Customs and coordinator of the French mission; from Spain, there participated representatives of the Ministerio de Fomento – Dirección General de la Marina Mercante and SASEMAR (Spanish Maritime Safety Agency). Moreover, the Directeur de la flotte et de la navigation maritime from the Ministère du Transport Tunisien participated as an observer.

3.2.5. Aerial and satellite monitoring systems used in OSCAR-MED

3.2.5.1. Aerial surveillance with aircraft

All the countries of the western Mediterranean basin had replied positively to this initiative, and France, Italy and Spain confirmed their participation by making a surveillance aircraft available. Italy carried out the operational part of the mission using the ATR 42 *Manta 02* (Figure 3.16) from the 3rd Nucleo Aereo di Pescara, with 14 crew members and equipped with SLAR, Torretta EOST with IR, ATV and Long Range and radar for searching and light for searching at night.



Figure 3.16. ATR 42 'Manta 02' from the Italian Coast Guard.

Spain provided CN-235 of SASEMAR, with 11 crewmembers and equipped with SLAR, Scanner IR/UV, LFS, MWR, radar and AIS.

France provided two Customs F406 POLMARs, with 16 crewmembers, equipped with SLAR, IR/UV scanner, AIS, SATCOM and MWR/LLTV.

Flights were performed within the survey area (along the axis Genoa-Barcelona) during both day and night hours between Tuesday 13 October (0900 hrs local time) and Thursday 15 October (1800 hrs local time). Aircraft were used in the monitoring activities following a flight plan of 20 hours for each country. Moreover, surveillance at sea was ensured by a French anti-pollution vessel, while the Italian coast guard patrol *CP 905* of the was in Genoa harbour, ready to move if needed.

3.2.5.2. The CleanSeaNet monitoring system

The European Maritime Safety Agency (EMSA) supported the operation by providing satellite images analysed for oil slick detection through the CleanSeaNet service.

On the basis of Directive 2005/35 on ship-sourced pollution and the introduction of penalties for infringements, EMSA provides the CleanSeaNet oil spill monitoring service to the national maritime administrations of 24 coastal states, consisting of 22 European member states, Croatia and Norway. This technical assistance focuses on tracing potential discharges by satellite monitoring and, when required, satellite monitoring during an oil pollution emergency. The service began in April 2007 and provides oil pollution alerts and analysed satellite Synthetic Aperture Radar (SAR) images to national contact points responsible for operational follow-up actions in coastal states.

During OSCAR-MED operation EMSA provided 3 satellite image reports during the 3-day operation as reported in Table 3.3 Figure 3.17 presents the areas covered by the 3 images.

Satellite name	platform	Date of acquisition	Time of acquisition
ENV		13/10/2009	09:41:29
RS-1		14/10/2009	17:29:58
RS-1		15/10/2009	05:42:22

Table 3.3. Summary table of the satellite images provided by CNS-EMSA for the OSCAR-MED operation.

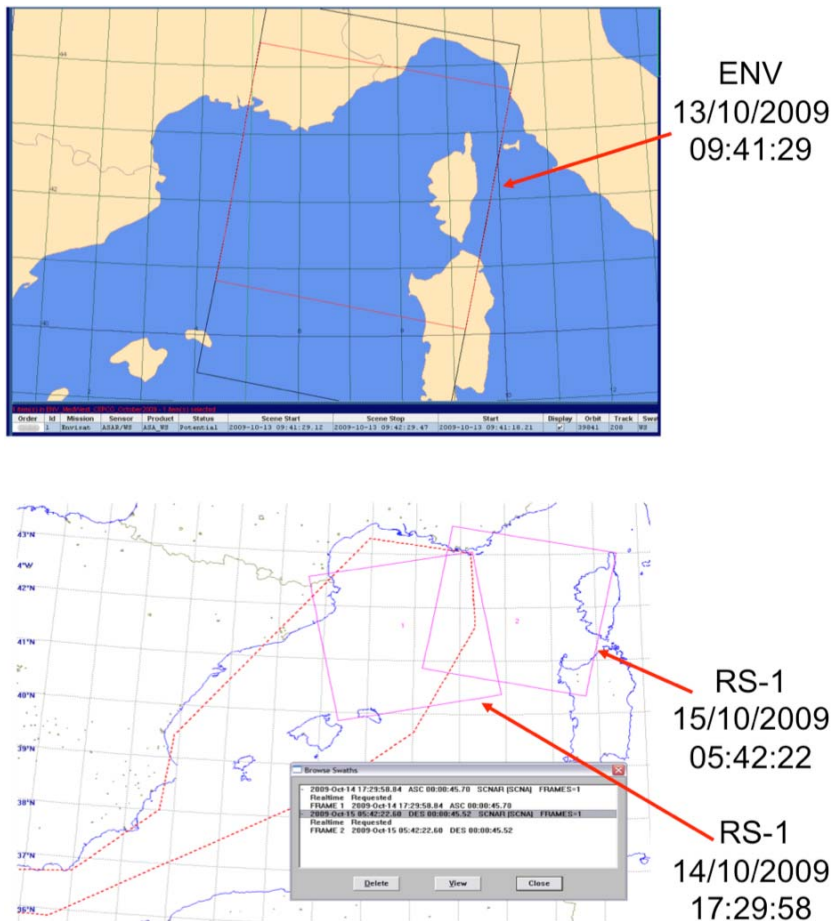


Figure 3.17. Areas covered by the 3 CNS satellite images provided by EMSA-CSN: the upper panel is related to the first ENVISAT image and the area that has been covered ENVISAT satellite passage on the 13 October 2009 at 09:41:29 is identified by the square shape inside the rectangular one. The lower panel presents the areas covered by the two images produced by Radarsat-1 satellite passages on the 14 October 2009 at 05:42:22 (square on the right) and 14 October 2009 at 17:29:58 (square on the left).

The image from ENVISAT identified 3 oil slick north west of Corsica Island (Figure 3.18) while the second and third satellite passage by RADARSAT-1 did not identified any oil slick. Based on the information provided in the report from EMSA-CSN on the ENVISAT passage ERO was activated and different oil spill forecasting system were activated. In figure 3.21 we present the results of the simulation carried out by IFREMER-PREVIMER system. Moreover based on the satellite information in Figure 3.18 aerial means from SASEMAR and Italian Coast Guard. EMSA-CSN report also provide shape file containing the information on the position of

the oil slick detected, this information is provided through a certain number of geo-located points. Figure 3.19 shows the shape of the oil slick detected from ENVISAT satellite and provided by EMSA-CSN.

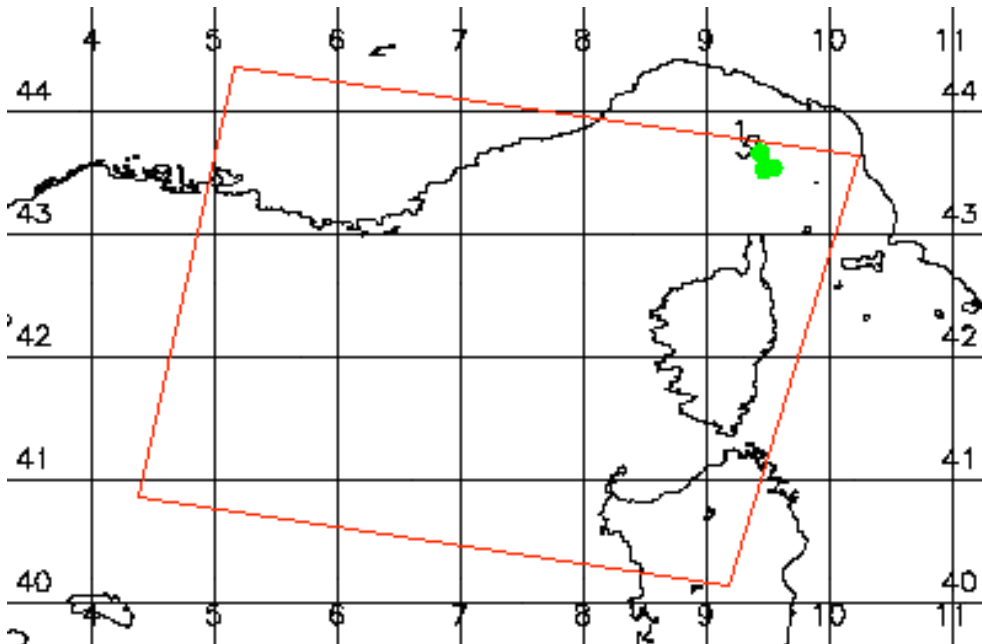


Figure 3.18. ENVISAT satellite passage area on the 13 October 2009 at 09:41:29 (red line), the presence of oil is highlighted with green dots (source EMSA-CSN report).

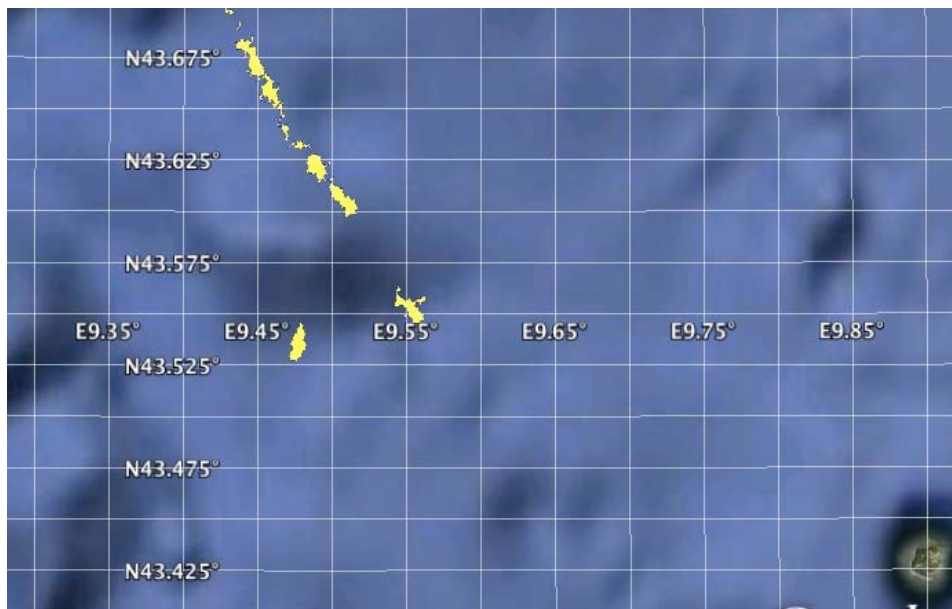


Figure 3.19. Position of the oil slicks as detected by ENVISAT passage of 13 October 2009 at 09:41:29 and provided by EMSA-CSN. The oil slicks are represented by a certain number of geo-located points (yellow).

3.2.6. ERO procedures and ERO-MOON monitoring and forecasting systems

After the formal establishment of ERO in September 2009, ERO started to operate and OSCAR-MED was the first operation in which ERO was acting in operational mode serving

REMPEC requests and providing real-time products. In September 2009 a first set of procedure to operate ERO and to communicate among ERO experts was drafted. These procedures have been refined on the basis of the OSCAR-MED operation and are described in the next paragraph.

3.2.6.1. ERO procedures

The ERO procedures are not fully activated yet, and for instance ERO-WEB is not implemented yet, so for the time being communication is carried out using e-mails and the assembling of the bulletins is done manually by the ERO manager on the basis of the ERO expert contributions sent by e-mail. A scheme of the ERO communication steps is presented in Figure 3.20.

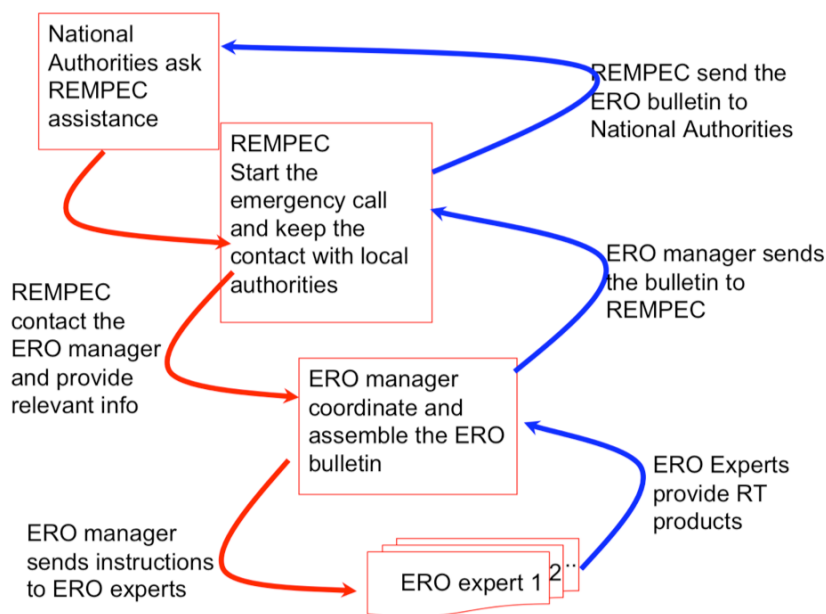


Figure 3.20. Scheme of ERO communication steps.

The following procedures describe the steps that have been designed to be followed after the request of support by REMPEC to the ERO:

- Phase1: REMPEC will contact by phone the ERO manager using the given telephone number and introduce him/herself. REMPEC informs him that an emergency call will be activated on ERO-WEB. The ERO manager can also be contacted using the email ero-manager@bo.ingv.it
- Phase2: REMPEC activates the emergency call on ERO-WEB by filling the dedicated form with the relevant information (accident location, accident time...). Once the available information has been included, ERO-WEB sends an automatic e-mail with all the information uploaded (preliminary info sheet) to the ERO manager and REMPEC. An sms is also sent to the ERO manager with the relevant information.

- Phase3: The ERO manager acknowledges reception of the emergency call (via e-mail, telephone call). In this phase the ERO manager could ask for clarifications on the provided information. The ERO manager will then activate the emergency call on ERO-WEB and an e-mail and sms will be sent through ERO-WEB to all the ERO partners (ero@bo.ingv.it). In this e-mail the ERO manager will also propose which ERO partners should participate in the emergency call on the basis of accident location and the characteristics of their systems and products:

1. Forecasting model domains
2. Availability of ancillary data (wind, waves, SST)
3. Availability of satellite oil spill observations

Invited ERO partners will have to acknowledge their participation in the emergency call (logging in into ERO-WEB with their account and confirming or denying participation; an e-mail will be sent by ERO-WEB to the ERO manager). The ERO partners that positively confirm are defined as activated partners.

- Phase4: The ERO manager will decide, consulting ERO activated partners if need be, the technical details needed to run the models and to produce the outputs:
 1. graphical details (palette scale, domain of the figures to be produced...) on the basis of the time of the accident and location;
 2. information needed to run the models that may be not available at first (duration of the spill, type of oil...);
 3. output frequency of oil spill forecast, duration of the forecast;

If points 2 and 3 are not available at the very beginning of the emergency, the technical sheet will be used to issued a meteoceanographic bulletin (see P-6).

The ERO manager will send a new e-mail though ERO-WEB with this info (technical sheet) to the activated partners. The technical sheet contains the preliminary info sheet.

Note: the technical sheet can be re-issued at any time when new information became available. The ERO manager will update the information on ERO-WEB and this will be sent to the activated partners

- Phase5: ERO activated partners will start at this point the simulations and will start to process their data (satellite...). Once available, results of the simulation and satellite products will be uploaded by each activated partner onto ERO-WEB. ERO activated partners, once they have finished uploading their information (figures, texts...), submit the contribution. An automatic acknowledgment is sent to the ERO manager (mentioning the product issued and the related technical sheet version used).

- Phase6: ERO will first issue an ERO bulletin (ERO manager creates/exports this bulletin on ERO-WEB) in a few hours, with meteo-oceanographic information (to be fully established after the November meeting) in the sub-region of interest. This first bulletin is issued only if in the early hours there is not enough information to run the oil spill models, in the case where all the information is available, this bulletin is issued with the inclusion of the oil spill forecast (see P8).
- Phase7: The ERO manager discusses the results with the ERO activated experts. If the first bulletin is issued only with meteo-ocean info, the procedure restarts at ERO phase4 with the preparation of the complete technical sheet.
- Phase8: The ERO manager delivers the second ERO bulletin with the oil spill forecasts from all the available systems within 6-12 hours
- Phase9: ERO will continue to follow the emergency case until REMPEC requests support, issuing updated bulletins on a daily basis.
- Phase10: ERO, after each REMPEC call, will prepare a short note on possible improvements of procedures and protocols and lessons learnt. The objective is to improve the procedures step by step. REMPEC and users may be asked to fill an evaluation report including the feedback from the users and estimate of the advantage (timing, kind of information...) of the service. MOON partners will be asked to assess the cost in terms of personnel hours, computing, etc.
- Phase11: ERO will decide how to disseminate the information to the public on a case-by-case basis.

The second release of the bulletin may contains less model outputs, meaning that ERO may decide to take out less realistic output. The web structure should have a backup and alternative site, and this will be describing in a separate document. The backup could be at the Hellenic Centre for Marine Research.

3.2.6.2. ERO forecasting models used in OSCAR-MED

MOON basin-scale forecasting products (MFS and MERCATOR) and 4 sub-regional MOON forecasting systems (PREVIMER, Western Med regional model, 2 ESEOO) were used to provide current and surface temperature forecasts, and some of them to force several oil spill models (MEDSLIK, MOTHY, IFREMER oil spill model).

MEDSLIK-II was used coupled with hourly time resolution oceanographic fields from the Mediterranean Forecasting System (MFS-<http://gnoo.bo.ingv.it/mfs>) (Pinaridi et al., 2003).

The MERCATOR forecasting system was used to force the MÉTÉOFRANCE oil spill model MOTHY. This system is fully operational in the context of MPRES-JCOM. The PREVIMER forecasting system from IFREMER, nested in MFS, was used to force the IFREMER trajectory model. The Western Mediterranean Regional Model forecasting system by CNR-IAMC provided current and SST forecasts. The ESEOO Balearic forecasting system, nested in MFS, provided current and SST forecasts. The ESEOO MED forecasting system, nested in MFS, provided current and SST forecasts. Moreover, the ECMWF and SKIRON atmospheric forecasting systems provided wind forecasts. USAM/CNMCA (Italian Met Office) provided through INGV the ECMWF forecast. The SKIRON and PREVIMER forecasting systems provided wave forecasts. To be mentioned that the service provided by SKYRON team appeared well organized and based on automatic procedure; this simplified a lot the provision of zoomed products and the downloading procedure. The SKIRON ftp service was considered very efficient and more operational if compared with the products sent by email.

The ERO manager, with the help of the ERO colleagues participating in the operation in Toulon, collected the different figures sent by ERO experts and prepared a bulletin including expert comments. The bulletin was then printed and distributed to the OSCAR-MED participants. An example of the content of the oceanographic and meteorological part of the ERO bulletin is presented in Figure 3.21 (surface currents) 3.22 (sea surface temperature), 3.23 (waves) and 3.24 (winds).

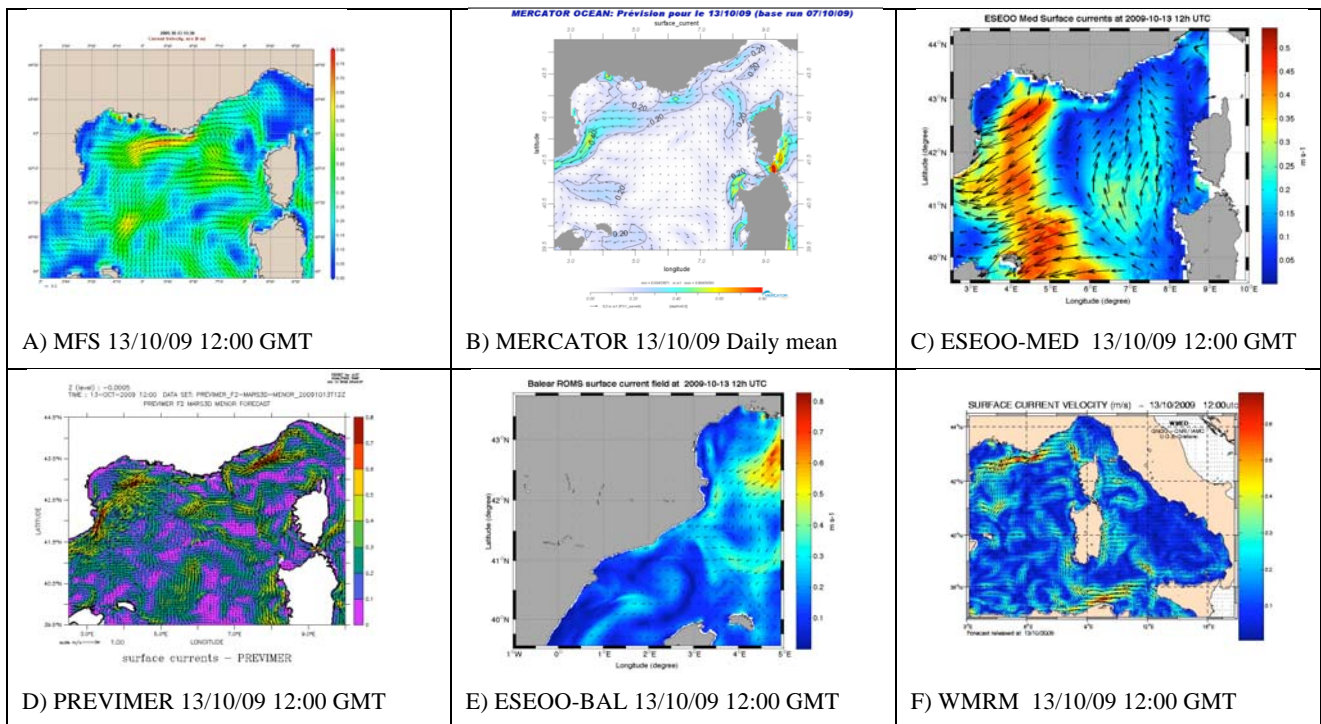


Figure 3.21. Example of the content of the oceanographic part of the ERO bulletin distributed in the context of the OSCAR-MED operation: surface currents (m/s) forecasts for 13/10/2009 from 2 different basin (A and B) and 4 sub-regional (C, D, E and F) forecasting systems.

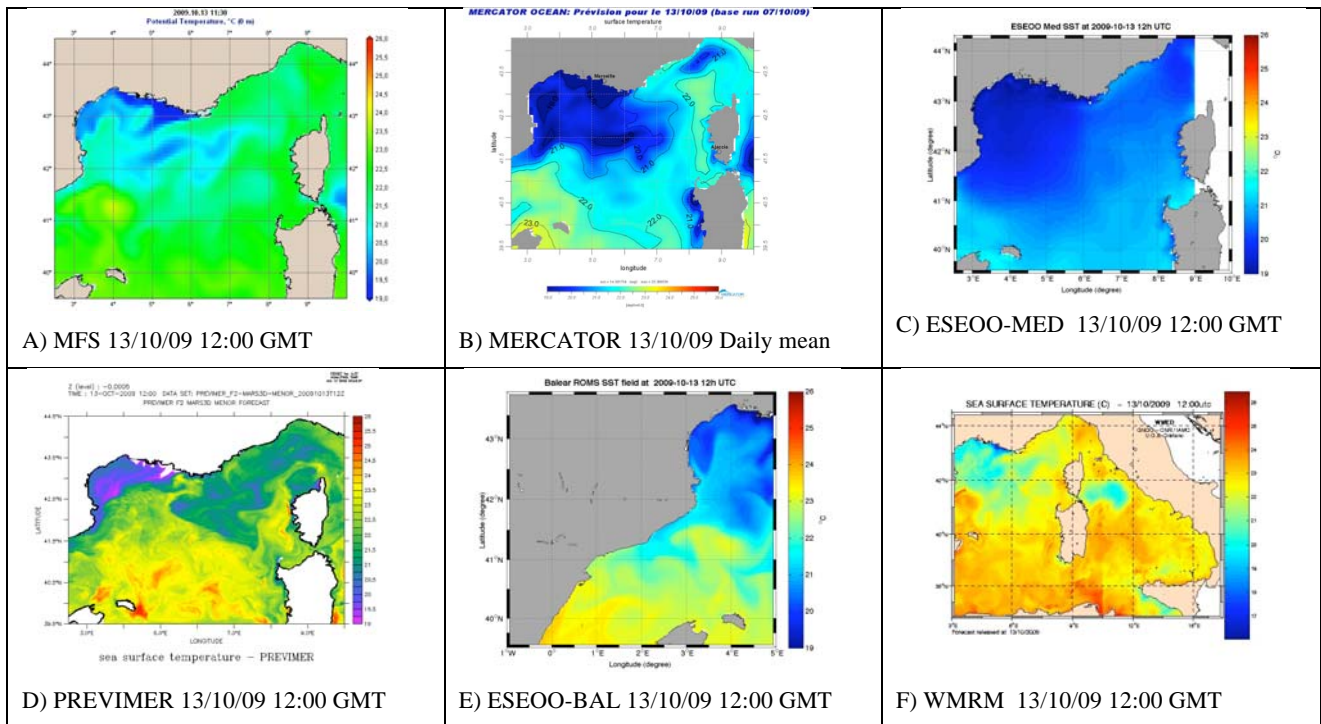


Figure 3.22. Example of the content of the oceanographic part of the ERO bulletin distributed in the context of the OSCAR-MED operation: sea surface temperature (°C) forecasts for 13/10/2009 from 2 different basin (A and B) and 4 sub-regional (C, D, E and F) forecasting systems.

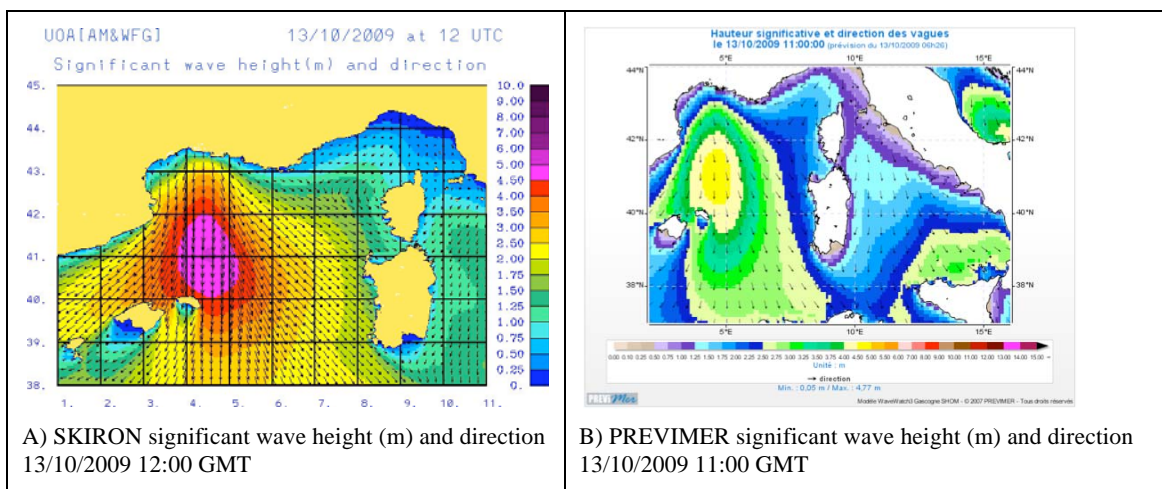


Figure 3.23. Example of the content of the wave part of the ERO bulletin distributed in the context of the OSCAR-MED operation: significant wave height and direction at 10 m (m/s) forecasts for 13/10/2009 from 2 forecasting systems (A) SKIRON from IASA and (B) PREVIMER from IFREMER.

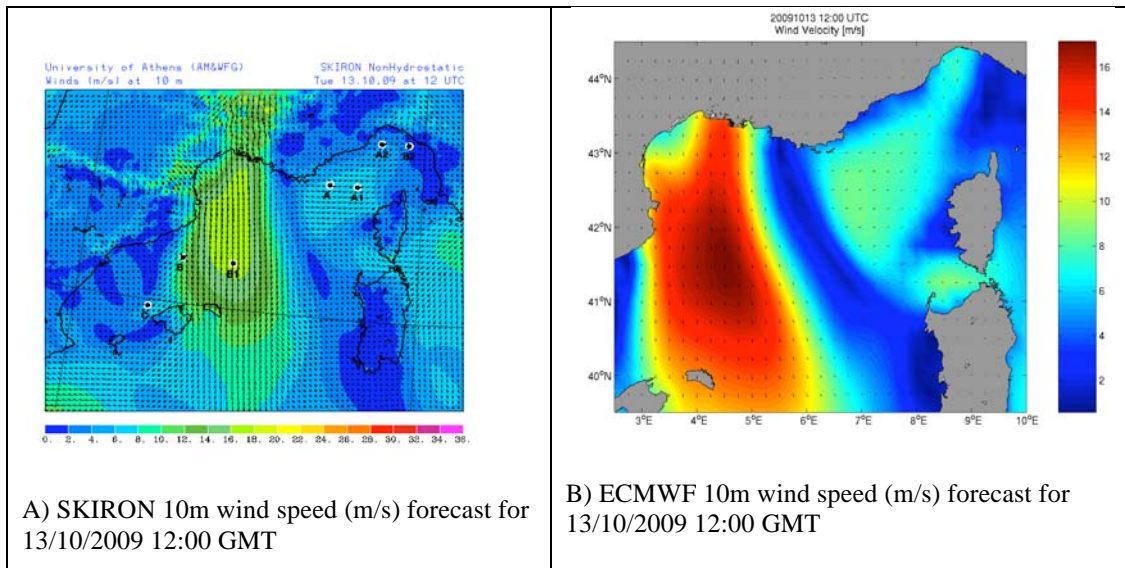


Figure 3.24. Example of the content of the meteorological part of the ERO bulletin distributed in the context of the OSCAR-MED operation: wind speed at 10 m (m/s) forecasts for 13/10/2009 from 2 forecasting systems (A) SKIRON from IASA and (B) ECMWF from USAM/CNMCA.

In addition to the meteo-oceanographic information presented above, ERO provided oil spill forecasts of the detected oil spills. The oil spill forecast was also commented upon by the ERO experts. An example of an oil spill forecast of OS1 detected by satellite produced by IFREMER with the PREVIMER system is presented in Figure 3.25. The image (Figure 3.25) also presents the satellite observation (OS1, OS2 and OS3) and the aerial observations by SASEMAR and Italian Coast Guard. In this case the forecast results show the slick is moving in the correct direction but in the simulation the slick moves more slowly than according to observation.

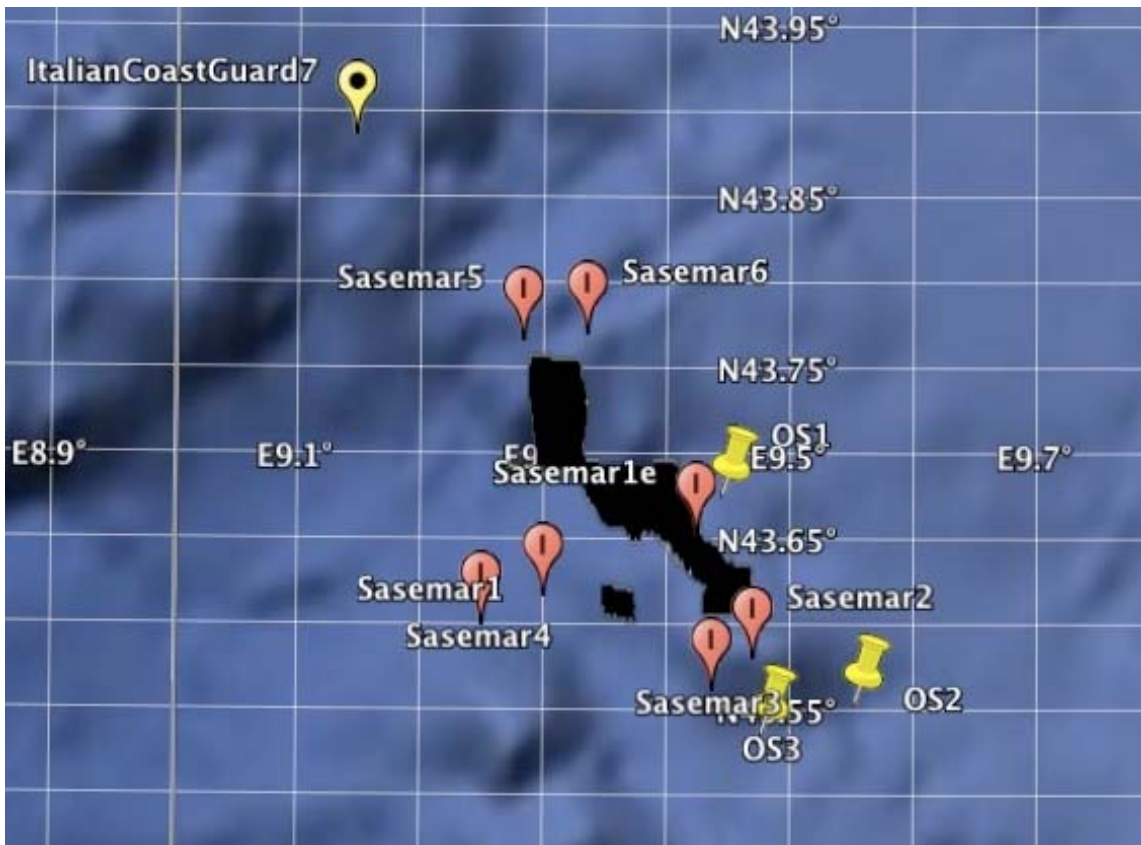


Figure 3.25. The yellow pins marked OS1, OS2 and OS3 represent the central position of the 3 slicks detected by CSN at 9:41 of 13 October 2009. The red pointers marked Sasemar 1 to 6 represent the oil slicks observed by the SASEMAR airplane around 12:00 UTC on 13 October 2009. SASEMAR observations show a northwestward movement of the slicks. The yellow pointer marked ItalianCoastGuard7 represents the observation of a slick in the area at 3:00 UTC on 14 October. The black slick represent the forecast at 3:00 UTC on 14 October made by the MFS-PREVIMER system of OS1 (using the information on the observed shape of the slick from satellite and not only the central position of the slick).

3.2.7. The operational activities

The OSCAR-MED operation was carried out through a continuous aerial surveillance (24h/day) of the identified sea area by Italian, Spanish and French aircraft. In addition, 3 satellite images were received from CSN with 30' from satellite passage and ERO provided meteo-oceanographic and oil spill forecasts (24h/day).

The following products were delivered by ERO during the 3 days of operations:

- ERO provided daily meteo-oceanographic bulletin for the entire domain of operation including: surface currents, Sea Surface Temperature (SST), waves, wind at 10 m. (3 bulletins issued during OSCAR-MED).
- Zoom meteo-oceanographic bulletins for the area where slicks were detected (2 bulletins issued during OSCAR-MED)
- Oil spill drift forecast starting from satellite images or from aerial observation:
 - o Quick and dirty bulletin within half an hour (image and/or position)

- Full report with meteo-ocean zoom forecast and oil spill forecast with the inclusion of expert comments and uncertainty estimation (4-5 hours)

The oil spill forecasts were provided for the following detections:

- Ligurian Sea oil spill detected by satellite on 13 October 11:40 UTC, confirmed by Spanish airplane on 12:00 UTC and by Italian airplane on 14 October 4:00 UTC
- *Aidabella* oil spill
- *Marlin Trade* oil spill
- *Cartage* oil spill

3.2.8. Results of the operation

Throughout the operation the following results were achieved:

- three oil spills which were detected by satellite were identified and confirmed by aircraft;
- the oil spill forecasting models were in some cases validated by observations made by the surveillance aircraft;
- three ships were caught red-handed, two of them while discharging mineral oil within the French Ecological Protected Zone (EPZ). The two polluting ships are being investigated by the French authorities;
- fourteen observers attended the operation participated in the surveillance flights and contributed to a fruitful exchange of knowledge and expertise.

3.2.9. Conclusions

The OSCAR-MED operation, which represents the follow-up of previous activities carried out by REMPEC in the field of illicit discharges from ships, is perfectly in line with Specific Objective 6 of the Regional Strategy for the Prevention of, and Response to, Marine Pollution from Ships, and has fully demonstrated that regional cooperation, particularly in terms of surveillance and investigation, represents a key issue for combating illicit discharges in the Mediterranean Sea.

It was duly noted that this kind of operations should be carried out in the future on a regular basis and also extended to other areas of the Mediterranean Sea which are well known for being threatened by illicit discharges.

REMPEC is looking forward to supporting the carrying out of other similar initiatives within the Mediterranean basin.

The Coordinated Surveillance Operation in the Western Mediterranean (OSCAR-MED) was organized in October 2009 by REMPEC, demonstrating the importance of MOON products for combating marine pollution and the ERO's capabilities of coordinated real-time support (1-2 hour response).

OSCAR-MED demonstrated that this kind of surveillance operation could contribute to the important activity of validation of oil spill models.

There is a need for higher-detail ERO procedures to be more effective and the users have underlined the need to better define different product levels (quick and dirty bulletins and complete ones).

It was evident that there is a need to enforce, through REMPEC, MOON's relationship with national responsible organizations (SASEMAR, Italian Coast Guard...).

4 Example of end-user service

4.1 Introduction

This chapter aims to describe an activity carried out by INGV in collaboration with a user to develop a prototype of Decision Support Systems (DSSs) designed on the basis of user requirements.

The work consists of identifying and analysing user characteristics and requirements and then identifying and building a combination of software, hardware and procedures to make available services and products based on operational oceanography products. The application presented is the Adriatic Sea Decision Support System (ADRI-DSS), built to supply a viewing, discovery and transformation service to the user, ARPA-DAPNHE. This activity is done in collaboration with colleagues at INGV that provided technical and IT assistance and in fact the ADRI-DSS web site and structure has been technically implemented by Dr Vladyslav Lyubartsev (CMCC/INGV).

4.2 An environmental DSS for the Adriatic Sea

ADRI-DSS consists of an on-line service built upon a set of integrated operational oceanography products. The present initial version of ADRI-DSS offers a viewing and transformation service of local in-situ observations and is built to support the Emilia-Romagna coastal monitoring system for marine environment and ecosystem health. The target user is the Oceanography Section of the Regional Environment Protection Agency from Emilia-Romagna (Italy), ARPA-EMR. In the next version, ADRI-DSS will integrate Adriatic Sea monitoring and forecasting system (AFS) products. Specifically, ADRI-DSS will support the daily action of the oceanographic section of ARPA-EMR, ARPA-DAPHNE, providing all the available products (forecast, observations, simulations) from the Adriatic Forecasting System. The product is shaped as required by the user and for the time being ADRI-DSS makes the routine observations that the user carries out on a weekly basis available. In the coming future, model simulation and forecasts and satellite observations and indicators will also be made available by ADRI-DSS. The products presently available on ADRI-DSS are described in the following paragraphs and are presented in Table 4.1. ADRI-DSS has been developed within the ECOOP project (European COastal-shelf sea OPERational Observing and forecasting system Integrated Project).

Data provider	Area	Products delivered
ARPA-DAPNHE	Emilia-Romagna coastal zone	In-situ observations

Table 4.1. Data provider, area of coverage and products delivered to ADRI-DSS.

4.3 The ARPA-DAPHNE monitoring network and data input to ADRI-DSS

ARPA-DAPHNE is the regional environmental protection agency for Emilia Romagna, and carries out regular cruises in the Emilia-Romagna marine and coastal domain.

The ARPA-DAPHNE monitoring network is based on 41 stations distributed from the Po delta region to the town of Cattolica and from the coast to 10 km offshore, and has as its objective to:

- Define intensity and extension of micro-alga blooms in the marine area from the Po river delta to the town of Cattolica.
- Identify the phytoplankton species that produce the blooms
- Control the effects that may derive from the different phases of the evolution of the bloom (anomalous water colours, ipoxya and anoxya of bottom, benthic organism mortality, etc.)
- Measure the nutrient concentrations (Phosphorous, Nitrogen) and their spatial and temporal distribution
- Determine the main physical and chemical water parameters (temperature, salinity, dissolved oxygen, pH, chlorophyll, transparency, turbidity), their temporal and spatial variability in relationship to eutrophication phenomena and meteo-marine conditions.

The cruises are conducted on a weekly basis over the station network presented in Figure 4.1.

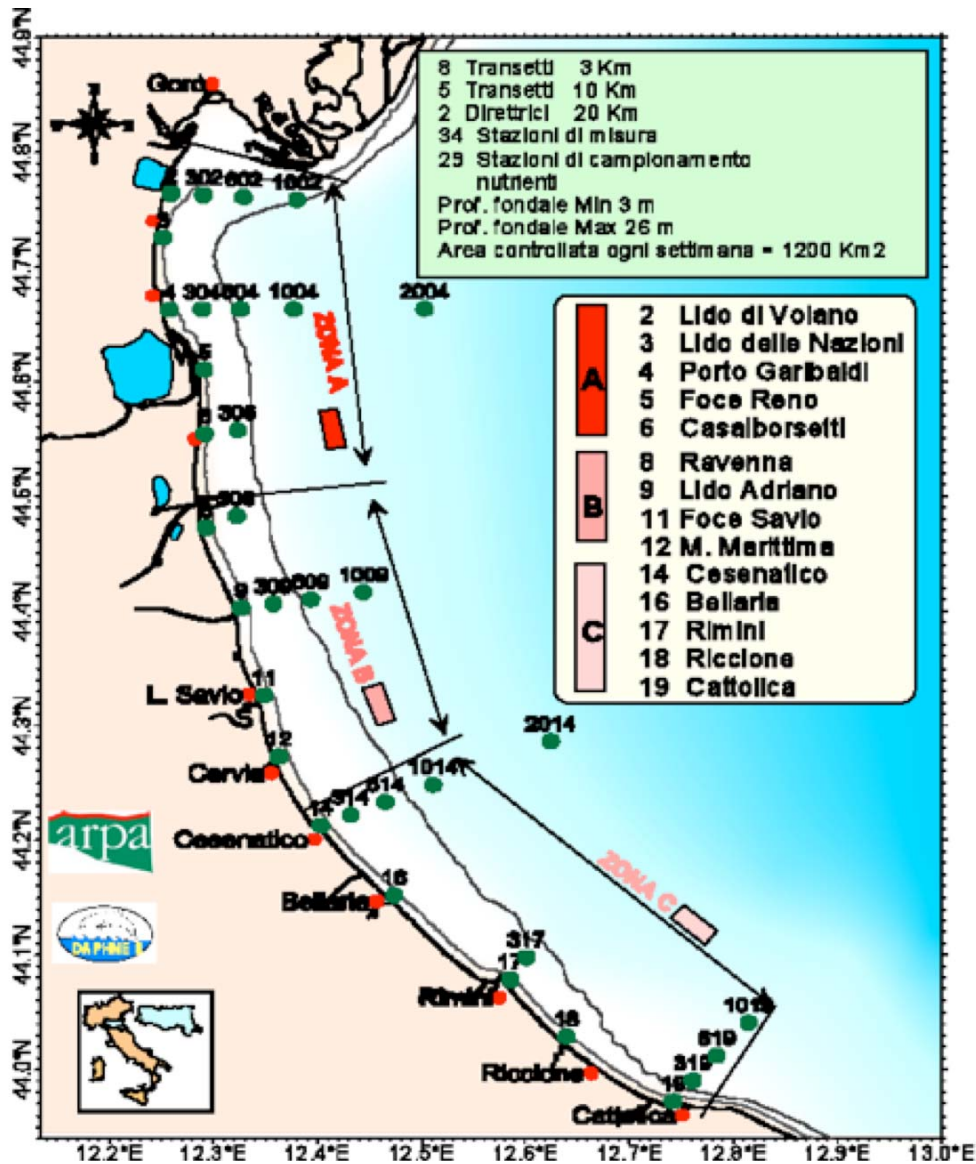


Figure 4.1. ARPA-DAPHNE monitoring network along the Emilia-Romagna coastal strip.

In-situ data collected are used to publish weekly bulletins and yearly reports. Data were delivered regularly to INGV in the framework of previous Italian projects and now this transmission has started again in the framework of ECOOP. Moreover, an agreement for data exchange has been settled between INGV and ARPA-DAPHNE. For each station the following parameters are measured:

- Temperature (°C)
- Salinity (psu)
- Oxygen (mg/L)
- pH
- Transparency (m)
- Chlorophyll-a (µg/L)

The dataset provided to INGV and included in ADRI-DSS starts in 1997 and is updated regularly after each monitoring campaign performed by ARPA-DAPHNE.

4.4 ARPA-DAPHNE user requirements

Several meetings were carried out to propose ADRI-DSS design to ARPA-DAPHNE, to identify user requirements and to show the ADRI-DSS present version and define further improvements.

ARPA-DAPHNE has strong capabilities of data analysis and transformation, but it was underlined that ADRI-DSS could improve ARPA-DAPHNE's ability to discover and visualize data. Moreover, ARPA-DAPHNE does not have an on-line viewing service and therefore ADRI-DSS could be the basis for such a service, which ARPA-DAPHNE could then offer to relevant stakeholders. ARPA-DAPHNE also underlined the relevance of an integrated system that in the next version will interconnect their in-situ dataset with AFS products.

ARPA-DAPHNE has contributed to improve ADRI-DSS by giving advice and defining specific requirements.

4.5 ADRI-DSS architecture

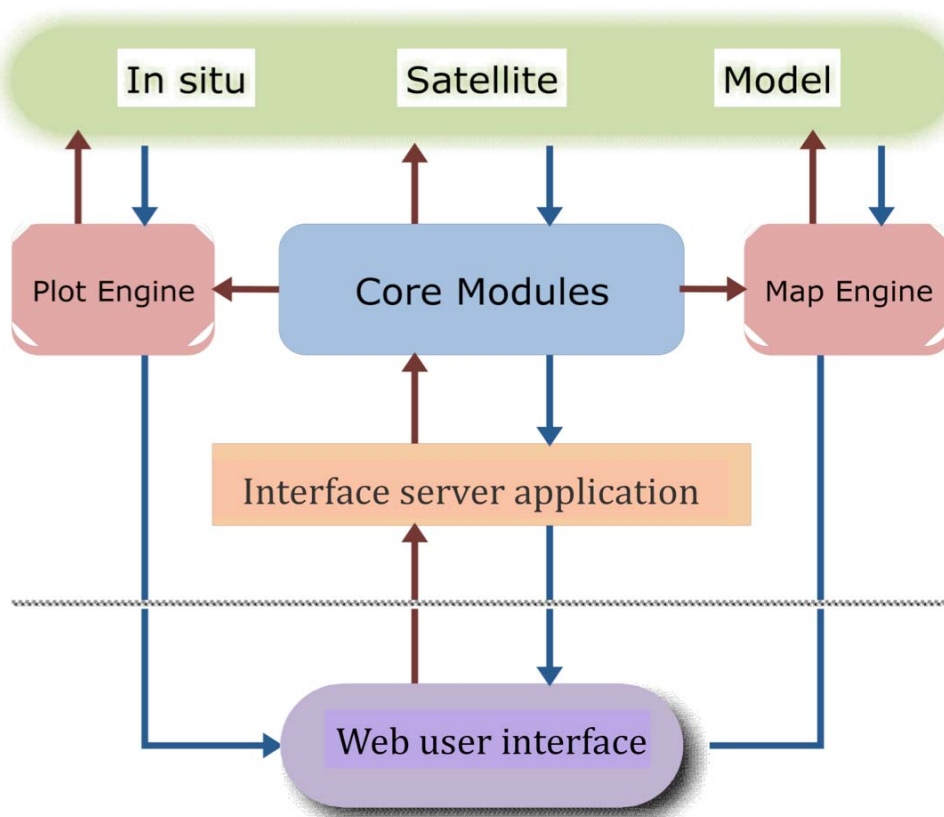


Figure 4.2. ADRI-DSS structure

The structure of ADRI-DSS (Figure 4.2) consists of a front-end server that receives user request, runs the corresponding core modules and composes the server response. Figure 4.2 presents the ADRI-DSS structure as it will be in the final version with access to the model and satellite products. Core modules are a set of functions to retrieve and process data, and pass data to graphics engines. ADRI-DSS is a web-based application available via Internet browsers with JavaScript capability. The server part is implemented on PHP (data management) and NCL (graphics production). NCL is NCAR Command Language, a free interpreted language designed specifically for scientific data processing and visualization (see <http://www.ncl.ucar.edu>). ADRI-DSS has been technically developed by Dr Vladyslav Lyubartsev (CMCC/INGV).

4.6 ADRI-DSS products

ADRI-DSS consists of a portal accessible by ARPA-DAPHNE with in-situ, the user can visualize and transform in-situ data at selected locations. The post-processing of the available datasets includes the extraction of time series and profiles, and some statistical analysis is also possible. The first implementation of ADRI-DSS is now available including ARPA-DAPNHE in-situ products, and appears as presented in Figure 4.3.

ADRI-DSS visualizes and analyses the following input data in the Northern Adriatic region:

- In-situ cruise data from (T, S, Chl-a and dissolved oxygen)

Products delivered:

- Profiles
- Time series
- Scatter plots
- Histograms
- Data availability

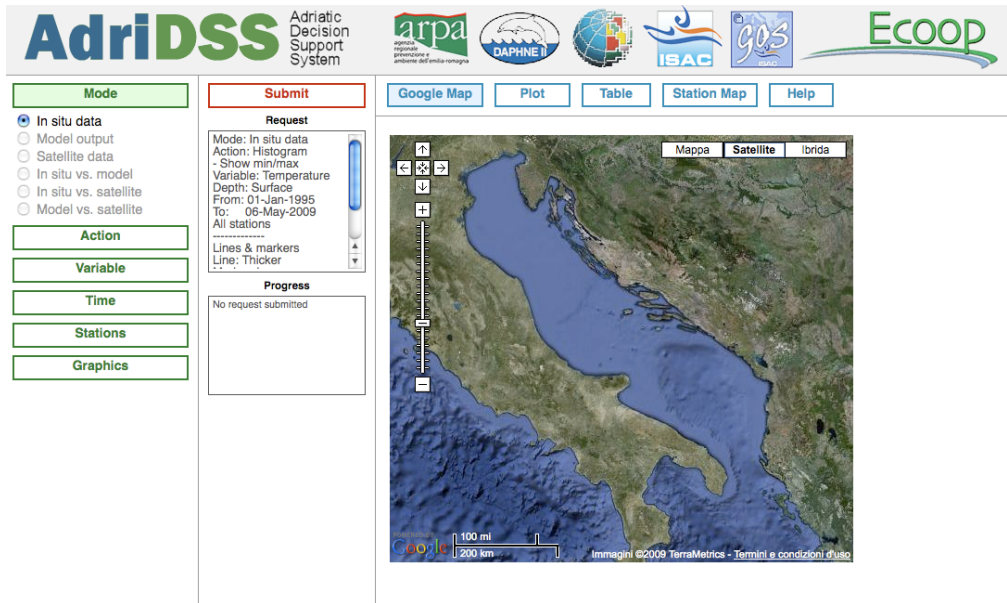


Figure 4.3. ADRI-DSS home page

ADRI-DSS is available at the following web site: http://gnoo.bo.ingv.it/ocean_op/ADRI-DSS/, and the website is password protected.

Once the mode has been selected, (currently only in-situ is developed) the user can select the type of action from the following options: profile, time series, histogram, scatterplot and data availability. The options are shown in Figure 4.4.

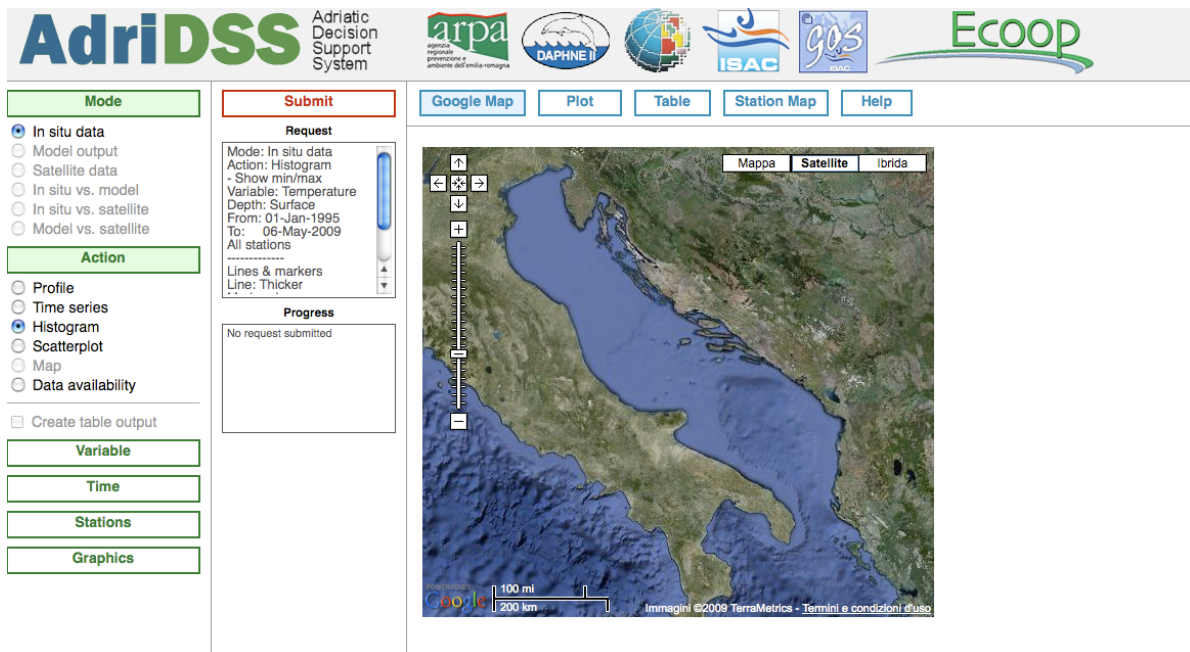


Figure 4.4. Mode and action selection

Once the 'action' has been selected, user should select the variable to be visualized, as shown in Figure 4.5.

Create table output

Variable

- Temperature
- Salinity
- Oxygen, %
- Oxygen, mg/l
- pH
- Chlorophyll-a
- Turbidity
- Bottom depth

Fixed depth Layer

Depth:

Time

Stations

Graphics

Figure 4.5. Variable (Temperature) and depth (surface) selection.

After the user has selected the variable, the time frame of analysis has to be decided.

After the time selection, the user should select the in-situ station to be analysed. The user can select from one station to all of them, using dynamically the menu in Figure 4.6.

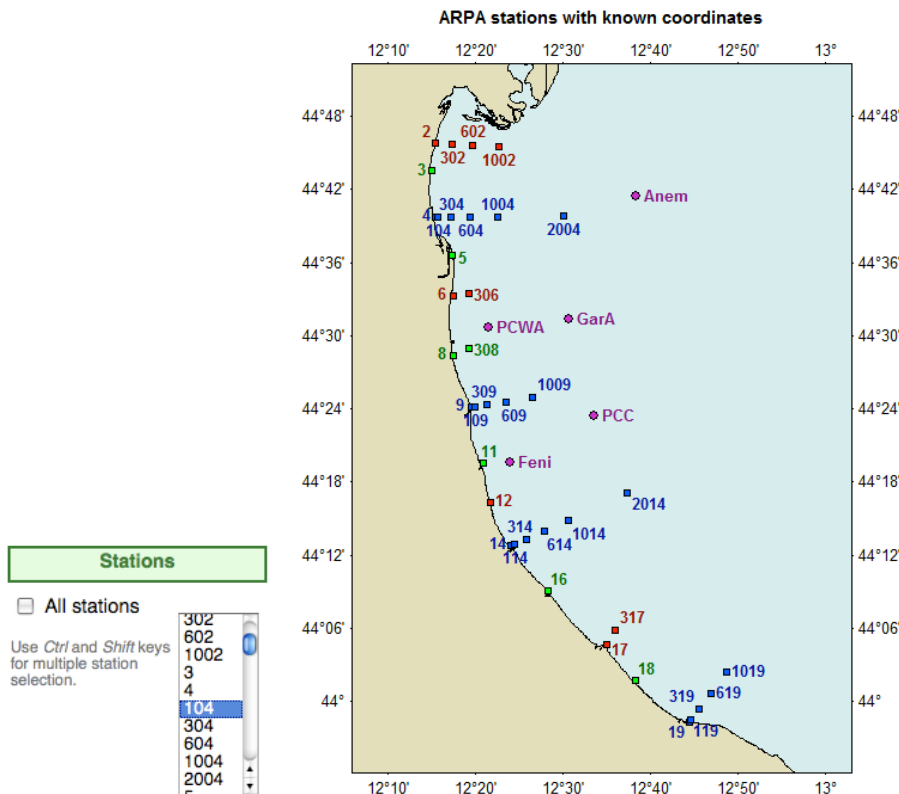


Figure 4.6. Station selection and station map

Data can be analysed at a certain depth, as a profile or aggregating them over several layers.

An example of a product from ADRI-DSS V1 is given in Figure 4.7, where Temperature and Chl-a variables time series are plotted as mean values (1-10m depth) for all the stations for the period 1 January 1998 to 31 December 2007. The plot shows that the two variables appear anti-correlated

and the maximum of Chl-a occurred in the period February-April, which is when the temperature reaches its minimum values.

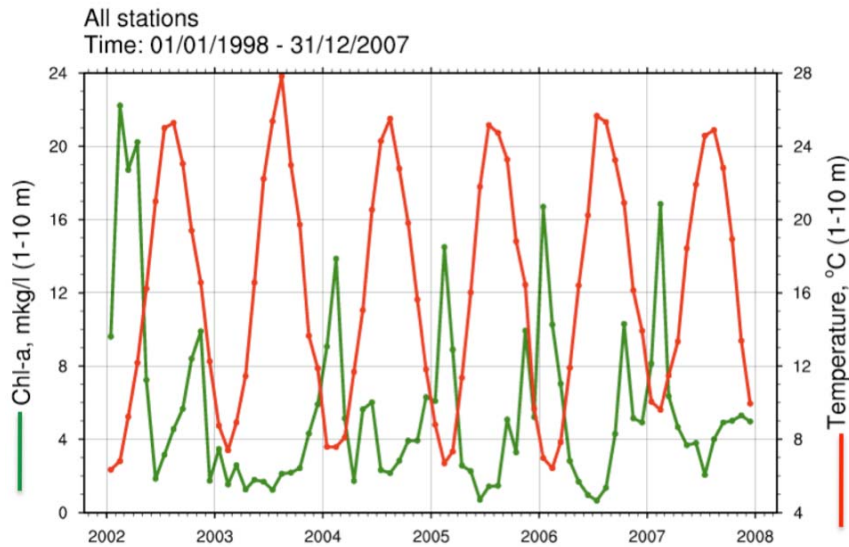


Figure 4.7. Example of time series plotted by ADRI-DSS. Chl-a and Temperature variables monthly means are plotted for all stations as average of the first 10m-depth from January 2002 to February 2010.

In ARPA-DAPHNE dataset the deepest measurement of each profile is marked for each profile and in ADRI-DSS we have identified this value as the bottom one. This approach allows us to analyse for each variable the values close to the bottom. An example of this type of analysis is done in figure 4.8 where we present timeseries of oxygen concentration at the bottom of the water column as calculated by ADRI-DSS in the northern part of the domain (stations n. 2, 102 and 302); this timeseries shows the anoxic events (oxygen concentration below 1 mg/l) recorded during 2005, 2006 and 2007 as also reported in ARPA-DAPHNE annual reports (ARPA-DAPHNE, 2005, 2006 and 2007).

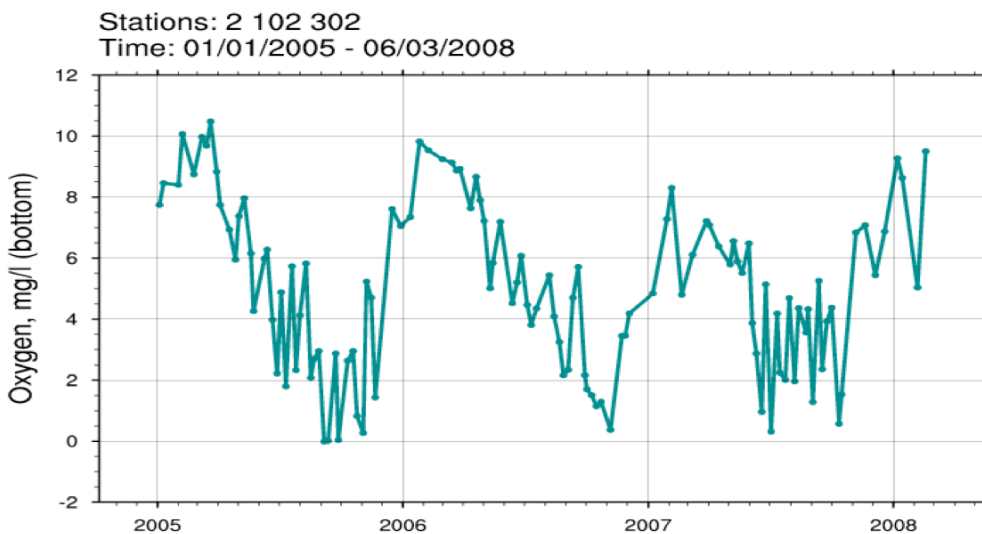


Figure 4.8. Timeseries of daily oxygen concentration [mg/l] at the bottom of the water column averaged on the three stations n. 2, 102, 302 for the period 1/01/2005-06/03/2008.

A series of profiles created in ADRI-DSS are shown in Figure 4.9, which presents the 2004 summer period (June-September) mean profile of temperature, salinity, chl-a, oxygen for station 1009.

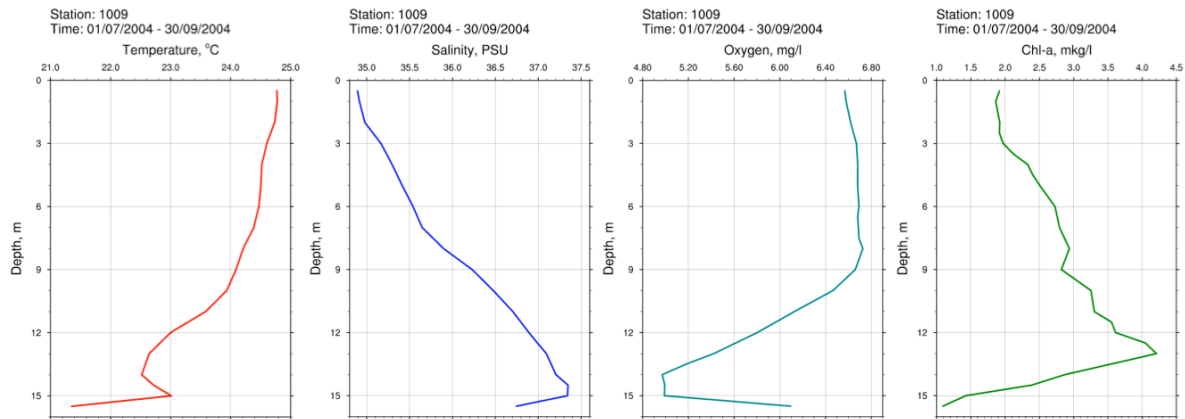


Figure 4.9. Examples of profile plotted by ADRI-DSS. Temperature [°C], salinity [PSU], Oxygen [mg/l] and Chl-a [µg/l] variables are plotted for stations 1009 as average from July 2004 to September 2004.

The following Figure 4.10 presents the scatterplot of surface Temperature and Salinity calculated for the period from 1 January 1995 to 2 February 2010. Figure 4.11 presents the histogram of frequency of surface sea temperature for station 1009 in the different classes for the period from 1 January 1995 to 2 February 2010.

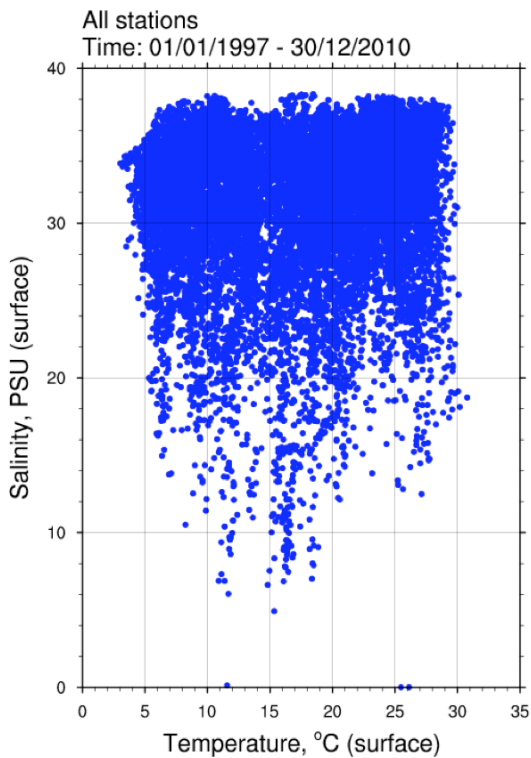


Figure 4.10. Example of scatterplot produced by ADRI-DSS. Salinity (y axis) and temperature (x axis) surface values are plotted for all stations from January 1995 to February 2010.

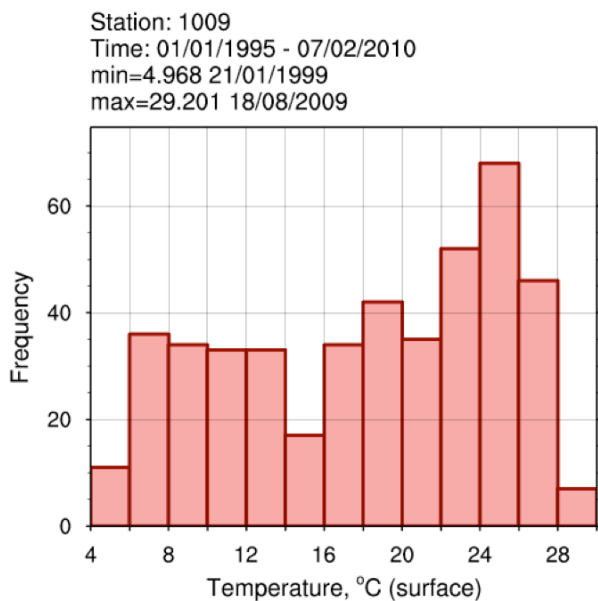


Figure 4.11 Example of histogram plotted by ADRI-DSS. Frequency of surface sea temperature for station 1009 in the different classes for the period from 1 January 1995 to 7 February 2010.

An example of data availability analysis is give in Figure 4.12, where the number of temperature profiles collected in all stations during the period 1 January 1998- 7 March 2010 is shown.

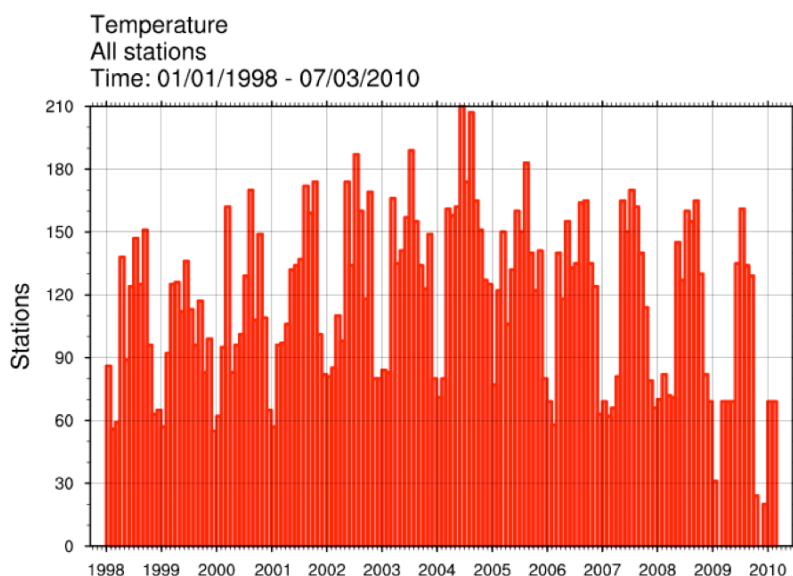


Figure 4.12. Temperature data availability for all stations from 1 January 1998 to 7 March 2010.

4.7 Conclusions

This first version of ADRI-DSS shows that is possible to develop web-based visualization service that also allows transformation of the products. This application will be further developed to also include model outputs and possibly other kind of products such as satellite observations and indicators. The product will develop towards the next version where the AFS (Adriatic Forecasting System, <http://gnoo.bo.ingv.it/afs>) model products will be compared with in-situ observations of

temperature and salinity collected by ARPA-DAPHNE itself. In the new version also hourly forecast from AFS will be available. The final aim of ADRI-DSS is to integrate selected products to support the monitoring activities of ARPA-DAPNHE and to improve ARPA-DAPHNE capabilities for the Emilia-Romagna marine environment status assessment. The system is already in this present version showing the potential of being used by ARPA-DAPHNE for data discovery, visualization and transformation in support to the monitoring activities and environmental assessment.

5 Conclusions

The work performed in this thesis identifies possible methodologies that could contribute to support the activities of several relevant stakeholders in the implementation of European Directives and international conventions for the protection of the European seas and the proper management of their resources.

The development of the proposed products, i.e., indicators and DSSs, is based on a continuous interaction with the main users identified: the EEA, REMPEC and ARPA-DAPHNE.

In Chapter 2 we have defined and implemented two main sets of indicators. The first one is dedicated to climate change state assessment that is evaluated in terms of SST anomalies long time series and SST trends of recent decades. SST anomalies long time series, based for recent decades on OO satellite products, and SST trends show the ability of assessing the climate change state and identifying the acceleration of ocean temperature increase over recent decades and regional differences in the European seas. The developed SST indicators have been included in two EEA reports (EEA, 2008 and in the '2010 EEA State of the Environment Report').

The second set of indicators is based on ocean colour products and aims to contribute to the state of the environment assessment and in particular the assessment of eutrophication evolution in terms of Chl-a trends and coastal water extension. The validation of Chl-a trends and concentrations estimated through remote sensing with in-situ ones has been performed. The comparison presented shows that the global ocean colour algorithm seems to overestimate Chl-a concentration but performs better if used to estimate trends; in fact, trends estimated by ocean colour products show similar slope and sign if compared with trends estimated by in-situ. Moreover, the regional daily dataset, Mediterranean CNR-SeaWIFS, used in the Mediterranean Sea seems to show a good comparison with in-situ data but further investigations need to be performed. The Chl-a trend pan-European indicator shows a large area with decreasing Chlorophyll-a concentrations in the Black Sea, in the Northern Adriatic Sea and in the Skagerrak, whereas a large area with increasing trends is observed in the Bay of Biscay and in the Baltic Sea.

The analysis has also revealed the need for regional ocean colour products to be available to develop support of the EEA indicator and that there is potential in a long-term trend analysis based on ocean colour because large-scale and in some cases even regional-scale changes appear to be

captured by the satellite images. In order to build confidence in this analysis, it is however clear that it needs to be based on the best possible regional products.

The pan-European Chl-a trend indicator has been included in the '2010 EEA State of the Environment Report'.

A second indicator based on ocean color products has been presented in its preliminary implementation showing marine waters influenced by river run-off and terrestrial inputs, also referred to as Case 2 waters has been presented. The indicator has been thought up for the EEA to present a qualitative influence of the influence of river and terrestrial inputs in the marine domain.

By comparing the indicators during two seasons (winter and summer 2009) it is evident that there is a seasonal variability in the extension of open ocean waters influenced by the river run-off and that this influence is larger in the winter period. The indicator is calculated for each season and is distributed by EEA on the Water Information System for Europe (WISE).

To show how accidental and illegal oil spill pollution can be monitored, managed and mitigated, we have selected two experiences that are presented in chapter 3. The first is the simulation of the Lebanese oil spill accident in 2006. The Lebanon oil pollution event is the largest oil pollution incident in the Eastern Mediterranean Sea so far. The oil spill affected most of the Lebanese coast and, as the oil spill was drifting northward for over one month, reached the southern Syrian coast. During the entire period of the Lebanese oil pollution crisis in July-August 2006, however, MOON was able to provide daily information on the displacement of the oil slicks. Our work shows that the technological innovation coming from operational oceanography, providing satellite images and real-time forecasts on water currents gives the possibility to precisely map the damage of oil spills even if very near the coasts. The satellite observing products used for oil slick detection and for validation of the MEDSLIK oil spill drift predictions were shown to be robust and capable of providing valuable operational information during this oil spill accident. Sensitivity experiments to different deterministic oil spill drift factors show that best results still require ad-hoc tuning of parameters such as the water current depth from the hydrodynamic model, and the wind drift factor and angle.

Our results indicate that both MFS and CYCOFOS models coupled to the MEDSLIK oil spill drift model show skill in reproducing the timing and transport of the oil, and comparison also shows that the CYCOFOS currents in MEDSLIK better represent the coastal trapping of the oil. This is due to the higher horizontal resolution of the CYCOFOS forecasting system, which allows the along-shore currents to be resolved better and permits the start of the oil spill closer to the coasts, near the real oil source. Coastal impact was observed to be heaviest from Jieh up to south of Beirut but also

significant impacts between Beirut and Chekka and northwards on the Syrian coast were reported. It is found that MEDSLIK coupled to MFS probably overestimates the northernmost part of the slick on the Syrian coast, even though validation of prediction is difficult because the quantities of oil that reached the northern Syrian shores were not clearly reported.

The second experience that we have shown to present how illegal oil spill pollution can be monitored, managed and mitigated is the OSCAR-MED operation organized by REMPEC in the western Mediterranean Sea. OSCAR-MED has demonstrated that regional cooperation, particularly in terms of surveillance and investigation, represents a key issue for combating illicit discharges in the Mediterranean Sea. During this operation the ERO, the MOON-REMPEC agreement Emergency Response Office, was activated and participated actively in providing real time meteorological and oceanographic products and oil spill forecast. OSCAR-MED demonstrated the importance of MOON products for combating marine pollution and the ERO's capabilities of coordinated real-time support (1-2 hour response). OSCAR-MED also demonstrated that this kind of surveillance operation could contribute to the important activity of validation of oil spill models. The operation also shown that there is a need for higher-detail ERO procedures to be more effective and the users have underlined the need to better define different product levels (quick and dirty bulletins and complete ones). During OSCAR-MED it was also evident that there is a need to enforce, through REMPEC, MOON's relationship with national responsible organizations (SASEMAR, Italian Coast Guard...).

Finally, in Chapter 4 of this thesis we present a first version of DSS for operational oceanography products matched with in-situ monitoring networks. ADRI-DSS shows that is possible to develop web-based visualization services that also allow transformation of the products. This application will be further developed also to include model outputs and possibly other kinds of products such as satellite observations and indicators. The system is already in this present version showing the potential of being used by ARPA-DAPHNE for data discovery, visualization and transformation in support of monitoring activities.

References

- Adamo M., D. C. (2007). Exploiting Sun glint Signatures From Meris and Modis Imagery in combination to SAR data to detect oil slicks. *Proc. Envisat Symposium*, ESA-SP-636.
- Ahlstrom, S. (1975). A mathematical model for predicting the transport of oil slicks in marine waters. *Res. Rept.*, Batelle Laboratories, Richland, Wash.
- Al-Rabeh A.H. (1994). Estimating surface oil spill transport due to wind in the Arabian Gulf. *Ocean Engineering*, Volume 21, Issue 5, July 1994, Pages 461-465
- Amato E. and Alcaro L. (2006). Oil spill in Lebanon: in situ observation. Proceeding of the Workshop on Monitoring activities related to the oil pollution in Lebanon. European Commission Joint Research Centre *EUR 22531 EN*.
- Ardhuin F., Marie L., Rasclé N., ; Forget P. and Rolabd Aron. (2009). Observation and Estimation of Lagrangian, Stokes, and Eulerian Currents Induced by Wind and Waves at the Sea Surface. *Journal of physical oceanography* ISSN 0022-3670. vol. 39, no11, pp. 2820-2838
- ARPA-DAPHNE annual report (2005). Rapporto Eutrofizzazione 2005. Available at: http://www.arpa.emr.it/cms3/documenti/daphne/download/RAPPORTO_2005.pdf
- ARPA-DAPHNE annual report (2006). Rapporto Eutrofizzazione 2005. Available at: http://www.arpa.emr.it/cms3/documenti/daphne/download/RAPPORTO_2006.pdf
- ARPA-DAPHNE annual report (2007). Rapporto Eutrofizzazione 2005. Available at: http://www.arpa.emr.it/cms3/documenti/daphne/download/RAPPORTO_2007.pdf
- Bignami F., Sciarra R., Carniel S., Santoleri R. (2007). The variability of Adriatic Sea coastal turbid waters from SeaWiFS imagery, *J. Geophys. Res.*, VOL. 112, C03S10, doi:10.1029/2006JC003518, 2007.
- Brander K. M., Blom G., Borges M. F., Erzini K., Henderson G., MacKenzie B. R., Mendes H., Ribeiro J., Santos A. M. P. and Toresen R. (2003). Changes in fish distribution in the eastern North Atlantic: Are we seeing a coherent response to changing temperature? *ICES Marine Science Symposia* 219: 261–270.

Brenner, S., (2003). High-resolution nested model simulations of the climatological circulation in the southeastern corner of the Mediterranean Sea. *Annal. Geophys.*, 21, 267-280.

Cazenave A., Dominh K., Guinehut S., Berthier E., Llovel W., Ramillien G., Ablain M. and Larnicol G. (2009). Sea level budget over 2003-2008: a reevaluation from GRACE space gravimetry, satellite altimetry and ARGO. *Global and Planetary Change*. Volume 65, Issues 1-2, January 2009, Pages 83-88

CSI021, (2009). Core Set of Indicators n. 021 - Nutrients in transitional, coastal and marine waters - Assessment published Jan 2009. Available at:
http://themes.eea.europa.eu/IMS/ISpecs/ISpecification20041007132008/IAssessment1204714151163/view_content

CSI023, 2009. Core Set of Indicators n.023 - Chlorophyll in transitional, coastal and marine waters - Assessment published Jan 2009. Available at:
http://themes.eea.europa.eu/IMS/ISpecs/ISpecification20041007132031/IAssessment1205412447537/view_content

Demirov E. and Pinardi N. (2002). Simulation of the Mediterranean Sea circulation from 1979 to 1993. Part I: The interannual variability, *J. Mar. Syst.*, 33-34 (C): 23-50

Dobricic, S. and Pinardi N. (2008). An oceanographic three-dimensional variational data assimilation scheme. *Ocean Modelling*, 22, 3-4, 89-105.

ECMWF User Guide to ECMWF forecasts products Version 4.0, 14 March 2007.(2005)
Meteorological Bulletin M3.2 available at:
http://www.ecmwf.int/products/forecasts/guide/user_guide.pdf

Edwards M. and Richardson A.J. (2004). Impact of climate change on marine pelagic phenology and trophic mismatch. *Nature* 430: 881-884

EEA, (2007). Europe's environment - The fourth assessment. Available at:
http://www.eea.europa.eu/publications/state_of_environment_report_2007_1

EEA, (2008). Impacts of Europe's changing climate - 2008 indicator-based assessment (http://www.eea.europa.eu/publications/eea_report_2008_4)

Emblow C. and Gelabert E. R., (2009). EEA - ETC report: Indicator Comparison in 2008 and 'next steps'. Available at:

http://water.eionet.europa.eu/ETC_Reports/Final_IC__Progress_Report_180509.pdf

EWGL, Experts Working Group For Lebanon. (2008). Lebanon marine and coastal oil pollution *international assistance action plan*.

Fingas M. F. and Brown C. E. (1997). Review on oil spill remote sensing. *Spill Science & Technology Bulletin* , 4 (4), 199-208.

Fiscella B., Giancaspro A., Nirchio F., Pavese P. and Trivero, P. (2000). Oil spill detection using marine SAR images. *International Journal of Remote Sensing* , 21 (18), 3561-3566.

GLA, Green Line Association. (2007). *LEBANON OIL SPILL July 2006 – July 2007*.

Gordon Hr. and Morel Ay. (1983). Remote assessment of ocean color for interpretation of satellite visible imagery: A review. *Springer-Verlag (Lecture Notes on Coastal and Estuarine Studies. Volume 4)*, 1983, 118 p

Guinehut S. and Larnicol G. (2008). Impacts of Europe's changing climate - 2008 indicator-based assessment (http://www.eea.europa.eu/publications/eea_report_2008_4)

Halpern B.S., Walbridge S., Selkoe K.A., Kappel C.V., Michelo F., D'Agrosa C., Bruno J.F., Casey K.S., Ebert C., Fox H.E., Fujita R., Heinemann D., Lenihan H.S., Madin E.M.P., Perry M.T., Selig E.R., Spalding M., Steneck R., Watson R. (2008). A global map of human impact on marine ecosystems. *Science* 319, 948–952.

HELCOM (Helsinki Commission) (2003). The Baltic Marine Environment 1999–2002. HELCOM, Helsinki, *Baltic Sea Environment Proceedings* 87.

Hu C., Müller-Karger F. E. , Taylor C., Myhre D., Murch B., and Odriozola A. L. (2003). MODIS Detects Oil Spills in Lake Maracaibo, Venezuela. *Eos*, 84, 33, 313-319.

Hunter J. R. (1987). The application of Lagrangian particle tracking technique to modelling of dispersant in the sea, in Numerical Modelling: Application to Marine Systems, edited by J. Noye, North Holland.

ICES (International Council for the Exploration of the Sea), (2003). Environmental Status of the European Seas. Copenhagen,
http://www.ices.dk/reports/germanqsr/23222_ICES_Report_samme.pdf (28.10.2008). (European Commission, 2005a).

ICES (International Council for the Exploration of the Sea), (2007). Report of the ICES Advisory Committee on the Fishery Management, Advisory Committee on the Marine Environment and Advisory Committee on Ecosystems, 2007. Book 8: Baltic Sea. ICES, Copenhagen, *ICES Advice* 2007, 8.

IMO/REMPEC and Joint UNEP/OCHA. (2006). IMO/REMPEC and Joint UNEP/OCHA Environment Unit mission in Syria, Final Report: Sampling at the border between Syria and Lebanon (Ph. Rene Nijenhuis).

IPCC (2007). Climate Change 2007: The Physical Science Basis - Summary for Policymakers Contribution of Working Group I to the Fourth Assessment Report of the Intergovernmental Panel on Climate Change. *Intergovernmental Panel on Climate Change*, Geneva, Switzerland.

Jha M. N., J. L. (2008). Advances in Remote Sensing for Oil Spill Disaster Management: State-of-the-Art Sensors Technology for Oil Spill Surveillance. *Sensors* , 8, 236-255.

Kallos, G. (1997). The Regional weather forecasting system SKIRON. *Proceedings of the Symposium on Regional Weather Prediction on Parallel Computer Environments*, 15-17 October 1997, Athens, Greece. Pp 9., ISBN: 960-8468-22-1.

Lardner R.W. and Zodiatis G. (1998). An operational Oil Spill model in the Levantine Basin (Eastern Mediterranean Sea). *International symposium on Marine Pollution*. 10 5-9

- Lardner R., Zodiatis G., Hayes D. and Pinardi N. (2006). Application of the MEDSLIK oil spill model to the Lebanese spill of July 2006. *European Group of Experts on satellite monitoring of sea based oil pollution, European Communities*. ISSN 1018-5593.
- Lavander S.J., Pinnkerton M. H., Froidefod J-M., Morales J., Aiken J. and Moore G. F. (2004). SeaWiFS validation in European coastal waters using optical and bio-geochemical measurements. *Int. J. Remote Sensing*, 10–20 April, 2004, Vol. 25, No. 7–8, 1481–1488
- Lombard A., Cazenave A., Guinehut S., Le Traon P.Y. and Cabanes C. (2006). Perspectives on present-day sea level change. *Ocean Dyn.*, 56,445-451, doi:10.1007/s10236-005-0046-x.
- Lotliker Aneesh A., M. S. (2008). Evaluation of Hi-Resolution MODIS-Aqua data for oil spill monitoring. *Proceedings of SPIE, the International Society for Optical Engineering*, 7150.
- Loureiro Maria L., Loomis John B. and Vázquez M. X. (2009). Economic Valuation of Environmental Damages due to the Prestige Oil Spill in Spain. *Environmental and Resource Economics*. 44, 4, 2009 537-553
- Mackay, D. and Paterson, S. (1980). Calculation of the evaporation rate of volatile liquids. *Proc. 1980 National Conf. on Control of Hazardous Material Spills, Louisville, Ky.*
- Mackay, D. and Leinonen, P.J. (1977). Mathematical model of the behaviour of oil spills on water with natural and chemical dispersion. *Tech. Review Report no. EPS-3-EC-77-19, Fisheries and Environment Canada.*
- Marpol convention (1973). Available at the web site: http://en.wikipedia.org/wiki/MARPOL_73/78
- Morel, A. and Prieur, L. (1977). Analysis of variations in ocean-colour. *Limnol. Oceanogr.*, 22: 709-722.
- O'Reilly, J. E. and 24 co-authors (2000). Ocean colour chlorophyll-a algorithms for SeaWiFS, OC2 and OC4: version 4. In *SeaWiFS Post Launch Calibration and Validation Analyses, vol. 11, edited by S. B. Hooker and E. R. Firestone* (Greenbelt, MD: NASA Goddard Space Flight Center), pp. 9–23.
- Otremba, Z., & Piskozub, J. (2001). Modelling of the optical contrast of an oil film on a sea surface. *Opt. Express.* , 9, 411-416.
- Otremba Z. and Piskozub J. (2004). Modelling the bidirectional reflectance distribution function (BRDF) of seawater polluted by an oil film. *Opt. Express*. 12., 12, 1671-1676.

Papadopoulos, A., P. Katsafados, and G. Kallos, (2002). Regional weather forecasting for marine application. *GAOS* Vol. 8, No 2-3, 219-237.

Pavlakakis P., Tarchi D., Sieber A., Ferraro G. and Vincent G. (2001). On the Monitoring of Illicit Vessel Discharges: A Reconnaissance Study in the Mediterranean Sea. *Joint Research Centre and DG – Environment. European Commission.*

Pinardi N., Allen I., Demirov E., De Mey P., Korres G. and Lascaratos A., Le Traon P.-Y., Maillard C., Manzella G. and Tziavos C.(2003). The Mediterranean ocean forecasting system: first phase of implementation (1998–2001). *Annales Geophysicae* 21, 3–20 c.

Pinardi N., Arneri E., Crise A., Ravaioli M. and Zavatarelli M. (2006). “The physical, sedimentary and ecological structure and variability of shelf areas in the Mediterranean Sea”. *The Sea* Vol. 14 (A. R. Robinson and K. Brink Eds.), Harvard University Press, Cambridge, USA, 1243-1330

Pond, S. and Pickard G.L.(1983). *Introductory Dynamical Oceanography*, 2nd edition, *Ed.Elsevier Butterworth-Heinemann.*

Prieur L. and Sathyendranath S. (1981). An optical classification of coastal and oceanic waters based on the specific spectral absorption curves of phytoplankton pigments, dissolved organic matter and other particulate materials. *Limnol. Oceanogr.*, 26(4): 671-689.

Rascle N., Arduin F. (2005). Wave-induced drift and Mixing. *Ocean-Europe 2005*

Reed M., Turner C. and Odulo, A. (1994). The role of wind and emulsification in modelling oil spill and surface drifter trajectories. *Spill Science and Technology Bulletin*, 1:2, 143–157.

REMPEC (2006). REMPEC News, from *SITREP 12 (Updated 25.08.2006) SPILL IN LEBANON:*
<http://www.rempec.org/newsmore.asp?id=182&lang=en>

Salmi T., Määttä A., Anttila P., Ruoho-Airola T. and Amnell T. (2002). Detecting trends of annual values of atmospheric pollutants by Mann-Kendall test and Sen'Slope estimates - the excel template application *Makesens*. Ilmatieteen laitos - Meteorologiska Institutet, Finnish Meteorological Institute. Helsinki 2002. *Publications on Air Quality No. 31*. Report code FMI-AQ-31.

Painopaikka: Edita Oyj

Salomon M. (2009). Recent European initiatives in marine protection policy: towards lasting protection for Europe's seas? *Environmental science & policy* 12 (2009) 359 – 366

Santoleri R., Volpe G., Marullo S. and Buongiorno Nardelli B. (2008). Open Waters Optical Remote Sensing of the Mediterranean Sea. *Remote Sensing of the European Seas*, edited by V. Barale and M. Gade, pp. 103-116, Springer

Shi Lijian, Z. X.-X. (2007). Oil Spill Detection by MODIS Images using Fuzzy Cluster and Texture Feature Extraction. *Ocean 2007 Europe*, 1-5., 06 18-21.

Sofianos S., Skliris N., Mantziafou A., Lascaratos A., Zodiatis, G., Lardner, R., Hayes D. and Georgiou G. (2006). Nesting operational forecasting models in the Eastern Mediterranean: active and slave mode. *Ocean Science Discussions*, 3, 1225-1254.

Southward A.J., Langmead O., Hardman-Mountford N.J., Aiken J., Boalch G.T., Dando P.R., Genner M.J., Joint I., Kendall M., Halliday N.C., Harris R.P., Leaper R., Mieszkowska N., Pingree R.D., Richardson A.J., Sims D.W., Smith T., Walne A.W, Hawkins S.J. (2005). Long-term oceanographic and ecological research in the western English Channel. *Adv Mar Biol* 47, 1-105.

Stachowicz J.J., Terwin J.R., Whitlatch R.B., Osman R.W. (2002). Linking climate change and biological invasions: ocean warming facilitates non-indigenous species invasion. *Proc Nat Acad Sc USA* 99, 15497-15500

Tonani, M., Pinardi N., Dobricic S., Pujol I. and Fratianni C. (2008). A high-resolution free-surface model of the Mediterranean Sea. *Ocean Sci.*, 4, 1-14.

Trenberth, K.E., Jones P.D., Ambenje P., Bojariu R., Easterling D., Klein Tank A., Parker D., Rahimzadeh F., Renwick J.A., Rusticucci M., Soden B. and Zhai P. (2007). Observations: Surface and Atmospheric Climate Change. In: *Climate Change 2007: The Physical Science Basis. Contribution of Working Group I to the Fourth Assessment Report of the Intergovernmental Panel on Climate Change* [Solomon, S., D. Qin, M. Manning, Z. Chen, M. Marquis, K.B. Averyt, M. Tignor and H.L. Miller (eds.)]. *Cambridge University Press*, Cambridge, United Kingdom and New York, NY, USA.

UNEP, (2007). Lebanon Post-Conflict Environmental Assessment. ISBN: 978-92-807-2794-4

<http://postconflict.unep.ch/publications.php?prog=lebanon>

Volpe G., Sanotleri R., Vellucci V., Ribera d'Alcalà M., Marullo S., D'Ortenzio F. (2007). The colour of the Mediterranean Sea: Global versus regional bio-optical algorithms evaluation and implication for satellite chlorophyll estimates. *Remote Sensing of Environment* 107 625–638

World Bank. (2007). Republic of Lebanon Economic Assessment of Environmental Degradation due to July 2006 Hostilities. World Bank.

Zodiatis, G., Lardner, R., Lascaratos, A., Georgiou, G., Korres, G., & Syrimis, M. (2003). High resolution nested model for the Cyprus, NE Levantine Basin, eastern Mediterranean Sea : implementation and climatological runs. *Annales Geophysicae* , 21, 221-236.

Zodiatis G., Lardner R., Hayes D., Georgiou G., Sofianos S., Skliris N. and Lascaratos A. (2008). Operational ocean forecasting in the Eastern Mediterranean: implementation and evaluation. *Ocean Science* , 4, 31-47.